

**SYNTHESIS AND EVALUATION OF NEW POTENT HIV-1  
PROTEASE INHIBITORS**



**A THESIS SUBMITTED IN PARTIAL FULFILLMENT  
OF THE REQUIREMENTS FOR  
THE DEGREE OF MASTER OF SCIENCE IN  
PHARMACY(PHARMACEUTICAL CHEMISTRY)  
FACULTY OF GRADUATE STUDIES  
MAHIDOL UNIVERSITY**

**2005**

**ISBN 974-04-6357-6**

**COPYRIGHT OF MAHIDOL UNIVERSITY**

Thesis  
Entitled

**SYNTHESIS AND EVALUATION OF NEW POTENT HIV-1  
PROTEASE INHIBITORS**



*Narumol Phosrithong*

Ms. Narumol Phosrithong  
Candidate

*Jiraporn Ungwitayatorn*

Assoc. Prof. Jiraporn Ungwitayatorn, Ph.D.  
Major-Advisor

*Chanpen Wiwat*

Assoc. Prof. Chanpen Wiwat, Ph.D.  
Co-Advisor

*Rassmidara Hoonsawat*

Assoc. Prof. Rassmidara Hoonsawat, Ph.D.  
Dean  
Faculty of Graduate Studies

*Ampol Mitrevej*

Prof. Ampol Mitrevej,  
Ph.D.  
Chair  
Master of Science in Pharmacy  
Programme in Pharmaceutical Chemistry  
Faculty of Pharmacy

Thesis

Entitled

**SYNTHESIS AND EVALUATION OF NEW POTENT HIV-1  
PROTEASE INHIBITORS**

was submitted to the Faculty of Graduate Studies, Mahidol University  
for the degree of Master of Science in Pharmacy (Pharmaceutical Chemistry)

On  
August 1, 2005

*Narumol Phosrithong*

Ms. Narumol Phosrithong

Candidate

*Jiraporn Ungwitayatorn*

Assoc. Prof. Jiraporn Ungwitayatorn,

Ph.D.

Chair

*Onoomar Poobrasert*

Asst. Prof. Onoomar Poobrasert,  
Ph.D.

Member

*Chanpen Wiwat*

Assoc. Prof. Chanpen Wiwat,  
Ph.D.

Member

*Rassmidara Hoonsawat*

Assoc. Prof. Rassmidara Hoonsawat, Ph.D.

Dean

Faculty of Graduate Studies  
Mahidol University

*Ampol Mitrevej*

Prof. Ampol Mitrevej, Ph.D.

Dean

Faculty of Pharmacy  
Mahidol University

## ACKNOWLEDGEMENTS

I am sincerely indebted to my thesis advisor, Associate Professor Dr. Jiraporn Ungwitayatorn, for her kindness, helpful, valuable supervision, guidance and constructive criticism during my entire study.

My sincere and grateful appreciation are also expressed to Associate Professor Dr. Chanpen Wiwat, my co-advisor, for her guidance and correction in bioassay section.

I sincerely wish to thank Assistant Professor Dr. Onoomar Poobrasert, Department of Pharmaceutical Chemistry, Faculty of Pharmacy, Silpakorn University, for being a member of the defense committee.

A special acknowledgement extends to Department of Pharmaceutical Chemistry, Faculty of Pharmacy, Mahidol University, for providing research facilities and supporting the important information. As well, my special appreciation gives to my fellow graduate students at the Faculty of Pharmacy, Mahidol University, and other persons who have not been mentioned here for their help, friendship and encouragement.

Finally, I wish to express my gratitude and infinite thanks to my family for their love, concern, encouragement and precious spiritual support throughout my life.

Narumol Phosrithong

## SYNTHESIS AND EVALUATION OF NEW POTENT HIV-1 PROTEASE INHIBITORS

NARUMOL PHOSRITHONG 4537370 PYPE/M

M.Sc. in Pharm (PHARMACEUTICAL CHEMISTRY)

THESIS ADVISORS: JIRAPORN UNGWITAYATORN, Ph.D. CHANPEN WIWAT, Ph.D.

### ABSTRACT

A new series of chromone derivatives has been designed based on the previous 3D QSAR, CoMFA and CoMSIA studies. Ten derivatives of this series have been synthesized by one-pot cyclization reaction using DBU as a base. All compounds at concentration 12.5  $\mu\text{g/mL}$  were evaluated for their *in vitro* enzyme inhibitory activity by HPLC assay using recombinant HIV-1 protease enzyme expressed in *E.coli* and anthranilyl His-Lys-Ala-Arg-Val-Leu-(*p*-NO<sub>2</sub>-Phe)-Glu-Ala-Nle-Ser-NH<sub>2</sub> as substrate. The results showed that the inhibitory activity of the synthesized compounds were in the range of 35-88 % inhibition. The three most potent compounds, 7-hydroxy-2-(4'-*tert*-butylphenyl)-3-(4''*tert*-butylbenzoyl) chromone **1**, 6-hydroxy-2-(3'-methoxyphenyl)chromone **7**, and 6-hydroxy-2-(3'-trifluoromethylphenyl) chromone **10**, possessed IC<sub>50</sub> values of 6.89  $\mu\text{M}$ , 23.35  $\mu\text{M}$ , and 26.92  $\mu\text{M}$ , respectively.

The results from this study correspond to the previous 3D QSAR, comparative molecular field analysis (CoMFA) and comparative molecular similarity indices analysis (CoMSIA) studies that compounds in this chromone series with substituted phenyl and substituted benzoyl groups at position 2 and 3 of the benzopyran nucleus, respectively showed high potency. Moreover, both *meta* and *para* position of the phenyl and benzoyl rings should contain bulky substituents. The hydrogen bond donor substituent(s) should be presented in ring A of the benzopyran nucleus

KEY WORDS: HIV-1 PROTEASE / CHROMONE DERIVATIVES

99 P. ISBN 974-04-6357-6

การสังเคราะห์และประเมินประสิทธิผลของสารใหม่ที่มีฤทธิ์สูงในการยับยั้งเอนไซม์เอชไอวี-1 โปรตีเอส.  
(SYNTHESIS AND EVALUATION OF NEW POTENT HIV-1 PROTEASE INHIBITORS)

นฤมล โพธิ์ศรีทอง 4537370 PYPE / M

ภ.ม. (เภสัชเคมี)

คณะกรรมการควบคุมวิทยานิพนธ์ : จิรภรณ์ อังวิทยาธร, Ph.D., จันทร์เพ็ญ วิวัฒน์, Ph.D.

### บทคัดย่อ

การวิจัยนี้ได้ทำการออกแบบสารซึ่งเป็นอนุพันธ์โครโมนตัวใหม่จำนวน 10 อนุพันธ์ตามผลของการศึกษาหาความสัมพันธ์เชิงปริมาณระหว่างโครงสร้างทางเคมีและการออกฤทธิ์ของยาแบบ 3 มิติ ด้วยวิธี comparative molecular field analysis (CoMFA) และวิธี comparative molecular similarity indices analysis (CoMSIA) และทำการสังเคราะห์ด้วยวิธี one-pot cyclization โดยใช้ DBU เป็นเบส จากนั้นทดสอบฤทธิ์ในการยับยั้งเอนไซม์เอชไอวี-1 โปรตีเอสของอนุพันธ์โครโมนที่สังเคราะห์ได้ด้วยวิธี HPLC โดยใช้เอนไซม์ recombinant HIV-1 protease ซึ่ง expressed ในเชื้อ *E. coli* และใช้ anthranilyl His-Lys-Ala-Arg-Val-Leu-(*p*-NO<sub>2</sub>-Phe)-Glu-Ala-Nle-Ser-NH<sub>2</sub> เป็น substrate โดยใช้ความเข้มข้นของสาร 12.5 ไมโครกรัม/มิลลิลิตร พบว่าสารทั้ง 10 อนุพันธ์สามารถยับยั้งเอนไซม์ได้ในระหว่าง 35-88 % inhibition โดยสารที่สามารถยับยั้งเอนไซม์เอชไอวี-1 โปรตีเอสได้สูงที่สุด 3 อนุพันธ์ได้แก่ 7-hydroxy-2-(4'-*tert*-butylphenyl)-3-(4'-*tert*-butylbenzoyl) chromone **1**, 6-hydroxy-2-(3'-methoxyphenyl) chromone **7**, and 6-hydroxy-2-(3'-trifluoromethylphenyl) chromone **10** สารทั้ง 3 มีค่า IC<sub>50</sub> เท่ากับ 6.89 ไมโครโมลาร์, 23.35 ไมโครโมลาร์, และ 26.92 ไมโครโมลาร์ ตามลำดับ.

การวิจัยครั้งนี้ให้ผลสอดคล้องกับการศึกษาหาความสัมพันธ์เชิงปริมาณระหว่างโครงสร้างทางเคมีและการออกฤทธิ์ของยาแบบ 3 มิติ ด้วยวิธี comparative molecular field analysis (CoMFA) และวิธี comparative molecular similarity indices analysis (CoMSIA) กล่าวคือ อนุพันธ์ของโครโมน ที่ประกอบด้วยหมู่ phenyl และ benzoyl ที่ตำแหน่งที่ 2 และ 3 ของ benzopyran nucleus ตามลำดับ จะให้ผลการยับยั้งเอนไซม์เอชไอวี-1 โปรตีเอสที่สูง นอกจากนี้หมู่แทนที่ที่ตำแหน่ง *meta* และ *para* ของ phenyl และ benzoyl ring ควรเป็นหมู่แทนที่ที่มีขนาดใหญ่ สำหรับ ring A ของ benzopyran nucleus ควรมีหมู่ที่มีคุณสมบัติเป็น hydrogen bond donor.

99 หน้า ISBN 974-04-6357-6

## CONTENTS

	Page
ACKNOWLEDGEMENT	iii
ABSTRACT	iv
LIST OF TABLES	viii
LIST OF FIGURES	ix
LIST OF SCHEMES	xi
LIST OF ABBREVIATIONS	xii
CHAPTER	
I INTRODUCTION	1
II LITERATURE REVIEW	3
A. AIDS and molecular biology of HIV-1 virus	3
B. The development of HIV-1 agent	8
C. Antiretroviral agents	13
D. HIV-1 protease inhibitory activity test	28
III CHEMICAL EXPERIMENTAL	30
A. Equipment and chemicals	30
B. Methods	31
1. 7-Hydroxy-2-(4'- <i>tert</i> -butylphenyl)-3-(4"- <i>tert</i> -butyl - benzoyl) chromone <b>1</b>	33
2. 7-Hydroxy-2-(3'-chlorophenyl)-3-(3"-chlorobenzoyl) chromone <b>2</b>	35
3. 7,8-Dihydroxy-2-(3'-chlorophenyl)-3-(3"-chlorobenzoyl) chromone <b>3</b>	36
4. 7,8-Dihydroxy-2-(4'-methoxyphenyl)-3-(4"- methoxybenzoyl) chromone <b>4</b>	37

## CONTENTS (Cont.)

	Page
5. 7,8-Dihydroxy-2-(3'-methoxyphenyl)-3-(3''-methoxy benzoyl) chromone <b>5</b>	38
6. 5,7-Dihydroxy-2-(3'-methoxyphenyl) 3-(3''-methoxy benzoyl) chromone <b>6</b>	39
7. 6-Hydroxy-2-(3'-methoxyphenyl)chromone <b>7</b>	40
8. 6-Hydroxy-2-(3'-chlorophenyl) chromone <b>8</b>	41
9. 6-Hydroxy-2-(4'-fluorophenyl) chromone <b>9</b>	42
10. 6-Hydroxy-2-(3'-trifluoromethylphenyl) chromone <b>10</b>	43
<b>IV. BIOLOGICAL EXPERIMENTAL</b>	44
A. Equipment and reagents	44
B. Methods	45
HPLC assay	45
<b>V RESULTS AND DISCUSSION</b>	48
A. General discussion	48
B. Synthesis of chromone derivatives by one-pot cyclization reaction	50
C. HIV-1 protease inhibitory activity testing	63
<b>VI CONCLUSION</b>	72
<b>REFERENCES</b>	74
<b>APPENDIX</b>	87
<b>BIOGRAPHY</b>	99

## LIST OF TABLES

Table		Page
1	Approved anti HIV-1 drugs	14
2	Composition of the HPLC assay mixture	46
3	Structures of the previously synthesized chromone derivatives	49
4	Structures of chromone derivatives synthesized in this study	50
5	Melting point (m.p.) and % yield of chromone derivatives	54
7	The inhibitory activity of the synthesized chromone compounds	65
8	IC <sub>50</sub> determination of 7-hydroxy-2-(4'- <i>tert</i> -butylphenyl)-3-(4''- <i>tert</i> -butyl-benzoyl) chromone <b>1</b>	66
9	IC <sub>50</sub> determination of 6-hydroxy-2-(3'-methoxyphenyl) chromone <b>7</b>	67
10	IC <sub>50</sub> determination of 6-hydroxy-2-(3'-trifluoromethylphenyl) chromone <b>10</b>	68
11	The IC <sub>50</sub> values of compounds <b>1</b> , <b>7</b> , <b>10</b> and clinically approved HIV-1 PIs	69

## LIST OF FIGURES

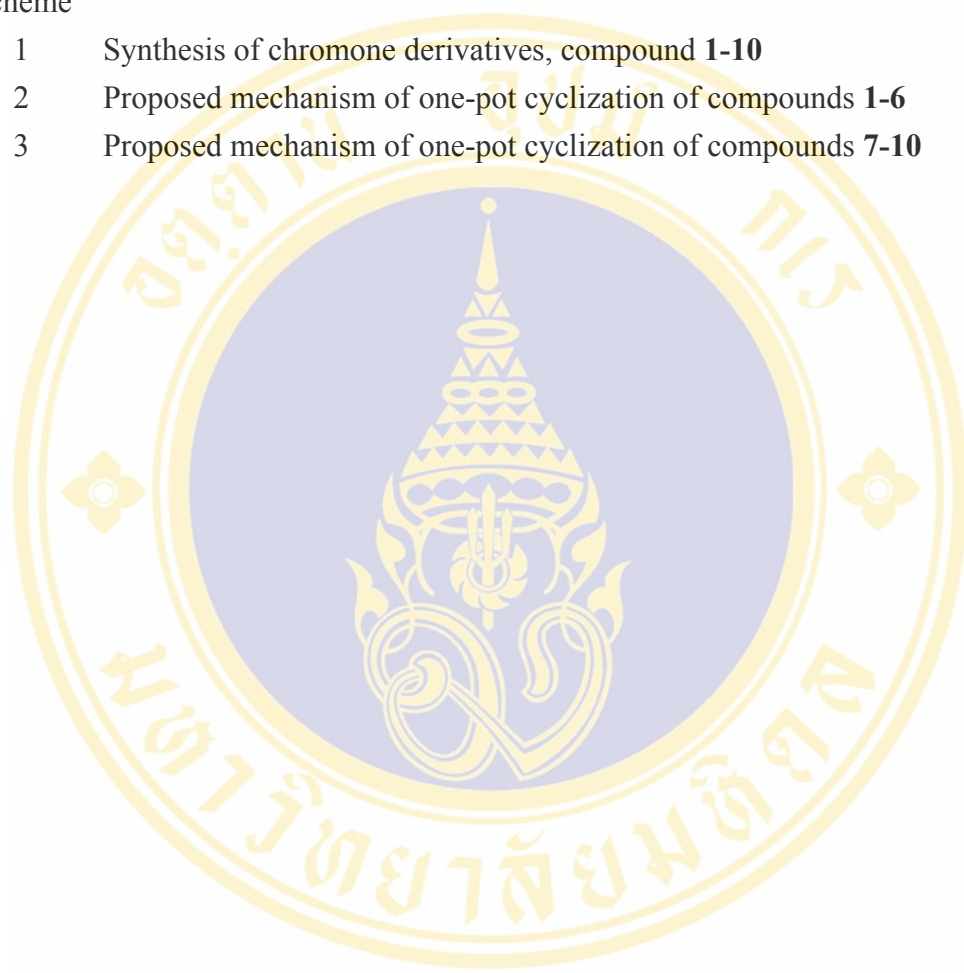
Figure		Page
1	The natural history of HIV infection	4
2	Number of people living with HIV/AIDS–total: 39.4 million (Dec. 2004).	4
3	The viral genome of HIV-1	6
4	Schematic drawing of the HIV-1 virion	6
5	Schematic drawing of the HIV-1 replication cycle	7
6	Structure of the HIV-1 reverse transcriptase and the location of the NRTI and NNRTI binding sites	9
7	Structure of the HIV-1 protease binding site	11
8	Standard nomenclature for substrate residues and their corresponding binding sites	11
9	Schematic representation of the HIV-1 protease cleavage mechanism	12
10	Hydrogen-bonding interactions between a cyclic peptidomimetic inhibitor and HIV-1 protease	13
11	Structures of US FDA approved NRTIs	16
12	Structures of US FDA approved NNRTIs	18
13	Structures of clinically approved anti HIV-1 protease drugs	21
14	Design concept of indinavir	23
15	Structure of enfuvirtide	27
16	Chromatograms of HIV-1 PR inhibitory activity assay	47
17	IR spectrum of 7-hydroxy-2-(4'- <i>tert</i> -butylphenyl)-3-(4''- <i>tert</i> -butylbenzoyl) chromone <b>1</b>	55
18	<sup>1</sup> H NMR spectrum (300 MHz, DMSO) of 7-hydroxy-2-(4'- <i>tert</i> -butylphenyl)-3-(4''- <i>tert</i> -butylbenzoyl) chromone <b>1</b>	57
19	EI mass spectra of 7-hydroxy-2-(4'- <i>tert</i> -butylphenyl)-3-(4''- <i>tert</i> -butylbenzoyl) chromone <b>1</b>	58

**LIST OF FIGURES (Cont.)**

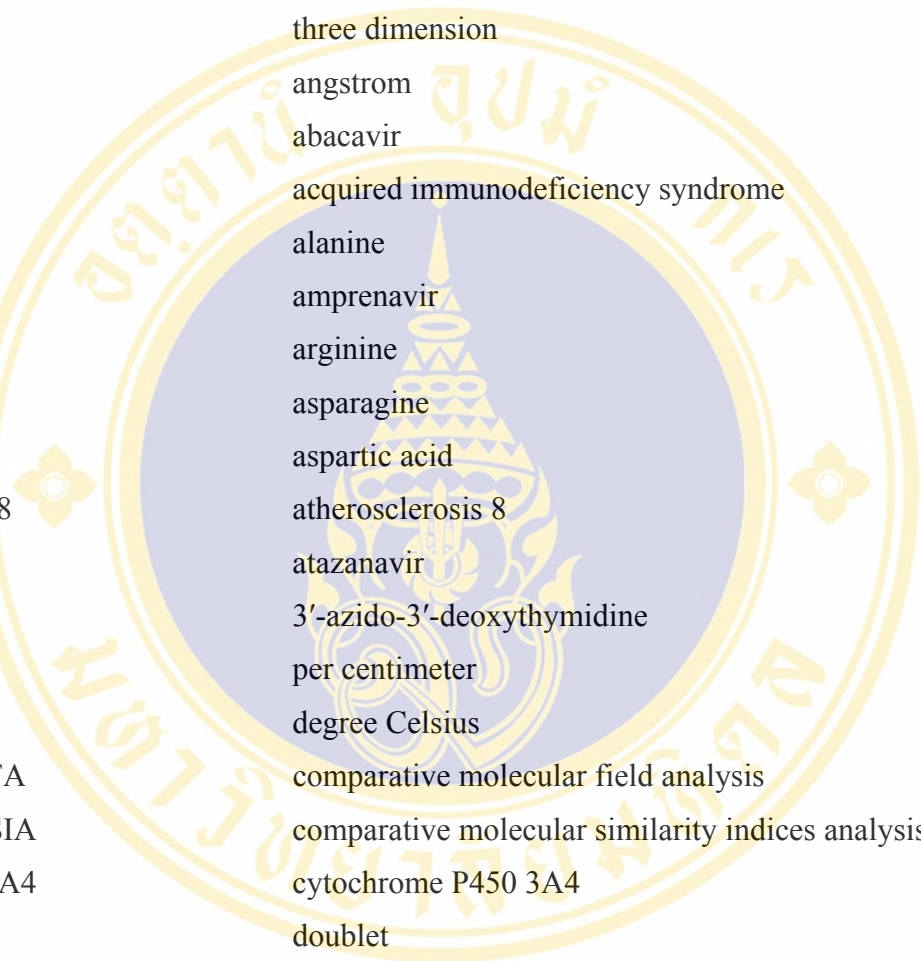
Figure		Page
20	Proposed fragmentation mechanism of 7-hydroxy-2-(4'- <i>tert</i> -butylphenyl)-3-(4''- <i>tert</i> -butylbenzoyl) chromone <b>1</b>	59
21	IR spectrum of 6-hydroxy-2-(4'-fluorophenyl) chromone <b>9</b>	60
22	<sup>1</sup> H NMR spectrum (300 MHz, DMSO) of 6-hydroxy-2-(4'-fluorophenyl) chromone <b>9</b>	61
23	EI mass spectra of 6-hydroxy-2-(4'-fluorophenyl) chromone <b>9</b>	62
24	Proposed fragmentation mechanism of compound <b>9</b>	62
25	HPLC profile of a reaction mixture of HIV-1 PR and substrate incubated for 2 hours at 37 °C	64
26	The % inhibition vs. log concentration profile of compound <b>1</b>	66
27	The % inhibition vs. log concentration profile of compound <b>7</b>	67
28	The % inhibition vs. log concentration profile of compound <b>10</b>	68
29	CoMSIA contour maps	71

## LIST OF SCHEMES

Scheme		Page
1	Synthesis of chromone derivatives, compound <b>1-10</b>	51
2	Proposed mechanism of one-pot cyclization of compounds <b>1-6</b>	52
3	Proposed mechanism of one-pot cyclization of compounds <b>7-10</b>	53



## LIST OF ABBREVIATIONS



3D	three dimension
Å	angstrom
ABC	abacavir
AIDS	acquired immunodeficiency syndrome
Ala	alanine
APV	amprenavir
Arg	arginine
Asn	asparagine
Asp	aspartic acid
ATH-8	atherosclerosis 8
ATZ	atazanavir
AZT	3'-azido-3'-deoxythymidine
cm <sup>-1</sup>	per centimeter
°C	degree Celsius
CoMFA	comparative molecular field analysis
CoMSIA	comparative molecular similarity indices analysis
CYP3A4	cytochrome P450 3A4
d	doublet
Da	dalton
$\delta$	chemical shift
DBU	1,8-diazabicyclo [5,4,0] undec-7-ene
ddC	2',3'-dideoxycytidine
ddI	2',3'-dideoxyinosine
DLV	delavirdine
DMSO	dimethyl sulfoxide
DNA	deoxyribonucleic acid
d4T	2',3'-dihydro-2',3'-dideoxythymidine
DTT	dithiothreitol

## LIST OF ABBREVIATIONS (Cont.)

EFV	efavirenz
<i>env</i>	envelope glycoprotein
et al	and others
ETC	emtricitabine
FTIR	Fourier transform infrared spectroscopy
g	gram
<i>gag</i>	group-specific antigen
Gly	glycine
gp	glycoprotein
His	histidine
HIV-1	human immunodeficiency virus type-1
<sup>1</sup> H NMR	proton nuclear magnetic resonance
Hz	hertz
IC <sub>50</sub>	50% inhibitory concentration
Ile	isoleucine
IN	integrase
IND	indinavir
% IR	percentage of inhibitory ratio
<i>J</i>	coupling constant
K <sub>i</sub>	inhibitory constant
L	liter
LTR	long terminal repeat
$\lambda$	wave length
Leu	leucine
Lys	lysine
m	multiplet
Met	methionine
mg	miligram
MHC	major histocompatibility complex

## LIST OF ABBREVIATIONS (Cont.)

<i>MHz</i>	<i>megahertz</i>
mL	milliliter
mM	millimolar
mmol	millimole
m.o.i.	multiplicity of infection
m.p.	melting point
mRNA	messenger ribonucleic acid
MS	mass spectrometry
MT-4	metallothionein IV
MW	molecular weight
<i>nef</i>	negative factor
NFV	nelfinavir
Nle	norleucine
nM	nanomolar
nm	nanometer
NNRTIs	non-nucleoside reverse transcriptase inhibitor
NRTIs	nucleoside reverse transcriptase inhibitors
NVP	nevirapine
PBMC	peripheral blood mononuclear cell
Phe	phenylalanine
PIs	protease inhibitors
<i>pol</i>	polymerase enzyme activity
PR	protease
Pro	proline
QSAR	quantitative structure-activity relationship
$r^2$	square correlation coefficient
<i>rev</i>	regulatory of expression of virion protein
$R_f$	retardation factor
RNA	ribonucleic acid

## LIST OF ABBREVIATIONS (Cont.)

RNase H	ribonuclease H
RT	reverse transcriptase
RTV	ritonavir
s	singlet
SAR	structure activity relationship
Ser	serine
st	stretching
t	triplet
TAR	transactivation response
<i>tat</i>	transactivator of transcription
<i>t</i> -butyl	tertiary butyl
3TC	2',3'-dideoxy-3'-thiacytidine
TDF	tenofovir
TFA	trifluoroacetic acid
Thr	threonine
TLC	thin layer chromatography
Trp	tryptophan
Tyr	tyrosine
Val	valine
<i>vif</i>	viral infectivity factor
<i>vpr</i>	viral protein R
<i>vpu</i>	viral protein U
vs.	versus
$\mu\text{g}$	microgram
$\mu\text{L}$	microlitre
$\mu\text{M}$	micromolar

## CHAPTER I

### INTRODUCTION

Human immunodeficiency virus (HIV) is the causative agent of acquired immune deficiency syndrome (AIDS). The rapid spread of the disease has stimulated discovery of therapeutic agent to arrest the replication of the virus. Characterization of the HIV life cycle has highlighted many different targets for potential drug intervention. These include inhibition of virus adsorption, viral fusion, viral uncoating and inhibition of the viral replicative enzymes such as reverse transcriptase (RT), integrase (IN) and HIV protease (PR). One promising possibility to interrupt the viral life cycle is the use of inhibitors of the virally encoded protease which is indispensable for viral maturation (1-4).

HIV-1 PR is a virally encoded enzyme involved in posttranslational processing of the *gag* and *gag-pol* gene products into the functional core proteins and other essential replicative viral enzymes. It is an essential component of the replicative cycle since inhibition of HIV-1 PR leads to production of immature noninfectious viral progeny and hence prevention of further propagation of the virus (5). A large number of inhibitors have been designed, synthesized, and assayed. Seven HIV-1 protease inhibitors now utilized in the treatment of AIDS, i.e., saquinavir, indinavir, ritonavir, nelfinavir, amprenavir, atazanavir and fosamprenavir, have been approved by the US FDA and are being used in combination with RT inhibitors (6-13).

Although the peptide-derived inhibitors are potent HIV-1 PR inhibitors, they are typically not suitable drug candidate. The early problems of peptidic protease inhibitors, i.e., poor oral bioavailability and severe side effects caused by the necessarily high doses of the inhibitors, have strengthened the development of non-peptidic protease inhibitors that promised better bioavailability and/or pharmacokinetic properties (14-20).

The previous three-dimensional quantitative structure-activity relationship (3D QSAR) approach, comparative molecular field analysis (CoMFA) and comparative molecular similarity indices analysis (CoMSIA) studies of a new series of HIV-1 PR

inhibitors, chromone derivatives, suggested that the bulkiness substituents of benzoyl ring at position 3 and the phenyl ring at position 2 of the chromone nucleus would prefer to interact with the hydrophobic S1 subsite of the enzyme. Substituents at least at position 7 and 8 of a chromone nucleus should be OH or other hydrogen bond donor group to interact with Asp25 and Asp25' (21). Introduction of electron donating group to position 4' of phenyl ring and 4'' of benzoyl ring resulted in lower % inhibition comparing to the others containing electron withdrawing group. The compound containing 7,8-dihydroxyl derivatives exhibited higher % inhibition comparing to the rest in this series (22).

The aim of this study is to synthesize more compounds in the chromone series with modifying substituents of the chromone structure based on the previous CoMFA, and CoMSIA studies and evaluate for their *in vitro* HIV-1 PR inhibitory activity by HPLC assay (23). All compounds were synthesized using one-pot cyclization reaction with DBU as a base (24). Their structures were characterized by <sup>1</sup>H NMR, mass spectrometry, infrared spectrophotometry and elemental analysis.

## CHAPTER II

### LITERATURE REVIEW

#### A. AIDS and molecular biology of HIV-1 virus

##### 1. Acquired immunodeficiency syndrome (AIDS)

Acquired immunodeficiency syndromes (AIDS) was first major epidemic caused by a previously unknown pathogen to appear during the 20<sup>th</sup> century. The etiologically agents of AIDS was later determined to be human immunodeficiency virus (HIV), a member of the lentivirus subfamily of retrovirus (25). HIV is subdivided into two distantly related types, HIV-1 and HIV-2. HIV-1 is more prevalent and more pathogenic than HIV-2. HIV-1 is responsible for infections globally, whereas HIV-2 is found predominantly in countries of West Africa. More than 95 % of HIV infected people live in the developing world (26).

The consequence after infection is a severe immunosuppression resulting from destruction of CD4 positive T-helper lymphocytes and macrophage. HIV can remain latent or chronically expressed at a low level for extended periods (averages about 10 years from initial infection to clinical disease). Follow this prolonged disease-free period, the CD4 cell-count decreases to a level at which the immune system is no longer effective against opportunistic pathogens, resulting in the emergence of multiple infections, tumors, and ultimately, death (26).

The course of the HIV infection is reflected by the concentration of the CD4 positive T-helper lymphocytes in the blood (Figure 1). Normally the concentration is 800-1200 cells/mm<sup>3</sup> but in the final phase of the disease the number is less than 200 cells/mm<sup>3</sup> of blood (27).

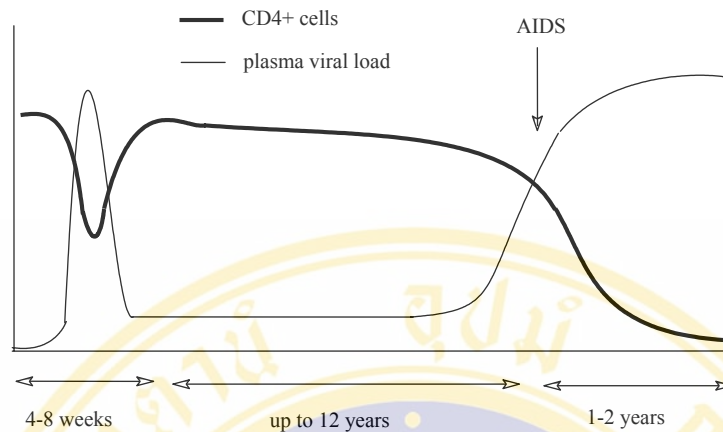


**Figure 1.** The natural history of HIV infection (28).

During the past two decades, the epidemic of HIV infection and AIDS has spread worldwide (29). It is the third largest cause of death as a result of infectious disease after heart disease and cancer, respectively (30). The total number of people living with HIV rose in 2004 to reach its highest level. At the end of 2004 the World Health Organization (WHO) estimated that 35.9-44.3 million people globally were living with HIV (Figure 2) and approximately 4.9 million people who acquired HIV in 2004 (31).

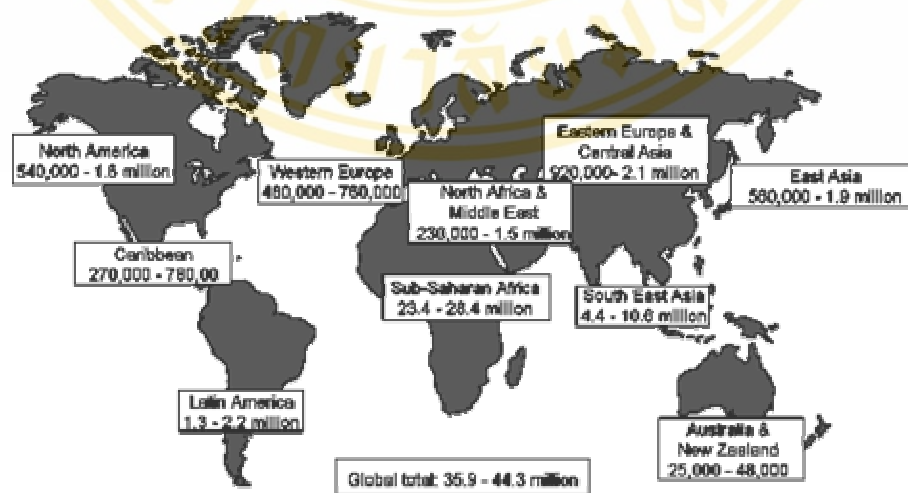


**Figure 2.** Number of people living with HIV/AIDS—total: 39.4 million (Dec.2004) (31).

## 2. The viral genome

The genomic complexity and heterogeneity of HIV underlie its pathogenicity. The 9 kilobase single-stranded HIV RNA genome consists of ten open reading frames encoding structural genes, i.e., *gag*, *env*, *pol*, regulatory genes i.e., *tat*, *rev*, and accessory genes i.e., *nef*, *vif*, *vpr*, and *vpu* (Figure 3) (32). The structural genes are essential for retroviral replication. The *gag* gene encodes the precursor for virion capsid proteins. The *env* gene encodes the two major envelope glycoproteins, gp120 and gp 41. These glycoproteins become embedded all over the host cell membrane and this membrane ultimately becomes the viral envelope as the virus "buds" out of cell as it completes its maturation process (33). The *pol* gene encodes the viral enzymes protease, reverse transcriptase, and integrase. These enzymes are produced as a *gag-pol* precursor polyprotein, which is processed by viral protease. The regulatory genes are required for control of the viral replication cycle. The *tat* acts as a potent transcriptional activator by binding to the transactivation response (TAR) element of the HIV long terminal repeat (LTR) to mediate viral gene expression. The *tat* gene produces proteins which turn on other HIV genes, greatly increasing the activity of the virus. Without *tat*, HIV is largely or totally inactive (34, 35). The major role of *rev* is to regulate the expression of HIV proteins by controlling the export rate of mRNAs (36). The accessory genes products perform important functions related to virion maturation, release and infectivity. The *nef* interacts with host cell signal transduction proteins, down regulates expression of cell-surface proteins (CD4 and MHC Class I), and can induce apoptosis in non-infected cells. The *vif* promotes virion maturation and infectivity. The *vpr* is involved in targeting the nuclear localization of preintegration complexes, arrests infected cells at G2 phase of cell cycle, and inhibits cell division (37). The *vpu* acts in the degradation of CD4 in the endoplasmic reticulum and the enhancement of virion release from the plasma membrane (38).

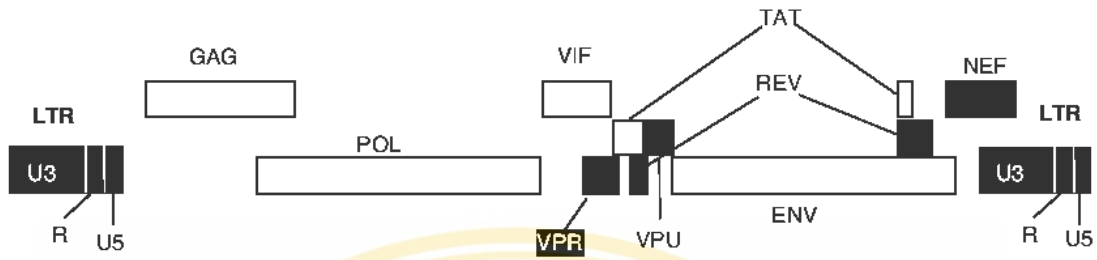


**Figure 3.** The viral genome of HIV-1 (39).

### 3. HIV-1 virion

The mature HIV-1 virion is a roughly spherical particle with a diameter of approximately 110 nm. The outer surface of the virus is enveloped by a lipid bilayer that is derived from the membrane of the host cell. The envelope is acquired during virion budding and is studded with approximately 72 spikes formed by the two major viral envelope glycoprotein, gp 120 and gp 41. The gp 120 are anchored to the virus via interactions with the transmembrane protein (gp 41). A shell of matrix (p 17) lines the inner surface of the viral membrane and a conical capsid core particle comprising of the capsid protein (p 24) is located in the center of the virus. The capsid particle encapsidates two copies of the unspliced viral genome, stabilized by nucleocapsid protein (p7) and also contains three essential viral enzymes: reverse transcriptase (p64), integrase (p32), and protease (p10) (40). Major histocompatibility complex (MHC) is protein complex on surface of cells. MHC presents antigens to CD4. The schematic drawing of the HIV-1 virion is shown in Figure 4.

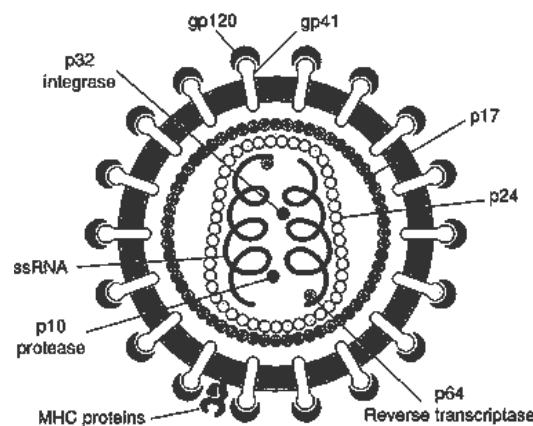


**Figure 4.** Schematic drawing of the HIV-1 virion (41).

#### 4. The replication cycle of HIV-1

HIV infection begins with the interaction of the HIV glycoprotein (gp) 120 with the CD4 receptor on the surface of the target cell (Figure 5). Following CD4 binding, a center material change in the HIV gp 120/gp 41 complex is induced by interaction of gp 120 with the chemokine receptors CCR5 or CXCR4. This change in conformation exposes gp 41 and allowing it to initiate fusion of the membranes (42). After the fusion of membranes, the nucleocapsid enters the cytoplasm. The viral RNA, still enclosed in the viral capsid, is uncoated in a process aided by capsid proteins (p24) and cellular protein called cyclophilins (43). After uncoating process, reverse transcription of the viral RNA generates a double-stranded DNA copy (cDNA) of the genome (44). The newly formed HIV DNA enters the host cell nucleus and integrates into the host cell genome via the action of the viral integrase leading to the formation of a provirus. The provirus may remain inactive for several years, producing few or no new copies of HIV. When the host cell receives a signal to become active, the provirus uses a host enzyme called RNA polymerase to create copies of the HIV genomic material, as well as shorter strands of RNA called messenger RNA (mRNA). The mRNA is used as a blueprint to make long chains of HIV proteins. The HIV life cycle final event is the maturation of cell-free particles upon action of HIV-1 protease (HIV-1 PR) (45). HIV-1 PR cleaves the polyproteins into functional enzymes and structural proteins. These matured viruses, if assembled correctly, are then capable of productive function when they encounter appropriate target cells and start the new replication cycles.

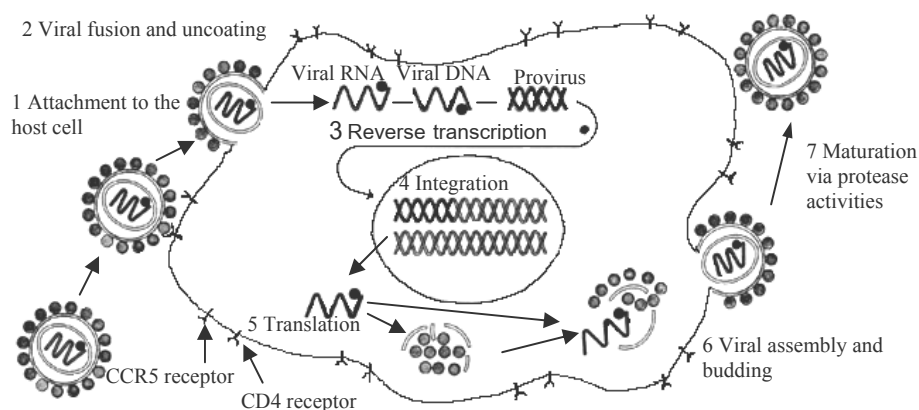


**Figure 5.** Schematic drawing of the HIV-1 replication cycle (46).

## **B. The development of anti HIV-1 agents**

The current treatment for HIV/AIDS involves utilizing combination of a number of drugs. Although this therapy can suppress viral loads to below detectable levels, suppression has been observed to be reversible, especially once drug therapy is stopped (47). In addition, issues of patient adherence, drug toxicity, the emergence of multidrug-resistant phenotypes, and the presence of persistent reservoirs of virus replication have highlighted the need to develop alternative therapeutic approaches utilizing other targets essential in the viral replication cycle.

Many steps in the HIV life cycle can be considered as a potential target for antiviral chemotherapy. The key in selective antiviral therapy is therefore to identify any process that is essential for the replication of the virus, but not for the survival of the cell (48). The gained knowledge about the replication cycle of the HIV virus has led to the extraction of virus-specific processes. Predominantly, scientists have focused their attentions on the following processes: 1) viral binding to target cells, 2) virus cell fusion, 3) virus uncoating, 4) reverse transcription of viral genomic RNA, 5) viral integration, 6) gene expression, and 7) protease activity. So far, the two strategies 4 and 7 have been proven to be the most successful in the search for drugs that can be used for treatment of AIDS (49, 50). These two targets will be described briefly in the following sections.

### **1. HIV-1 reverse transcriptase**

Reverse transcriptase (RT) is essential for the life cycle of HIV because it converts the single stranded genomic RNA into the double stranded DNA version which is subsequently integrated into the host chromosome and passed on to all progeny cells (51). The HIV-1 RT molecule is a heterodimer consisting of a 560 residue chain (call p66) and a second chain comprising the initial 440 residues of p66 (call p51). Crystal structures of HIV RT reveal that the p66 subunit folds into five domains named finger, palm, thumb, connection, and RNase H and that the p51 subunit comprises the first four domain of p66 (Figure 6) (52). Whilst the equivalent domains from each subunit have a broadly similar fold, especially the finger and thumb domains, their relative arrangement in the two subunits is radically different (52, 53). The p66/p51 HIV-1 RT heterodimer contains one DNA polymerization

active site and one RNase H active site, both of which reside in the p66 subunit at spatially distinct regions. Although the p51 subunit contains the same amino acid sequence that comprises the DNA polymerase domain of the p66 subunit, the polymerase active site in p51 is not functional (54).

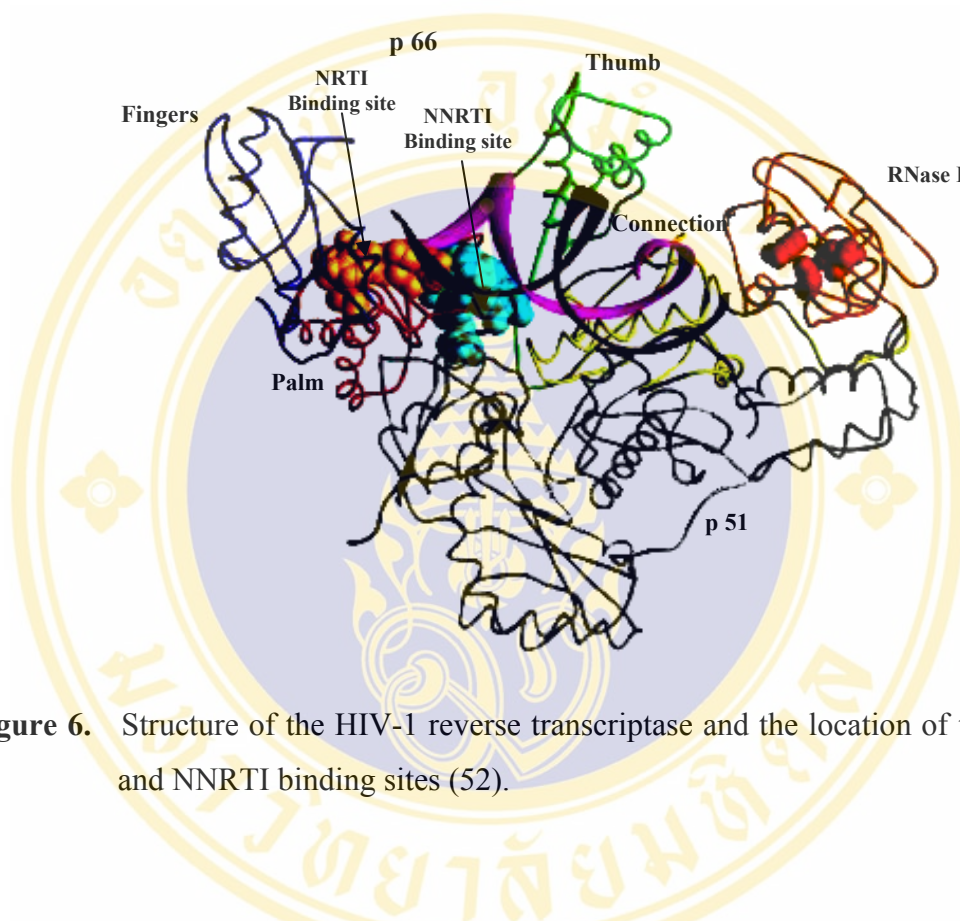


**Figure 6.** Structure of the HIV-1 reverse transcriptase and the location of the NRTI and NNRTI binding sites (52).

Because of its pivotal role in the HIV life cycle, HIV RT is a primary target for antiretroviral agents. Two major classes of inhibitors that inhibit the polymerase activities of HIV-1 RT have been identified, nucleoside/nucleotide reverse transcriptase inhibitors (NRTIs), and non-nucleoside reverse transcriptase inhibitors (NNRTIs). NRTI binds at the polymerase active site. The polymerase active site, as defined by the three aspartic acid residues Asp 110, Asp 185 and Asp 186 resides in the palm subdomain (54). NRTI mimics normal active site substrates of HIV-1 RT but lack the 3'-OH group required for DNA chain elongation, which causes premature termination of the growing viral DNA strand (55, 56). NNRTI binds to a hydrophobic pocket on HIV-1 RT ca. 10-15 Å from the NRTI site (polymerase active site) and is primarily consisted of Leu100, Lys101, Lys103, Val106, Thr107, Val108, Val179,

Tyr181, Tyr188, Val189, Gly190, Phe227, Trp229, Leu234, and Tyr318 in p66 (57). The putative entrance of the pocket is proposed to be located at the interface of the p66/p51 heterodimer and is primarily formed by Pro95, Leu100, Lys101, Lys103, Val179, and Tyr181 of p66 (57, 58). The side chains of several residues, especially those of Tyr181 and Tyr188, assume significant conformational changes on the binding of NNRTIs. This binding event alters the conformation of active site residues hampering normal enzymatic activity (Figure 6) (56, 59).

## 2. HIV-1 protease

HIV-1 protease (HIV-1 PR) is a symmetrical homodimer enzyme. It belongs to the family of aspartic proteases, which have two aspartic acid residues at the active site (60). This was confirmed through pepstatin A inhibition, an aspartic protease selective inhibitor, and by site-directed mutagenesis of the active site Asp25, which led to abolition of the catalytic activity (61). The aspartic proteases are well-characterized group of enzymes that can be found in vertebrates, plants, in addition to in fungi. Examples of the aspartic proteases are pepsin, cathepsin D, renin, chymosin, penicillopepsin, plasmepsins and *Rhizopus* pepsin (62, 63). General feature of HIV-1 PR structure is illustrated in Figure 7. Its *C*<sub>2</sub> symmetric homodimeric structure is consisting of two identical 99-amino acid chains (64). The active site, with the two catalytic aspartate residues Asp25 and Asp25', is located at the interface between the two monomers. Two  $\beta$ -hairpin structures, called 'flaps', are positioned over the active site. They undergo structural changes on binding of the inhibitor molecule. In the unliganded protease structure, the conformation of the flaps is open, thereby exposing the active site, whereas in the ligand complex, the flaps form a roof over the active site and the ligand. The flaps cover to a large extent of the bound ligand. This arrangement is advantageous for the design of inhibitors, because it offers a large number of tight interactions between the enzyme and the inhibitor (64, 65). The PR dimer forms a series of subsites, i.e., S<sub>3</sub>, S<sub>2</sub>, S<sub>1</sub>, S<sub>1</sub>', S<sub>2</sub>', and S<sub>3</sub>' which correspond to the binding sites of P<sub>3</sub>, P<sub>2</sub>, P<sub>1</sub>, P<sub>1</sub>', P<sub>2</sub>', and P<sub>3</sub>' residues of substrate, where the scissile bond is located between the P<sub>1</sub> and P<sub>1</sub>' positions (Figure 8) (66, 67).

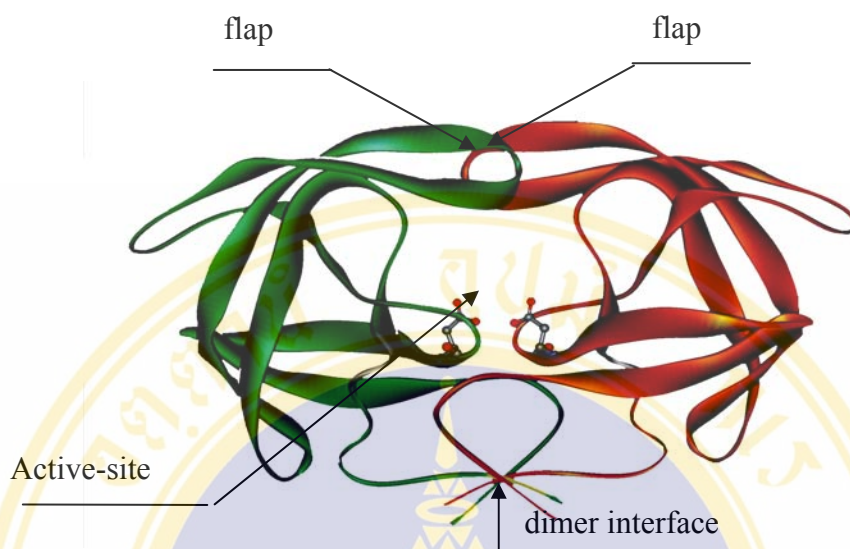


**Figure 7.** Structure of the HIV-1 protease binding site (68).

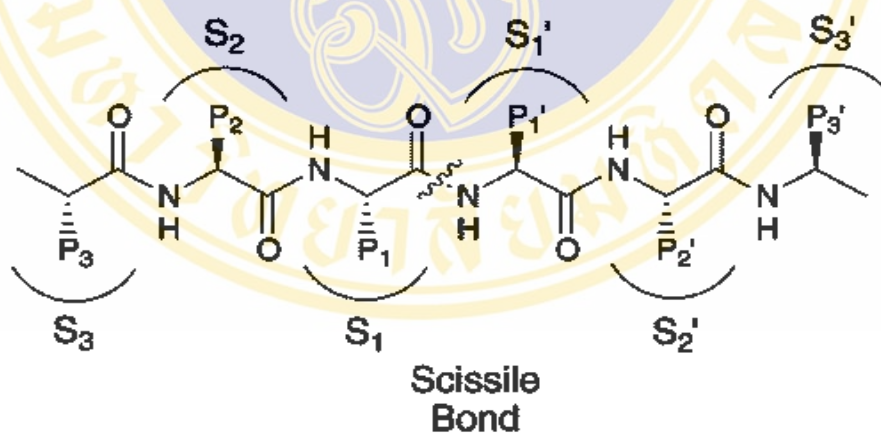


**Figure 8.** Standard nomenclature for substrate residues and their corresponding binding sites (66).

HIV-1 PR catalyzes the hydrolysis of specific peptide bonds within the HIV-1 *gag* and *gag-pol* polyproteins to generate the various structural and functional proteins essential for viral replication (69). It cleaves the p55 *gag* precursor into the four structural proteins, forming the core of the virion, p17, p24, p8 and p7. It also processes the p160 *gag/pol* precursor to liberate the structural elements just mentioned, and enzymes of the virus, i.e., the protease itself, the reverse transcriptase, and the endonuclease or integrase. Catalytic mechanism for substrate hydrolysis by aspartic protease is shown in Figure 9 (62). The scissile amide bond undergoes nucleophilic attack by a water molecule which is itself partially activated by a deprotonated catalytic aspartic acid residue. The protonated aspartic acid donates a proton to the amide bond nitrogen, generating a zwitterionic intermediate which collapses to the cleaved products. The water molecule that binds between the enzyme (Ile50 and Ile50') and inhibitor is thought to position a peptide substrate, stretching the peptide bond out of planarity toward a tetrahedral transition state which is stabilized by a second water molecule (Figure 10) (62).

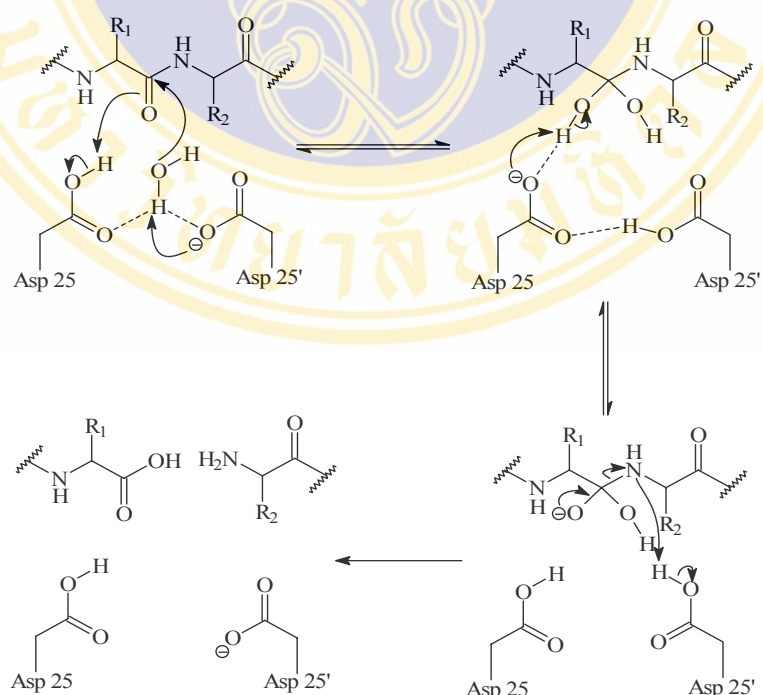


**Figure 9.** Schematic representation of the HIV-1 protease cleavage mechanism (62).

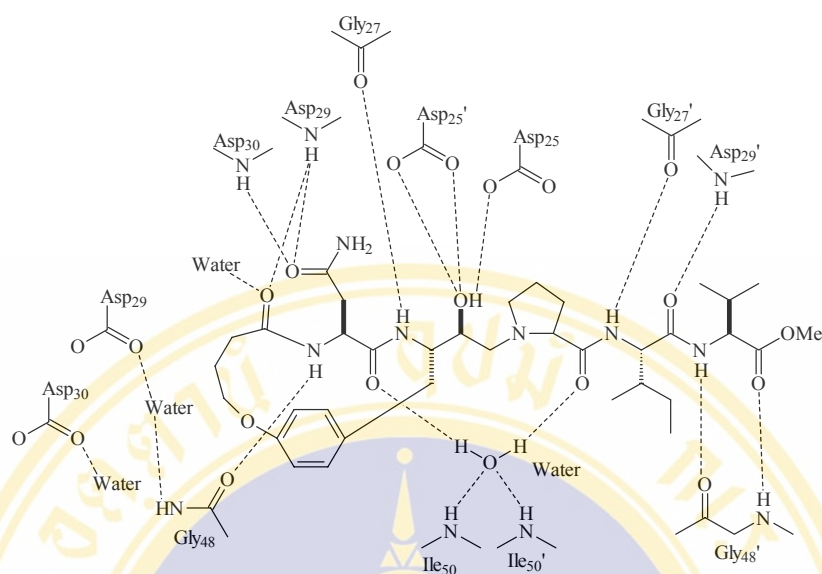


**Figure 10.** Hydrogen-bonding interactions between a cyclic peptidomimetic inhibitor and HIV-1 protease (62).

### C. Antiretroviral agents

Currently, there are 20 antiretroviral drugs in 3 mechanistic classes were already approved for the treatment of HIV infection, i.e., HIV-1 RT inhibitors, HIV-1 PR inhibitors and HIV entry inhibitors (Table 1).

#### 1. Nucleoside reverse transcriptase inhibitors (NRTIs)

NRTIs acting as alternative substrates or “false building blocks”, they compete with physiological nucleotides, differing from these only by a minor modification in the sugar (ribose) molecule. The incorporation of nucleoside s aborts DNA synthesis, as phosphodiester bridges can no longer be built to stabilize the double strand. NRTIs are converted to the active metabolite only after endocytosis, whereby they are phosphorylated to the active triphosphate derivatives. NRTIs are important components of almost all AIDS combination regimens. Although they are potent inhibitors of HIV replication, and are rapidly absorbed when taken orally, they can cause a wide spectrum of side effects (70). The currently available NRTIs are zidovudine (AZT), didanosine (ddI), zalcitabine (ddC), stavudine (d4T), lamivudine (3TC), abacavir (ABC), tenofovir, and emtricitabine (ETC), structures as shown in Figure 11.

**Table 1.** Approved anti HIV-1 drugs.

Class	Generic name	Trade name	Company	Approval
NRTIs	Zidovudine (AZT)	Ritovir	GlaxoSmithkline	1987
	Didanosine (ddI)	Videx	Bristol Mayers Squibb	1991
	Zalcitabine (ddC)	Hivid	Hoffman-LaRoche	1992
	Stavudine (d4T)	Zerit	Bristol Mayers Squibb	1994
	Lamivudine (3TC)	Epivir	GlaxoSmithkline	1995
	Abacavir (ABC)	Ziagen	GlaxoSmithkline	1998
	Tenofovir (TDF)	Viread	Gilead Science	2001
	Emtricitabine (ETC)	Emtriva	Gilead Science	2003
	NNRTIs	Nevirapine (NVP)	Viramune	Boeringer-Ingelheim
Delavirdine (DLV)		Rescriptor	Pharmacia & Upjohn	1997
Efavirenz (EFV)		Sustiva	DuPont Merck	1998
PIs	Saquinavir (SQV)	Invirase	Hoffman-LaRoche	1995
	Ritonavir (RTV)	Norvir	Abbott Laboratories	1996
	Indinavir (IND)	Crixivan	Merck & Co.	1996
	Nelfinavir (NFV)	Viracept	Pfizer	1997
	Amprenavir (APV)	Agenerase	GlaxoSmithkline	1999
	Lopinavir/ritronavir	Kaletra	Abbott Laboratories	2000
	Atazanavir (ATZ)	Reyataz	Bristol Mayers Squibb	2003
	Fosamprenavir	Lexiva	GlaxoSmithKline	2003
	Fusion inhibitor	Enfuvirtide (T-20)	Fuzeon	Hoffman-LaRoche

3'-Azido-3'-deoxythymidine (AZT, Zidovudine, Retrovir<sup>®</sup>) was the first antiretroviral agent to be put on the market in 1987 (70). Early therapeutic interventions in asymptomatic individuals showed an initial clinical benefit but was not appear to be maintained for a prolonged period. The anti-HIV-1 activity of AZT stimulated the evaluation of a wide variety of nucleoside derivatives. AZT can cause severe side effect such as bone marrow suppression (71). AZT showed an IC<sub>50</sub> value of 0.002  $\mu$ M in MT-4 cells infected at a multiplicity of infection (m.o.i.) of 0.01 (72).

2',3'-Dideoxyinosine (ddI, Didanosine, Videx<sup>®</sup>) is a nucleoside analog that has been well investigated and shown good efficacy in numerous randomized studies(70). Didanosine was approved by the US FDA for the treatment of patients in whom AZT treatment had failed or who had become intolerant to AZT. The most serious side effect of didanosine is pancreatitis (73). Didanosine showed an *in vitro* IC<sub>50</sub> range from 2.5-10  $\mu$ M in lymphoblastic cell lines and 0.01-0.1  $\mu$ M in monocyte/macrophage cell cultures (74).

2',3'-Dideoxycytidine (ddC, zalcitabine, Hivid<sup>®</sup>) is an analog of the nucleoside deoxycytidine. In 1993, ddC was approved for used in combination with AZT for HIV infection. The side effect of ddC is peripheral neuropathy whose symptoms involve tingling, burning, pain or numbness in the hands or feet (75). In laboratory and clinical isolates, the IC<sub>50</sub> value of 30  $\mu$ M in ATH8 cell infected with HIV-1(IIIB) strain (76).

2',3'-Didehydro-3'-deoxythymidine (d4T, stavudine, Zerit<sup>®</sup>) was the second thymidine analog introduced after AZT. Stavudine is one of the more effective nucleoside analogs currently in clinical use for HIV infection (77). Stavudine was approved by the US FDA for the treatment of patients who are intolerant to zidovudine or didanosine. Stavudine can cause the same side effect as ddC, i.e., peripheral neuropathy (78). Stavudine shows an IC<sub>50</sub> value of 19  $\mu$ M in MT-4 cell infected with HIV-1(IIIB) strain (79).

2',3'-Dideoxy-3'-thiacytidine (3TC, lamivudine, Epivir<sup>®</sup>) has potent antiretroviral activity *in vitro* with good oral bioavailability, and less toxicity than AZT. Lamivudine is frequently used as a component in Combivir<sup>®</sup> (lamivudine and zidovudine) and Trizivir<sup>®</sup> (abacavir, zidovudine and lamivudine). Its main disadvantage is rapid development of resistance, and a single point mutation (M184V)

is sufficient for loss of effectiveness. The major reported side effects of lamivudine are pancreatitis and peripheral neuropathy (70, 80). Lamivudine showed an *in vitro*  $IC_{50}$  value of  $0.4 \mu M$  in MT-4 cells infected at a m.o.i. of 0.01 (72).

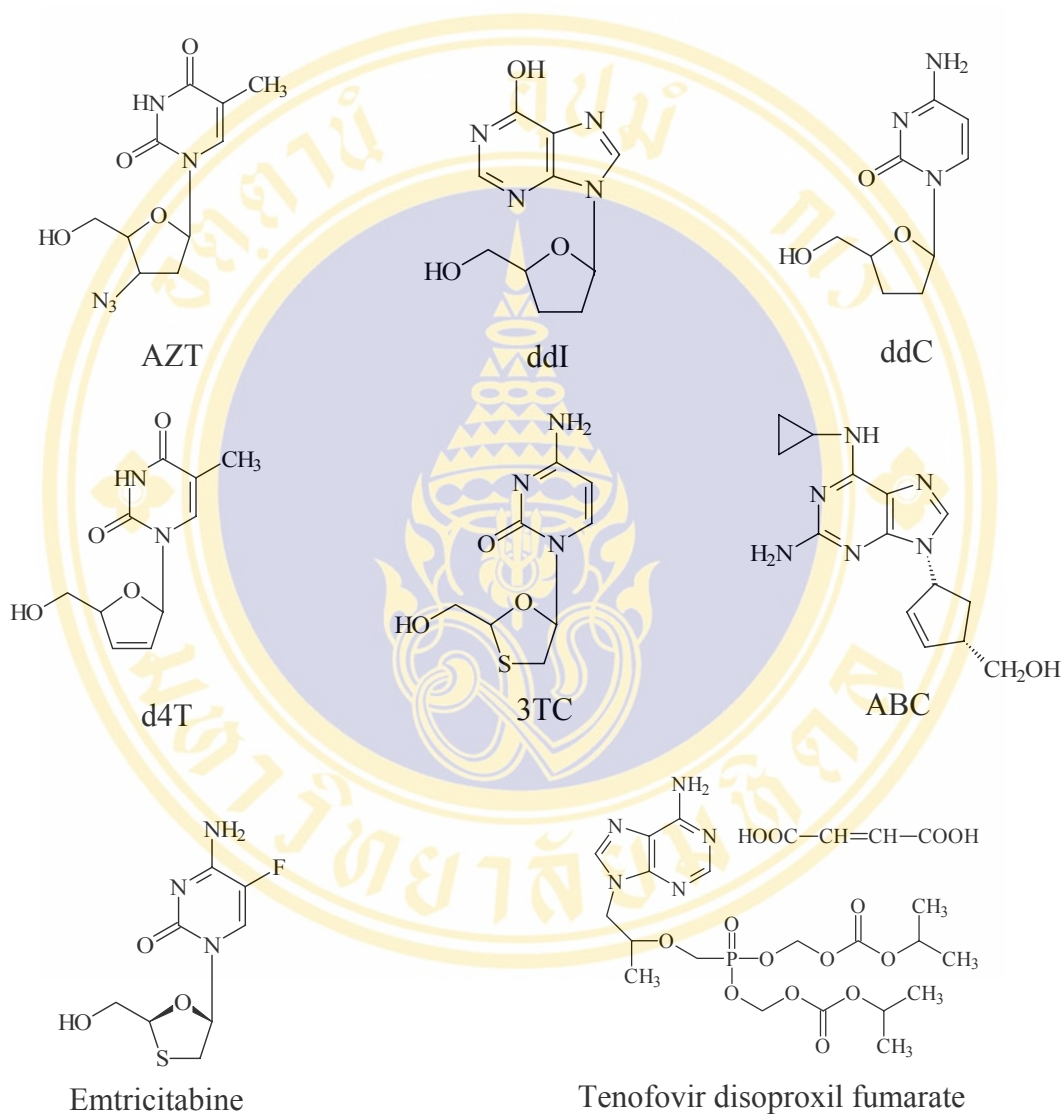


**Figure 11.** Structures of US FDA approved NRTIs.

Abacavir (ABC, Ziagen<sup>®</sup>) is a potent and mostly well-tolerated nucleoside with good CNS penetration due to its capable of crossing the blood-brain barrier. It has been well tolerated but the main side effect being hypersensitivity reactions, which sometime can be dangerous. Strains that are resistant to AZT or lamivudine are generally sensitive to abacavir, whereas strains that are resistant to AZT and lamivudine are not sensitive to abacavir. Abacavir is given orally and has a high bioavailability of 83 %. It is metabolized primarily through alcohol dehydrogenase or gluconyl transferase (70, 81). When tested with normal human peripheral blood lymphocytes against fresh clinical isolates of HIV-1 obtained from antiretroviral drug-naive patients, the mean 50% inhibitory concentration (IC<sub>50</sub>) was 0.26  $\mu$ M (0.07  $\mu$ g/ml); the corresponding IC<sub>50</sub> of zidovudine (ZDV), didanosine (ddI), and zalcitabine (ddC) were 0.23, 0.49, and 0.03  $\mu$ M, respectively (82).

Tenofovir (Viread<sup>®</sup>) acts as a false building block similarly to nucleoside analogs, targeting the enzyme reverse transcriptase. However, in addition to the pentose and nucleic base it is monophosphorylated, and is therefore referred to as a nucleotide. The more accurate description of the substance is tenofovir disoproxil fumarate which is a prodrug of tenofovir (83). Tenofovir showed an *in vitro* IC<sub>50</sub> value of 29  $\mu$ M in PBMC cell infected with HIV-1(IIIB) strain (84).

Emtricitabine (ETC, Emtriva<sup>®</sup>) is a synthetic nucleoside analog of cytosine. Emtricitabine is the (-) enantiomer of a thio analog of cytidine and it differs from other cytidine analogs by a fluorine in the 5 position. Emtricitabine, in combination with other antiretroviral agents, is FDA approved for the treatment of HIV infection in adults age 18 and older. Emtricitabine can cause some side effects, including nausea, vomiting, abdominal pain, lack of appetite, weight loss, difficulty breathing, and fatigue (85, 86, 87). Emtricitabine showed an *in vitro* IC<sub>50</sub> value more than 100  $\mu$ M in PBMC cell infected with HIV-1(LAV) strain (88).

## 2. Nonnucleoside reverse transcriptase inhibitors (NNRTIs)

NNRTIs were first described in 1990. In contrast to the NRTIs, they are not “false” building blocks, but rather bind directly and non-competitively to the enzyme, at a position in close proximity to the substrate-binding site for nucleosides (70). A number of competition experiments suggest that various NNRTIs bind to the same or overlapping sites on HIV-1 RT. A crystal structure of RT complexed with the nonnucleoside nevirapine indicates that nevirapine is bound in a hydrophobic pocket close to the polymerase active site. Most of NNRTIs binding conformations are butterfly-like shape (89). Several amino acids residues critical for conferring resistance to other NNRTIs are also located in or near this pocket (especially codon groups 100-108 and 181-190), supporting the suggestion that these inhibitors are binding at similar sites (90). Since NNRTIs target at a nonsubstrate binding site of the RT, they do not require activation through cellular metabolism. The most significant problem with NNRTIs is resistance, with a high risk of cross-resistance. One point mutation on position 103 (Lys103Asp) of the hydrophobic binding site is sufficient to eliminate an entire class of drug. Point mutations may occur very rapidly. Resistance has even been described in maternal transmission prophylaxis, in mothers who had taken nevirapine only once during delivery (91). The currently available NNRTIs are nevirapine, delavirdine, and efavirenz, structures as shown in Figure 12.

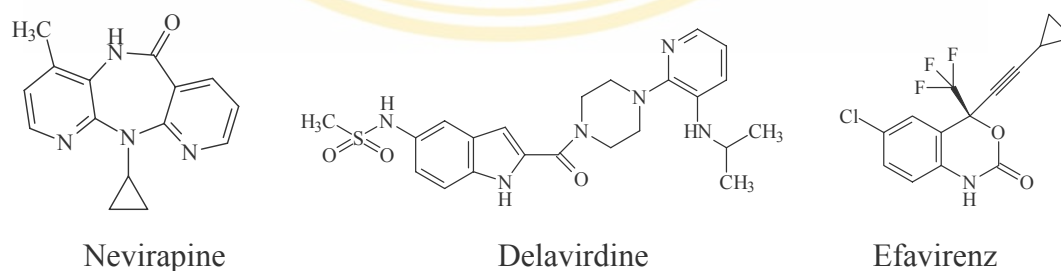


**Figure 12.** Structures of the approved NNRTIs.

Nevirapine (Viramune<sup>®</sup>), the dipyrindodiazeponone derivative, was the first licensed NNRTI. Nevirapine was found from a several derivatives of pyridobenzodiazepinones and dipyrindodiazeponones. Structure-activity relationship studies of this series have demonstrated that the diazeponone N-11 position needs an alkyl group e.g. ethyl or cyclopropyl group and 7-position of the pyridobenzodiazepinones or 4-position of the dipyrindodiazeponones requires a lipophilic group such as methyl group (92). In rare cases, it may cause serious hepatic toxicity. Nevirapine was approved by US FDA in 1996 (70). Nevirapine shows IC<sub>50</sub> value of 0.04  $\mu$ M in MT-4 cells infected at a m.o.i. of 0.01 (72).

Delavirdine (Rescriptor<sup>®</sup>, U-90152S), the bisheteroaryl piperazine derivative, was the second NNRTI approved by US FDA. The development of delavirdine was based on the modification of the original molecule N-ethyl-2-[4-[4-methoxy-3,5-dimethylphenylmethyl]-1-piperazinyl]-3-pyridinamine (U-80493E). Replacement of the methylene linkage by carbonyl group and phenyl ring by indole ring greatly enhanced the HIV-1 RT inhibitory activity. Delavirdine with two aromatic groups, i.e., 5-methanesulfonamidoindole and 3-isopropylaminopyridine linking with carbonylpiperazine exhibited an IC<sub>50</sub> of 0.26  $\mu$ M against HIV-1 RT (wild-type) (93). Delavirdine exhibited good absolute bioavailability in preclinical studies and serum drug levels in excess of those needed for in vitro antiviral activity was safely maintained for prolonged periods of time. Delavirdine prevented the spread of HIV-1 in human lymphocytes significantly longer than AZT at the same concentration. Although delavirdine was less effective against the known non-nucleoside-resistant forms of HIV-1 RT (Tyr181Cys and Lys103Asp) as compared to wild-type RT, it still demonstrated significant activity against these mutant RTs in vitro (IC<sub>50</sub> 8  $\mu$ M) (50). Due to a high pill burden and the required three times daily dosing, delavirdine is currently rarely prescribed, although it is likely to be approximately as effective as nevirapine and efavirenz (94, 95).

Efavirenz (Sustiva<sup>®</sup>, Stocrin<sup>®</sup>) was the third NNRTI approved and the first in which it was demonstrated that NNRTIs were at least as effective as protease inhibitors. Efavirenz is a benzoxazinone derivative, consisting of chlorine atom at position 6, trifluoromethyl and cyclopropylethynyl at position 4 of benzoxazinone ring system. Efavirenz has shown good antiviral potency, high oral bioavailability, and

favorable profile against a number of mutant RTs. The most common side effects of efavirenz are rash, nausea, dizziness, diarrhea, headache and insomnia and it is contraindicated in pregnancy (96). Lipids are not as favorably affected as with nevirapine, but hepatotoxicity is less frequent (70). Efavirenz shows  $IC_{50}$  value of 80  $\mu M$  in MT-4 cell infected with HIV-1 (IIIB) strain and this is the lowest concentration that exhibited signs of cytotoxicity (97)

### 3. HIV-1 protease inhibitor

HIV-1 PIs are compounds which bind to the active site of HIV-1 PR and prevent the processing of viral polyprotein precursors (*gag* and *gag-pol*). This results in the production of immature, non-infectious viral particles, thus inhibiting the replication and proliferation of HIV (98). PIs are almost always used in combination with at least two other anti-HIV drugs. Anti-HIV drug combinations, sometimes called cocktails, can reduce the amount of HIV in the patients's body (99). Several PIs are in clinical trials and eight of them (structures as shown in Figure 13) have been approved for using in AIDS patients.

Saquinavir (Ro 31-8959, Invirase<sup>®</sup>, Fortovase<sup>®</sup>), from Hoffmann-La Roche was developed by substrate analogy, with replacement of the scissile dipeptide fragment of the natural substrate with a Phe-Pro hydroxyethylamine transition state insert (100). The basic design criterion relied on the observation that HIV-1 PR cleaves the sequences containing dipeptides Tyr-Pro or Phe-Pro. Mammalian proteases do not cleave peptide bonds followed by a proline; thus, this target promised selectivity. Because reduced amides and hydroxyethylamine isosteres most readily accommodate the amino acid moiety, they were chosen for further studies. Replacement of a proline at the P1' subsite by (S,S,S)-decahydroisoquinoline-3-carbonyl (DIQ) significantly improved the potency of the inhibitors (101). This general approach has previously been used with success by a number of researchers seeking to develop inhibitors of human renin. Following traditional SAR optimization, saquinavir emerged and became the first approved HIV-1 PI in December 1995. Saquinavir inhibits HIV-1 PR with a  $K_i$  value of 0.12 nM and shows specificity for that enzyme, with little inhibition of mammalian aspartyl proteases ( $IC_{50} > 10$  mM).

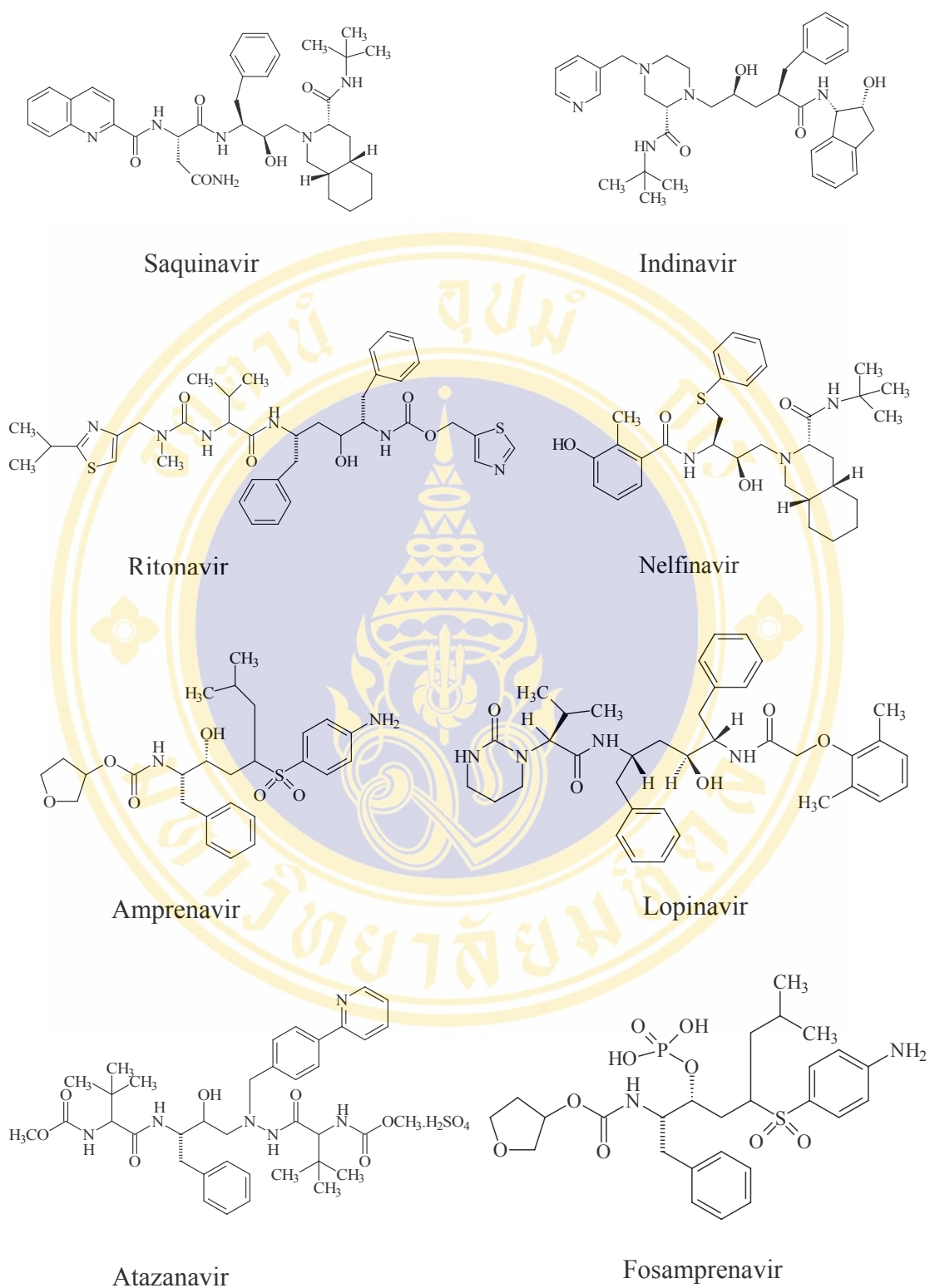
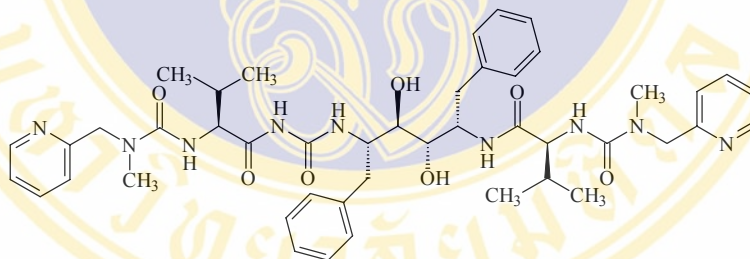


**Figure 13.** Structures of clinically approved anti HIV-1 PR drugs.

The first available formulation, Invirase<sup>®</sup>, was a hard gel capsule and provided dismal bioavailability of about 4% due to poor absorption and extensive first pass clearance. Fortovase<sup>®</sup> is a new version of saquinavir and is better absorbed by the body, it has a stronger anti-HIV effect than Invirase<sup>®</sup>. The anti-HIV effect of Fortovase<sup>®</sup> seems to be similar to other available PIs (100, 102, 103).

Ritonavir (ABT-538, Norvir<sup>®</sup>) was the symmetry of HIV-1 PR, and the first Abbott inhibitors (A-77003) were also symmetric (104). Researchers at Abbott initially sought to exploit the *C*<sub>2</sub> symmetry of HIV-1 PR by incorporating *C*<sub>2</sub> symmetry as an inhibitor design element. After extensive SAR investigation, which also involved partial desymmetrization, ritonavir emerged. The compound shows an IC<sub>50</sub> value against HIV-1 PR of 25 nM, and is both an inducer and potent inhibitor of cytochrome P450 3A4. The latter property has been used to advantage for increasing the half-life of coadministered drugs (105, 106, 107). Ritonavir achieved FDA approval as Norvir<sup>®</sup> in February 1996.



A-77003

Indinavir (MK-639, L-735,524, Crixivan<sup>®</sup>) was developed by Merck based on a transition-state mimetic concept (108), which had identified potent renin inhibitors based upon the PheΨ[CHOHCH<sub>2</sub>]Phe transition state insert (109). In order to improve solubility and bioavailability, the P1/P2 portion of L-685,434 was replaced, first by the Roche P1'/P2' decahydroisoquinoline *tert*-butylamide (Saquinavir) to generate L-704,486 (Figure 14), and subsequently by the pyridyl methylpiperazine moiety (110). Indinavir shows a K<sub>i</sub> value against HIV-1 PR of 0.34 nM and is effective in antiviral cell culture with IC<sub>50</sub> values of 25-100 nM. It is synergistic with both nucleoside and nonnucleoside RTIs, and is unique among currently approved PIs in having a low degree of protein binding (56% in human plasma). Indinavir therapy has been associated with kidney stones and urinary tract sludging, leading to the recommendation of increased fluid intake during its use. Indinavir was approved by FDA in March 1996 under the trade name Crixivan<sup>®</sup> (111).

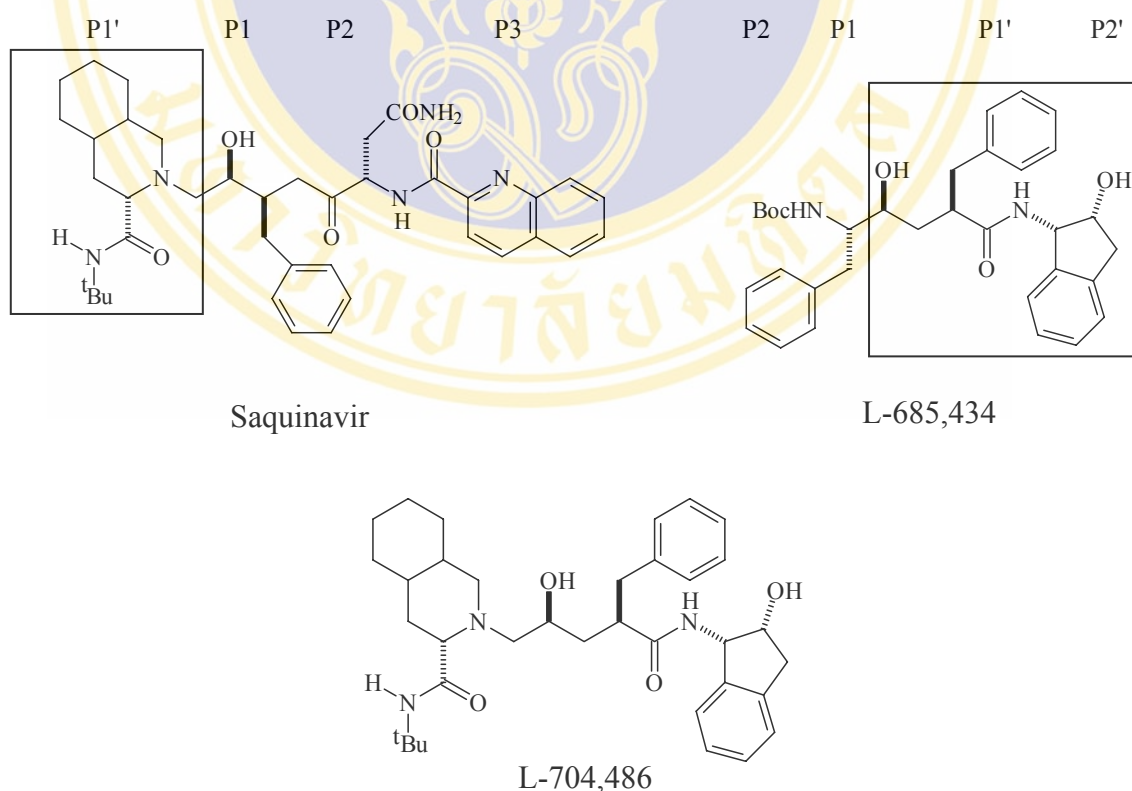


**Figure 14.** Design concept of indinavir (110).

Nelfinavir (AG-1343, Viracept<sup>®</sup>) was the first PI that was not a peptidomimetic, arose through a collaborative effort at Agouron and Lilly from a fusion of small peptidomimetic compounds with the Roche decahydroisoquinoline system. A key discovery during this evolution was the N-terminal 3-hydroxy-2-methylbenzoyl fragment, which subsequently found utility in other PIs (112). Nelfinavir showed a  $K_i$  value of 2 nM against HIV-1 PR with more than 78 % bioavailability. Nelfinavir was launched in the U.S. in March 1997 under the trade name Viracept<sup>®</sup> and was the first PI to be indicated for pediatric AIDS (119).

Amprenavir (VX-478, 141W94, Agenerase<sup>®</sup>) arose at Vertex from a structure-based design approach, which incorporated molecular weight minimization as a key goal. Its central core is identical to that of saquinavir, although both ends are quite different. The P2 group consists of tetrahydrofuran carbamate, whereas the P1'-P2' moieties consist of an isobutylphenyl sulfonamide with an added amide. This design gives amprenavir fewer chiral centers than saquinavir, facilitating synthesis and increasing water solubility to allow oral bioavailability as high as 40 %-70 %. Amprenavir inhibited HIV-1 PR with a  $K_i$  value of 0.6 nM. In humans, its pharmacokinetic properties, such as more than 70% bioavailability and long half-life (10 hours) are consistent with twice-daily dosing. Amprenavir was FDA approved as Agenerase<sup>®</sup> in April 1999. Under terms of a 1993 agreement, Glaxo Wellcome received rights to amprenavir in the U.S. and Europe (114, 115). Amprenavir in a combination with lamivudine and saquinavir was more potent than lamivudine or saquinavir alone, although less effective than indinavir (116).

Lopinavir is a second generation inhibitor from Abbott Laboratories, designed to preserve activity against Val 82 mutant virus arising with ritonavir therapy. The compound is based upon the same core insert as ritonavir but includes highly modified peripheral functionality. In particular, the P3 functionality interacts only minimally with Val 82, decreasing the sensitivity of the inhibitor to this particular mutation. Lopinavir shows a  $K_i$  value of 1.3 pM against HIV-1 PR and an antiviral  $IC_{50}$  value in cell culture of 6-17 nM. Administered alone, lopinavir is rapidly cleared from circulation (117, 118, 119). For this reason, the approved product Kaletra<sup>®</sup> is a formulation of lopinavir containing ritonavir, which blocks the metabolic degradation mediated by cytochrome P450 3A4 (CYP3A4) (120). Lopinavir/Ritonavir

(Lopinavir/r, Kaletra<sup>®</sup>), which contains both lopinavir and ritonavir, has been approved in both capsule and liquid formulations for adults and children greater than 6 months of age with HIV. Ritonavir may increase concentrations of lopinavir by more than 100-fold. This results in blood levels of lopinavir that enhance its effectiveness against HIV (121, 122). The new drug is used in combination with other anti-HIV drugs. It should be taken with food to increase absorption into the blood stream. The usual dose for adults is three capsules or 5.0 mL twice-daily. Kaletra<sup>®</sup> capsules contain 400 mg of lopinavir and 100 mg of ritonavir (122). Dyslipidemia appears to be a significant problem with lopinavir therapy. Kaletra<sup>®</sup> was approved in September 2000 (119).

Atazanavir (Reyataz<sup>®</sup>) is a once-daily PI that received approval by the Food and Drug Administration in June 2003. Atazanavir can cause increases in unconjugated bilirubin levels, which rarely leads to jaundice or scleral icterus. In contrast to comparators, atazanavir did not negatively impact the lipid profile. Similar to other PIs, atazanavir is metabolized by and inhibits CYP3A4 at clinically relevant concentrations, therefore, many potential drug interactions exist (123). Structure-activity studies with a series of azadipeptides designed to mimic the transition state of the peptide-cleavage reaction catalyzed by HIV-1 PR identified lead compounds that had either potent antiviral activity against mutant HIV-1 strains or good oral bioavailability, but not both. Lead optimization using X-ray structural data from an inhibitor-protease complex led to the discovery of atazanavir sulphate, which showed excellent antiviral activity with high oral bioavailability and could be used in combination with other antiretroviral agents (124). Atazanavir differs from the peptidomimetic PIs (e.g. saquinavir, nelfinavir) by its C<sub>2</sub> symmetric drug interaction concerns, chemical structure and was designed and synthesized based on X-ray studies of an enzyme dysazadipeptide complex (125, 126, 127). Atazanavir has an EC<sub>50</sub> of 35 nmol/L against a variety of HIV-1 isolates in different cell types and is a highly selective and effective inhibitor of the HIV-1 PR *in vitro* (K<sub>i</sub>, <1 nmol/L) (128).

Fosamprenavir (Lexiva<sup>®</sup>, Telzir<sup>®</sup>), also known as GW433908, is the latest PI for the treatment of HIV infection. It is an essentially inactive, highly water soluble phosphate ester prodrug of amprenavir. It was synthesized to enhance oral bioavailability and solubility of amprenavir, thus allowing a reduction in the pill

burden and offering the potential for improved patient compliance (98). Fosamprenavir calcium is a single stereoisomer with the (3*S*)(1*S*,2*R*) configuration (129). Fosamprenavir is rapidly and almost completely hydrolyzed to amprenavir and inorganic phosphate by cellular phosphatases in the gastrointestinal epithelium as it is absorbed. Amprenavir is metabolized in the liver by the CYP3A4 enzyme system. The two major metabolites resulted from the oxidation of the tetrahydrofuran and aniline moieties. Glucuronide conjugates of oxidized metabolites have been identified as minor metabolites in urine and feces (98). In clinical trials, fosamprenavir was studied alone or boosted with ritonavir in both HIV treatment-naïve and experienced-patient populations. In both patient populations, fosamprenavir decreased plasma HIV-1 RNA levels less than 400 copies/mL, increased CD4 cell counts from baseline, and increased the proportion of patients reaching undetectable viral load less than 50 copies/mL. Fosamprenavir demonstrated efficacy when used as a sole PI administered twice-daily or in combination with ritonavir-boosting as a once-daily regimen in treatment naïve patients. In treatment-experienced patients, ritonavir-boosting fosamprenavir regimens have not shown equivalent efficacy to lopinavir/ritonavir. Currently, the use of once-daily ritonavir-boosted fosamprenavir in patients who have previously been exposed to PIs is not recommended. Patients who received treatment with fosamprenavir demonstrated protease gene mutation different than those commonly seen with other PIs (except amprenavir). Fosamprenavir appears to have an adverse effect profile similar to that of other PIs (129). The most common adverse event reported were diarrhea, nausea, vomiting, fatigue, headache, abdominal pain, and rash. The plasma elimination half-life of amprenavir is approximately 7.7 hours. Excretion of unchanged amprenavir in the urine and feces is minimal (98). The recommended dosage of fosamprenavir for therapy naïve patients is 1,400 mg twice daily and for PI-experienced patients is 700 mg twice daily (13). Coadministration of food with fosamprenavir tablets appears to have little effect on amprenavir absorption (98). As a result, fosamprenavir may be taken with or without food (129). Fosamprenavir was approved by the FDA on October 20, 2003, for the treatment of HIV infection in adults in combination with other antiretroviral agents (98).

#### 4. Fusion inhibitors

Enfuvirtide (T-20, DP-178, Pentafuside<sup>®</sup>), the first in a new class of anti-HIV-1 drugs that inhibit the entry of the virus into cells, was approved by the US FDA in March 2003 for treatment of HIV-1 infection in treatment-experienced patients. Enfuvirtide is a synthetic 36 amino acids peptide (Figure 15) corresponding to residues 127-162 of the extracellular portion (ectodomain) of gp41 (or residues 643-678 in the gp160 precursor) of the HIV envelope glycoprotein. The molecular formula of enfuvirtide is  $C_{204}H_{301}N_{51}O_{64}$ , and its molecular weight is 4492 Da. (130, 131). Considering its large size, the manufacture of enfuvirtide is very complex, currently involving 106 steps in the chemical pathway to give a powder for subcutaneous injection (132). Because of the large size of the molecule and the complexity of the manufacturing process, enfuvirtide is expensive even by antiretroviral standards (133). Although enfuvirtide is the most expensive antiretroviral to date, the cost effectiveness of enfuvirtide has been explored and been demonstrated to be within currently acceptable thresholds for both the USA and UK (131). Enfuvirtide was approved for using with other anti-HIV drugs in the treatment of HIV infection and was approved for using in HIV infected adults and children 6 years of age or older whose HIV infection has not been controlled by other anti-HIV drugs.

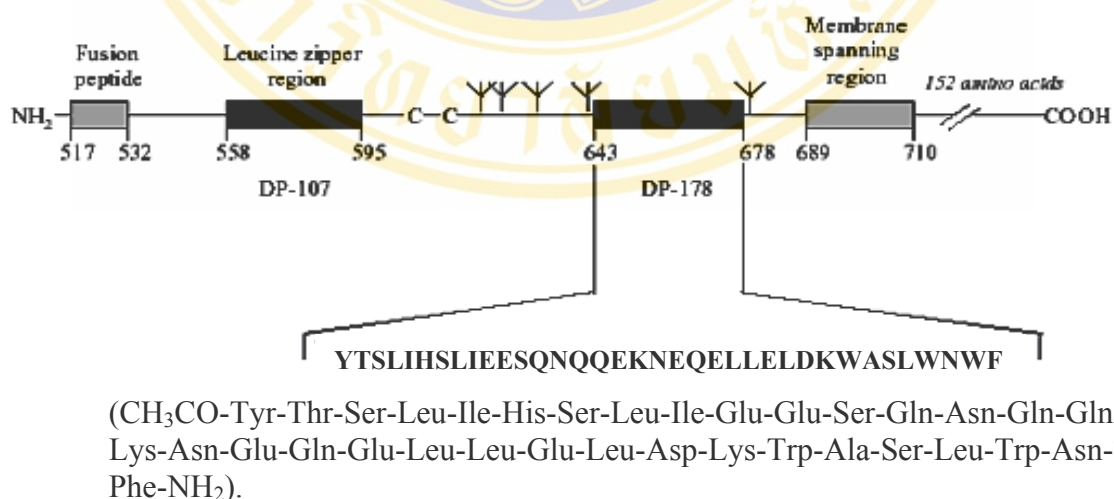


**Figure 15.** Structure of enfuvirtide (130, 131).

#### D. HIV-1 protease inhibitory activity test

Peptide substrates closely resembling in sequence the processing sites found within the HIV polyproteins have been used to develop peptidolytic assays. A variety of peptidolytic assays which have been reported for HIV-1 PR are i) separation of products from unreacted substrates by high-performance liquid chromatography (HPLC), ii) analysis of a peptide substrate containing an appropriate chromophoric residues, such as *p*-nitrophenylalanine, at one of its scissile positions by continuous spectrophotometric assay, iii) ion-exchange separation of the radiolabelled carboxylic product from its uncharged labeled substrate, and iv) continuous fluorometric analysis of a peptide substrate analog designed to be fluorogenic upon cleavage.

The most widely used peptidolytic assays for HIV-1 PR are HPLC and spectrophotometric assays. HPLC method is a stopped time assay using various concentrations of the peptide substrate incubated with the protease in small volumes (< 0.1 mL). After quenching with acid at selected times, the samples are subjected to reverse phase HPLC on octadecylsilane columns. The resulting peptidolytic products are thereby separated from the remaining substrate with linear gradients of acetonitrile in 0.1% trifluoroacetic acid with spectrophotometric detection of the peptides at 280 nm. The advantages of the HPLC assay are versatility (any soluble peptide substrate can be assayed) and sensitivity (reaction mixtures of 100  $\mu$ L containing  $\mu$ M concentrations of peptides can be analyzed) (23).

The principle of the spectrophotometric assay of HIV-1 PR is the analysis of the catalytic cleavage of peptide substrates bearing the chromogenic *p*-nitrophenylalanine. The cleavage of a peptide substrate containing a *p*-nitrophenylalanyl group at either the P1 or P1' position results in small shifts in the ultraviolet absorbance spectrum and a time course of absorbance can be generated by monitoring wavelengths between 300-330 nm. The spectrophotometric assay provides continuous monitoring of the initial rate, which upon extrapolation of the initial linear region of the time course to zero time, allows an accurate measure of the enzymatic initial rate. The use of an enzymatic time course also helps in evaluating the kinetics of inhibitors which are slow and/or tight binding (23).

An ion-exchange assay for HIV-1 PR using an immobilized substrate, Affi Gel 10-Gly-Gly-Gly-Gly-Val-Ser-Gln-Asn-Tyr-Pro-Ile-Val-Gln-[<sup>3</sup>H]Gly-OH has been devised. The Tyr-Pro bond of the substrate was hydrolyzed by the protease, releasing the radiolabeled cleavage product, Pro-Ile-Val-Gln-[<sup>3</sup>H]Gly-OH, into the supernatant. The pH optimum was found to be 6.0, and a high ionic strength was required for maximal activity. The ion-exchange assay is usable for convenient monitoring of purification procedures, and rapid screening of HIV-1 PIs (134).

A fluorometric method for measuring HIV-1 PR activity utilizing a synthetic peptide substrate (DABCYL-Ser-Gln-Asn-Tyr-Pro-Ile-Val-Gln-EDANS) for HIV-PR has been described by Wang and coworkers (135). The sequence of this substrate includes the HIV-PR cleavage site, along with two covalently modified amino acid residues, one that has been linked to a fluorophore (5-(aminoethyl)aminonaphthalene sulfonate, EDANS) and the other to an acceptor chromophore (4'-dimethylaminoazobenzene-4-carboxylate, DABCYL). The acceptor chromophore was chosen for maximal overlap of its absorbance with the emission spectrum of the fluorophore, resulting in quenching of the nearby fluorophore through resonance energy transfer. The fluorogenic peptide substrate has been demonstrated to be cleaved quantitatively by HIV-1 PR at the Tyr-Pro bond (136).

## CHAPTER III

### CHEMICAL EXPERIMENTAL

#### A. Equipment and chemicals

##### 1. Equipment

Analytical balance model 2842	Sartorius, USA
Chromato-VUE cabinet (Model CC-60)	UVP Inc., USA
Elemental analyzer (PE2400 series II)	Perkin Elmer, Germany
FTIR (FTIR 550)	Nicolet, USA
<sup>1</sup> H NMR (DPX-3000) spectrophotometer	Bruker, Switzerland
Magnetic stirrer (MR 3001K)	Heidolph, Germany
Mass spectrometer (MAT 90)	Finnigan, Germany
Melting point apparatus (model 9100)	Electrothermal , UK
Rotary evaporator	Eyela, Japan

##### 2. Chemicals

Acetone	J.T Baker, USA
Chloroform	J.T Baker, USA
3-Chlorobenzoyl chloride	Fluka, Switzerland
DBU (1,8-diazabicyclo[5,4,0]undec-7-ene)	Fluka, Switzerland
2,4-Dihydroxyacetophenone	Fluka, Switzerland
2,5-Dihydroxyacetophenone	Aldrich, USA
Dimethyl sulfoxide	Sigma, USA
Ethyl acetate	J.T Baker, USA
4-Fluorobenzoyl chloride	Aldrich, USA
Hexane	J.T Baker, USA
Hydrochloric acid	E. Merck, Germany

Methanol	J.T Baker, USA
4-Methoxybenzoyl chloride	Aldrich, USA
3-Methoxybenzoyl chloride	Aldrich, USA
Pyridine	Lab scan
Sea sand	Fluka, Switzerland
Silica gel F <sub>254</sub> (0.2 mm.)	E. Merck, Germany
Silica gel 60 No 1.07734	E. Merck, Germany
Sodium hydroxide	Fluka, Switzerland
Sodium sulfate	E. Merck, Germany
3-Trifluoromethylbenzoyl chloride	Aldrich, USA
2,3,4-Trihydroxyacetophenone	Aldrich, USA
2,4,6-Trihydroxyacetophenone	Aldrich, USA
4- <i>tert</i> -Butylbenzoyl chloride	Fluka, Switzerland

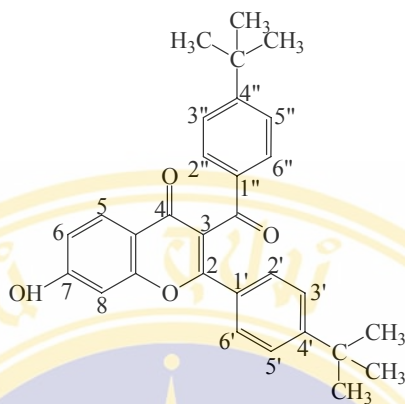
## B. Methods

All new compounds were characterized by spectroscopic methods, i.e., infrared (IR) spectroscopy, proton nuclear magnetic resonance (<sup>1</sup>H NMR) spectroscopy, mass spectroscopy (MS) and elemental analysis. IR spectra were recorded on FTIR Nicolet 550, using the potassium bromide pellet technique. <sup>1</sup>H NMR spectra were obtained on an ADVANCE 300 MHz Digital NMR Spectrophotometer (Bruker Switzerland DPX-3000). Chemical shifts were reported in ppm related to the internal standard, tetramethylsilane (TMS). The NMR solvent used was deuterated dimethylsulfoxide (DMSO,  $\delta_{\text{H}} = 2.54$  ppm). Mass spectra were determined on a MAT 90 (Finnigan) mass spectrometry using EI method. Percentage of carbon, hydrogen and nitrogen were obtained from a CHNS/O analyzer (Perkin Elmer PE2400 series II) and the results were within 0.4 % of theoretical values. Melting point of all products were determined on an Electrothermal model 9100 capillary melting point apparatus. The crude products were purified by column chromatography using silica gel, E. Merck (70-230 mesh) and recrystallization. Thin layer chromatography (TLC) was carried out on silica gel GF<sub>254</sub> coated aluminum sheets 20 x 20 cm (E. Merck) with spots visualized by UV light (254 nm). All

solvents were reagent grade and when necessary, were purified and dried by standard methods.



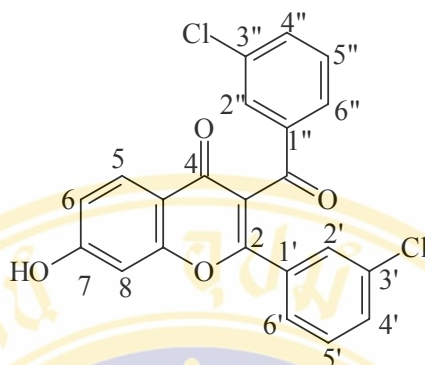
### 1. 7-Hydroxy-2-(4'-*tert*-butylphenyl)-3-(4''-*tert*-butylbenzoyl) chromone 1.



4-*tert*-Butylbenzoyl chloride (1.0 mL, 7.84 mmol) was added to a stirring solution of 2,4-dihydroxyacetophenone (0.4 g, 2.63 mmol) in pyridine (15 mL) at 120 °C. Then, DBU (1.2 mL, 8.03 mmol) was added dropwise to the stirring mixture. The reaction mixture was allowed to stir at 140-160 °C for 30 hours and pyridine was evaporated under vacuo. The mixture was poured into 5 mL of concentrated hydrochloric acid in 100 mL water and extracted with ethyl acetate (2 x 50 mL). The combined organic layers were washed with water (2 x 50 mL), dried over anhydrous sodium sulfate, and filtered. After evaporation, the crude product was hydrolyzed by the mixture of dioxane (2 mL), methanol (4 mL), water (1 mL) and 10 % NaOH (2 mL), and stirred at room temperature for 3-4 hours. The reaction mixture was acidified (pH 1.0) with 4N HCl and poured into 50 mL water, and then extracted with ethyl acetate (2 x 50 mL). The combined organic layers were washed with water (2 x 50 mL), dried over anhydrous sodium sulfate, and filtered. After evaporation, the crude product was purified by column chromatography (ethyl acetate/hexane [1:1]) to provide the white crystal (303 mg, 25.38 %); m.p. 271-273 °C; <sup>1</sup>H NMR 300 MHz (DMSO): δ 1.23 (s, 9H, 4'-*t*-butyl), 1.27 (s, 9H, 4''-*t*-butyl), 6.95 (dd, *J* = 7.95, 1.13, 1H, H6), 6.98 (d, *J* = 1.13 Hz, 1H, H8), 7.45 (d, *J* = 8.32 Hz, 2H, H3', H5'), 7.49 (d, *J* = 8.48 Hz, 2H, H3'', H5''), 7.55 (d, *J* = 8.32 Hz, 2H, H2', H6'), 7.82 (d, *J* = 8.48 Hz, 2H, H2'', H6''), 7.86 (d, *J* = 7.95 Hz, 1H, H5); FTIR (KBr) (cm<sup>-1</sup>): 3420 (O-H st.), 1683 (C=O st.), 1624 (C=C st.), 1459 (bending C-H), 1104 (C-O st.); EIMS: *m/z* (relative intensity) M<sup>+</sup> 454(37.92), 425(64.14), 397(100.00), 369(12.29), 321(8.81), 265(15.17). Anal. Calcd. for C<sub>30</sub>H<sub>30</sub>O<sub>4</sub> (454.56): C, 79.27; H, 6.65. Found: C, 79.09; H, 6.73.

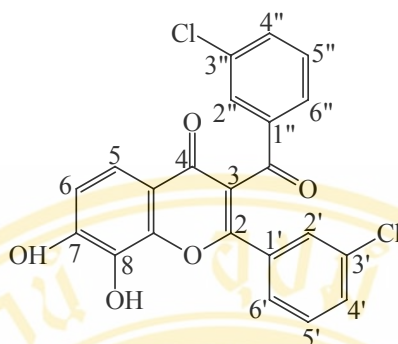
TLC (silica gel GF 254, ethyl acetate/hexane [1:1]).  $R_f$  of 2,4-dihydroxyacetophenone = 0.67, compound **1** = 0.54.



**2. 7-Hydroxy-2-(3'-chlorophenyl)-3-(3''-chlorobenzoyl) chromone 2.**

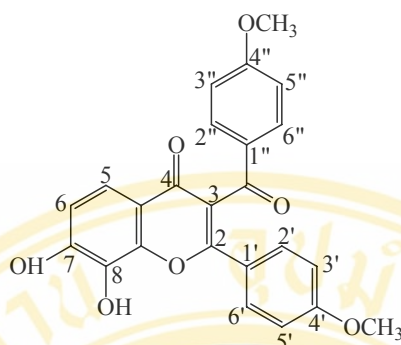
Compound **2** was synthesized by using the same procedure as described for compound **1** from 2,4-dihydroxyacetophenone (0.4 g, 2.63 mmol), 3-chlorobenzoyl chloride (1.0 mL, 7.81 mmol) and DBU (1.2 mL, 8.03 mmol). After hydrolysis and purification by column chromatography (ethyl acetate/hexane [1:1]), the desired compound **2** was obtained as a yellow crystal (250.12 mg, 23.14 %); m.p. 303-305 °C;  $^1\text{H}$  NMR 300 MHz (DMSO):  $\delta$  6.98 (dd,  $J = 8.13, 1.81$  Hz, 1H, H6), 7.00 (d,  $J = 1.81$ , 1H, H8), 7.44-7.58 (m, 4H, H5', H5'', H4', H6'), 7.68 (s, 1H, H2'), 7.70 (d,  $J = 1.67$  Hz, 1H, H4''), 7.86-7.91 (m, 2H, H5, H6''), 7.95 (d,  $J = 1.36$  Hz, 1H, H2''); FTIR (KBr) ( $\text{cm}^{-1}$ ): 3453 (O-H st.), 3072 (aromatic C-H st.), 1683 (C=O st.), 1624 (C=O st.), 1459 (C=C st.), 1393 (bending C-H), 1117 (C-O st.); EIMS:  $m/z$  (relative intensity)  $\text{M}^+$  410(29.73), 381(100.00), 299(17.56), 163(22.63), 139(8.50), 111(12.86). Anal. Calcd. for  $\text{C}_{22}\text{H}_{12}\text{O}_4\text{Cl}_2$  (411.24): C, 64.25; H, 2.94. Found: C, 63.94; H, 2.81. TLC (silica gel GF 254, ethyl acetate/hexane [1:1]).  $R_f$  of 2,4-dihydroxyacetophenone = 0.67, compound **2** = 0.41.

### 3. 7,8-Dihydroxy-2-(3'-chlorophenyl)-3-(3''-chlorobenzoyl) chromone 3.



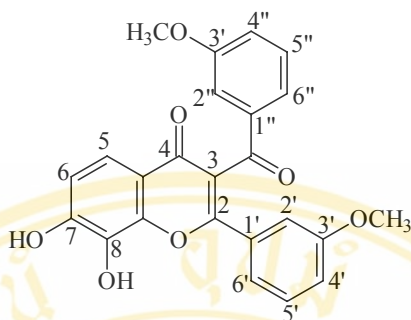
Compound **3** was synthesized by using the same procedure as described for compound **1** from 2,3,4-trihydroxyacetophenone (0.4 g, 2.38 mmol), 3-chlorobenzoyl chloride (1.0 mL, 7.81 mmol) and DBU (1.2 mL, 8.03 mmol). After hydrolysis and purification by column chromatography (chloroform/methanol [9:1]), the desired compound **3** was obtained as a yellow solid (116.61 mg, 11.50 %); m.p. 256-257 °C;  $^1\text{H}$  NMR 300 MHz (DMSO):  $\delta$  7.01 (d,  $J = 8.71$ , 1H, H6), 7.39 (d,  $J = 8.71$  Hz, 1H, H5), 7.45-7.58 (m, 4H, H5', H4', H5'', H4''), 7.69 (d,  $J = 6.87$  Hz, 1H, H6''), 7.76 (s, 1H, H2'), 7.88 (d,  $J = 7.69$  Hz, 1H, H6''), 7.96 (s, 1H, H2''); FTIR (KBr)( $\text{cm}^{-1}$ ): 3457 (O-H st.), 3078 (aromatic C-H st.), 1683 (C=O st.), 1628 (C=C st.), 1472 (bending C-H), 1150 (C-O st.); EIMS: m/z (relative intensity)  $\text{M}^+$  426(25.92), 397(100.00), 315(9.13), 163(23.88), 139(14.35), 111(17.84). Anal. Calcd. for  $\text{C}_{22}\text{H}_{12}\text{O}_5\text{Cl}_2 \cdot 0.25\text{H}_2\text{O}$  (431.74): C, 61.20; H, 2.92. Found: C, 61.25; H, 2.82. TLC (silica gel GF 254, chloroform/methanol [9:1]).  $R_f$  of 2,3,4-trihydroxyacetophenone = 0.50, compound **3** = 0.25.

#### 4. 7,8-Dihydroxy-2-(4'-methoxyphenyl)-3-(4''-methoxybenzoyl) chromone 4.

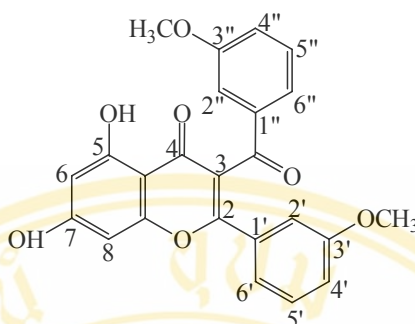


Compound **4** was synthesized by using the same procedure as described for compound **1** from 2,3,4-trihydroxyacetophenone (0.4 g, 2.38 mmol), 4-methoxybenzoyl chloride (1.0 g, 7.39 mmol) and DBU (1.2 mL, 8.03 mmol). After hydrolysis and purification by column chromatography (chloroform/methanol [9:1]), the desired compound **4** was obtained as a pale yellow solid (57.82 mg, 5.81%); m.p. 253-254 °C; <sup>1</sup>H NMR 300 MHz (DMSO): δ 3.74 (s, 3H, 4'-methoxy), 3.79 (s, 3H, 4''-methoxy), 6.91-6.99 (m, 5H, H<sub>6</sub>, H<sub>5'</sub>, H<sub>3'</sub>, H<sub>5''</sub>, H<sub>3''</sub>), 7.37 (d, *J* = 8.71 Hz, 1H, H<sub>5</sub>), 7.61 (d, *J* = 8.79, 2H, H<sub>2'</sub>, H<sub>6'</sub>), 7.84 (d, *J* = 8.76 Hz, 2H, H<sub>2''</sub>, H<sub>6''</sub>); FTIR (KBr) (cm<sup>-1</sup>): 3434 (O-H st.), 3131 (aromatic C-H st.), 1643 (C=O st.), 1617 (C=C st.), 1512 (bending C-H), 1400 (C-N st.), 1189 (C-O st.); EIMS: *m/z* (relative intensity) M<sup>+</sup> 418 (81.63), 389(100.00), 311(24.79), 159(24.87), 135(8.27). Anal. Calcd. for C<sub>24</sub>H<sub>18</sub>O<sub>7</sub>·0.75H<sub>2</sub>O (431.91): C, 66.74; H, 4.20. Found: C, 66.63; H, 4.36. TLC (silica gel GF 254, chloroform/methanol [9:1]). R<sub>f</sub> of 2,3,4-trihydroxyacetophenone = 0.50, compound **4** = 0.11.

### 5. 7,8-Dihydroxy-2-(3'-methoxyphenyl)-3-(3''-methoxybenzoyl) chromone 5.

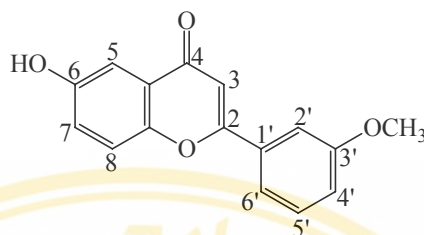


Compound **5** was synthesized by using the same procedure as described for compound **1** from 2,3,4-trihydroxyacetophenone (0.4 g, 2.38 mmol), 3-methoxybenzoyl chloride (1.0 g, 7.39 mmol) and DBU (1.2 mL, 8.03 mmol). After hydrolysis and purification by column chromatography (chloroform/methanol [9:1]), the desired compound **5** was obtained as a yellow solid (148.9 mg, 14.97 %); m.p. 255-257 °C;  $^1\text{H NMR}$  300 MHz (DMSO):  $\delta$  3.66 (s, 3H, 3'-methoxy), 3.85 (s, 3H, 3''-methoxy), 7.01 (d,  $J = 8.62$  Hz, 1H, H6), 7.05 (d,  $J = 9.17$ , 1H, H4'), 7.18 (s, 1H, H2'), 7.18-7.20 (m, 2H, H6', H5), 7.34 (d,  $J = 7.79$  Hz, 1H, H4''), 7.38 (s, 1H, H2'') 7.38-7.41 (m, 2H, H5', H5''), 7.47 (d,  $J = 7.79$  Hz, 1H, H6''); FTIR (KBr)( $\text{cm}^{-1}$ ): 3415 (O-H st.), 3091 (aromatic C-H st.), 1658 (C=O st.), 1580 (C=C st.), 1453 (bending C-H), 1194 (C-O st.); EIMS:  $m/z$  (relative intensity)  $M^+$  418(47.61), 390(24.60), 389(100.00), 267(30.82), 159(65.37), 135(33.03). Anal. Calcd. for  $\text{C}_{24}\text{H}_{18}\text{O}_7$  (418.40): C, 68.89; H, 4.34. Found: C, 68.38; H, 4.28. TLC (silica gel GF 254, chloroform/methanol [9:1]).  $R_f$  of 2,3,4-trihydroxyacetophenone = 0.50, compound **5** = 0.14.

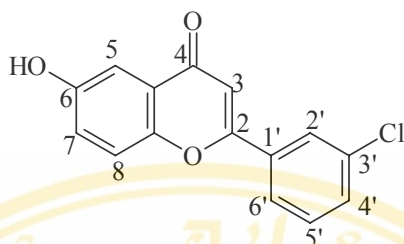
**6. 5,7-Dihydroxy-2-(3'-methoxyphenyl) 3-(3''-methoxybenzoyl) chromone 6.**

Compound **6** was synthesized by using the same procedure as described for compound **1** from 2,4,6-trihydroxyacetophenone (0.4 g, 2.15 mmol), 3-methoxybenzoyl chloride (1.0 mL, 7.34 mmol) and DBU (1.2 mL, 8.03 mmol). After hydrolysis and purification by column chromatography (ethyl acetate/hexane [1:1]), the desired compound **6** was obtained as a yellow solid (60.45 mg, 6.68 %); m.p. 167.2-168 °C;  $^1\text{H NMR}$  300 MHz (DMSO):  $\delta$  3.64 (s, 3H, 3'-methoxy), 3.76 (s, 3H, 3''-methoxy), 6.26 (d,  $J = 1.68$  Hz, 1H, H6), 6.51 (d,  $J = 1.68$ , 1H, H8), 7.05 (dd,  $J = 8.24, 2.49$  Hz, 1H, H4'), 7.10 (s, 1 H, H2'), 7.13 (dd,  $J = 8.24, 2.49$  Hz, 1 H, H6'), 7.21 (dd,  $J = 7.81, 2.25$  Hz, 1H, H4''), 7.34 (t,  $J = 8.24$  Hz, 1 H, H5'), 7.38 (t,  $J = 7.81$  Hz, 1 H, H5''), 7.41 (s, 1H, H2''), 7.54 (dd,  $J = 7.81, 2.25$  Hz, 1H, H6''); FTIR (KBr)( $\text{cm}^{-1}$ ): 3374 (O-H st.), 3078 (aromatic C-H st.), 1683 (C=O st.), 1650 (C=C st.), 1492 (bending C-H), 1163 (C-O st.); EIMS:  $m/z$  (relative intensity)  $\text{M}^+$  418(79.15), 389(100.00), 311(23.82), 284(43.26), 159 (24.49). Anal. Calcd. for  $\text{C}_{16}\text{H}_{12}\text{O}_4 \cdot 0.25\text{H}_2\text{O}$  (422.90): C, 68.16; H, 4.41. Found: C, 68.16; H, 4.32. TLC (silica gel GF 254, ethyl acetate/hexane [1:1]).  $R_f$  of 2,4,6-trihydroxyacetophenone = 0.36, compound **6** = 0.46.

### 7. 6-Hydroxy-2-(3'-methoxyphenyl)chromone 7.

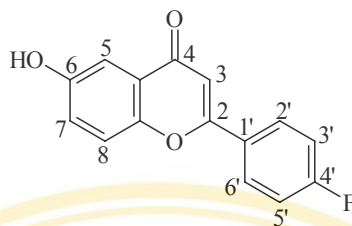


Compound 7 was synthesized by using the same procedure as described for compound 1 from 2,5-dihydroxyacetophenone (0.4 g, 2.63 mmol), 3-methoxybenzoyl chloride (1.0 mL, 7.34 mmol) and DBU (1.0 mL, 6.69 mmol). After hydrolysis and purification by column chromatography (ethyl acetate/hexane [1:1]), the desired compound 7 was obtained as a pink solid (85.94 mg, 11.97 %); m.p. 226-228 °C;  $^1\text{H}$  NMR 300 MHz (DMSO):  $\delta$  3.84 (s, 3H, 3'-methoxy), 6.98 (s, 1H, H3), 7.15 (d,  $J = 7.53$ , 1H, H4'), 7.25 (dd,  $J = 8.91, 2.75$  Hz, 1H, H7), 7.31 (d,  $J = 2.75$  Hz, 1H, H5), 7.47 (t,  $J = 7.53$  Hz, 1H, H5'), 7.57 (s, 1H, H2'), 7.64 (d,  $J = 7.53$  Hz, 1H, H6'), 7.65 (d,  $J = 8.91$  Hz, 1H, H8), 10.07 (s, 1H, C<sub>6</sub>-OH); FTIR (KBr)(cm<sup>-1</sup>): 3414 (O-H st.), 3170 (aromatic C-H st.), 2970 (aliphatic C-H st.), 1637 (C=O st.), 1617 (C=C st.), 1485 (bending C-H), EIMS: m/z (relative intensity) M<sup>+</sup> 268(100.00), 240(13.25), 136(40.56), 108(9.30). Anal. Calcd. for C<sub>16</sub>H<sub>12</sub>O<sub>4</sub> (268.27): C, 71.63; H, 4.51. Found: C, 71.45; H, 4.57. TLC (silica gel GF 254, ethyl acetate/hexane [1:1]). R<sub>f</sub> of 2,5-dihydroxyacetophenone = 0.59, compound 7 = 0.28.

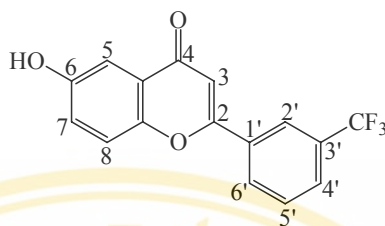
**8. 6-Hydroxy-2-(3'-chlorophenyl) chromone 8.**

Compound **8** was synthesized by using the same procedure as described for compound **1** from 2,5-dihydroxyacetophenone (0.4 g, 2.63 mmol), 3-chlorobenzoyl chloride (1.0 mL, 7.81 mmol) and DBU (1.0 mL, 6.69 mmol). After hydrolysis and purification by column chromatography (ethyl acetate/hexane [1:1]), the desired compound **8** was obtained as a yellow crystal (201.15 mg, 28.07 %); m.p. 247-248 °C;  $^1\text{H NMR}$  300 MHz (DMSO):  $\delta$  7.03 (s, 1H, H3), 7.25 (dd,  $J = 8.92, 2.85$  Hz, 1H, H7), 7.30 (d,  $J = 2.85$  Hz, 1H, H5), 7.55-7.66 (m, 2H, H5', H6'), 7.69 (d,  $J = 8.92$  Hz, 1H, H8), 8.04 (dd,  $J = 7.74, 1.15$  Hz, 1H, H4'), 8.13 (s, 1H, H2'), 10.10 (s, 1H, C<sub>6</sub>-OH) ; FTIR (KBr)(cm<sup>-1</sup>): 3341 (O-H st.), 3072 (aromatic C-H st.), 1630 (C=O st.), 1591 (C=C st.), 1479 (bending C-H); EIMS: m/z (relative intensity) M<sup>+</sup> EIMS: m/z (relative intensity) M<sup>+</sup> 272(100.00), 244(22.54), 136(76.07), 108(14.09). Anal. Calcd. for C<sub>15</sub>H<sub>9</sub>O<sub>3</sub>Cl (272.69): C, 66.07; H, 3.33. Found: C, 66.19; H, 3.19. TLC (silica gel GF 254, ethyl acetate/hexane [1:1]). R<sub>f</sub> of 2,5-dihydroxyacetophenone = 0.59, compound **8** = 0.39.

### 9. 6-Hydroxy-2-(4'-fluorophenyl) chromone 9.



Compound **9** was synthesized by using the same procedure as described for compound **1** from 2,5-dihydroxyacetophenone (0.4 g, 2.63 mmol), 4-fluorobenzoyl chloride (1.0 mL, 8.51 mmol) and DBU (1.0 mL, 6.69 mmol). After hydrolysis and purification by column chromatography (ethyl acetate/hexane [1:1]), the desired compound **7** was obtained as a pale yellow solid (41.30 mg, 6.84 %); m.p. 261-262.5 °C;  $^1\text{H NMR}$  300 MHz (DMSO):  $\delta$  6.95 (s, 1H, H3), 7.25 (dd,  $J = 8.93, 2.67$ , 1H, H7), 7.30 (d,  $J = 2.67$  Hz, 1H, H5), 7.41 (t,  $J = 8.78$  Hz, 2H, H3', H5'), 7.64 (d,  $J = 8.93$  Hz, 1H, H8), 8.13-8.17 (m, 2H, H2', H6'), 10.04 (s, 1H, C<sub>6</sub>-OH) ; FTIR (KBr)( $\text{cm}^{-1}$ ): 3295 (O-H st.), 3078 (aromatic C-H st.) 1649 (C=O st.), 1624 (C=C st.), 1479 (bending C-H), 1163 (C-O st.); EIMS:  $m/z$  (relative intensity)  $\text{M}^+$  256(72.87), 228(13.26), 136(100.00), 108(26.17). Anal. Calcd. for  $\text{C}_{15}\text{H}_9\text{O}_3\text{F}$  (256) C, 70.31; H, 3.51 Found: C, 70.30; H, 3.26. TLC (silica gel GF 254, ethyl acetate/hexane [1:1]).  $R_f$  of 2,5-dihydroxyacetophenone = 0.59, compound **9** = 0.32.

**10. 6-Hydroxy-2-(3'-trifluoromethylphenyl) chromone 10.**

Compound **10** was synthesized by using the same procedure as described for compound **1** from 2,5-dihydroxyacetophenone (0.4 g, 2.63 mmol), 3-trifluoromethylbenzoyl chloride (1.0 mL, 6.79 mmol) and DBU (1.0 mL, 6.69 mmol). After hydrolysis and purification by column chromatography (ethyl acetate/hexane [1:1]), the desired compound **7** was obtained as a pale yellow solid (24.10 mg, 2.99 %); m.p. 259.1-260.3 °C;  $^1\text{H NMR}$  300 MHz (DMSO):  $\delta$  7.15 (s, 1H, H3), 7.26 (dd,  $J = 8.96$ , 2.82, 1H, H7), 7.31 (d,  $J = 2.82$  Hz, 1H, H5), 7.72 (d,  $J = 8.96$  Hz, 1H, H8), 7.80 (t,  $J = 7.86$  Hz, 1H, H5'), 7.95 (d,  $J = 7.86$  Hz, 1H, H6'), 8.40 (m, 2H, H2', H4'), 10.06 (s, 1H, C<sub>6</sub>-OH); FTIR (KBr)(cm<sup>-1</sup>): 3434 (O-H st.), 3091 (aromatic C-H st.), 1639 (C=O st.), 1592 (C=C st.), 1471 (bending C-H), 1163 (C-O st.); EIMS:m/z (relative intensity) M<sup>+</sup> 306(65.39), 278(19.82), 136(100.00), 108(22.73). Anal. Calcd. for C<sub>16</sub>H<sub>9</sub>O<sub>3</sub>F<sub>3</sub> (306): C, 62.75; H, 2.94. Found: C, 63.26; H, 2.72. TLC (silica gel GF 254, ethyl acetate/hexane [1:1]). R<sub>f</sub> of 2,5-dihydroxyacetophenone = 0.59, compound **10** = 0.36.

## CHAPTER IV

### BIOLOGICAL EXPERIMENTAL

#### A. Equipment and reagents

##### 1. Equipment

Analytical balance model 2842	Satorius, Germany
High performance liquid chromatography	
- Column (BDS C <sub>18</sub> , 5 μm, 250 x 4.6 mm)	Hypersil <sup>®</sup> , USA
- High pressure pump, LC-10 AD	Shimadzu, Japan
- UV-Visible detector, SPD-10A	Shimadzu, Japan
Incubator	Thermolyne, USA
Micropipette 0.2-2 μL (Pipetman)	Gilson, France
Micropipette 1-10 μL (Pipetman)	Gilson, France
Micropipette 2-20 μL (Pipetman)	Gilson, France
Micropipette 20-200 μL (Pipetman)	Gilson, France
Micropipette 100-1000 μL (Model 5000)	Nichirio, Japan
Mini centrifuge (Model C-1200)	National Labnet. Co, USA
Ultrasonic bath	Branson 52, USA

##### 2. Reagents

Acetonitrile, HPLC grade	J.T.Baker, USA
Dimethyl sulfoxide	Sigma, USA
Dithiothreitol	Sigma, USA
Glycerol	Aldrich, USA
HIV-1 protease (H-9040, Lot. No. 9750004)	Bachem, Switzerland
Pepstatin A	Sigma, USA
Sodium acetate	Sigma, USA
Sodium chloride	Fluka, Switzerland

Substrate Anthranilyl (His-Lys-Ala-Arg-Val-Leu-  
(*p*-NO<sub>2</sub>-Phe)-Glu-Ala-Nle-Ser-Amide,

H-0811 Lot. No. 72H06801)

Sigma, USA

Trifluoroacetic acid

Fluka, Switzerland

## B. Methods

### HPLC assay

A stopped time HPLC assay was performed by incubating peptide substrate with the protease enzyme in small volumes (< 0.1 mL). A modified peptide, antranilyl His-Lys-Ala-Arg-Val-Leu-(*p*-NO<sub>2</sub>-Phe)-Glu-Ala-Nle-Ser-Amide, whose amino acid sequence corresponds to the p24-p15 cleavage site of viral polyprotein was used as a substrate. During the incubation, the substrate was hydrolyzed at the site of Leu and (*p*-NO<sub>2</sub>-Phe). After quenching with acid at selected times, the sample was subjected to reverse phase HPLC on octadecylsilane column. The resulting peptidolytic products were thereby separated from the remaining substrate using linear gradient of acetonitrile in 0.1 % trifluoroacetic acid (TFA) with spectrophotometric detection of the peptides at 280 nm. The percentage of relative inhibitory ratio (% IR) was calculated from the ratio of the substrate peak area to the hydrolysate peak area. The following reagents were prepared for the assays:

1. Antranilyl His-Lys-Ala-Arg-Val-Leu-(*p*-NO<sub>2</sub>-Phe)-Glu-Ala-Nle-Ser-Amide (1 μg/μL).
2. Substrate buffer (50 mM NaOAc, pH 4.9).
3. Inhibitors (chromone derivatives, 12.5 μg/mL).
4. Positive control (pepstatin A, 0.1 mM) dissolved in DMSO.
5. Assay buffer (50 mM NaOAc, pH 4.9, 200 mM NaCl, 5 mM dithiothreitol (DTT) and 10 % (v/v) glycerol in water).
6. Purified HIV-1 protease biosynthetic enzyme from *E.coli* (0.005 μg/μL).

**Table 2.** Composition of the HPLC assay mixture.

Reagents	Negative control ( $\mu\text{L}$ )	Positive control ( $\mu\text{L}$ )	Sample ( $\mu\text{L}$ )
Assay buffer	20.4	20.4	20.4
Substrate	1.6	1.6	1.6
50 % DMSO	1.6	-	-
Inhibitor	-	-	1.6
Pepstatin A	-	1.6	-
Enzyme	1.4	1.4	1.4
<b>Total volume</b>	<b>25.0</b>	<b>25.0</b>	<b>25.0</b>

HPLC condition:

Column	:	Hypersil <sup>®</sup> BDS C18, particle size: 5 $\mu\text{m}$ , 250 x 4.6 mm
Injection volume	:	20 $\mu\text{L}$
Solvent	:	A. 0.1 % trifluoroacetic acid in water B. acetonitrile/water (3:1)
Gradient	:	22.5 % to 40 % of solvent B in 12 minutes
Flow rate	:	1.5 mL/min
UV Detector	:	$\lambda$ 280 nm

The reaction mixture was incubated at 37 °C for 2 hours and then terminated by addition of 2.5  $\mu\text{L}$  of 10 % trifluoroacetic acid. The hydrolysate and the remaining substrate were quantitatively analyzed by reverse phase HPLC with a gradient of solvent B (22.5 % - 40 %) at a flow rate of 1.5 mL/min. The elution profile was monitored with UV-visible detector (SPD-10A) at 280 nm. The hydrolysate and substrate were eluted at 5.9 and 10.1 min, respectively (Figure 16). The percentage of relative inhibitory ratio (% IR) of a compound on HIV-PR is calculated as follows:

$$\% \text{ IR} = \frac{(A_{\text{Negative control}} - A_{\text{Sample}})}{A_{\text{Negative control}}} \times 100 \quad (\text{A is a relative peak area of the hydrolysate}).$$

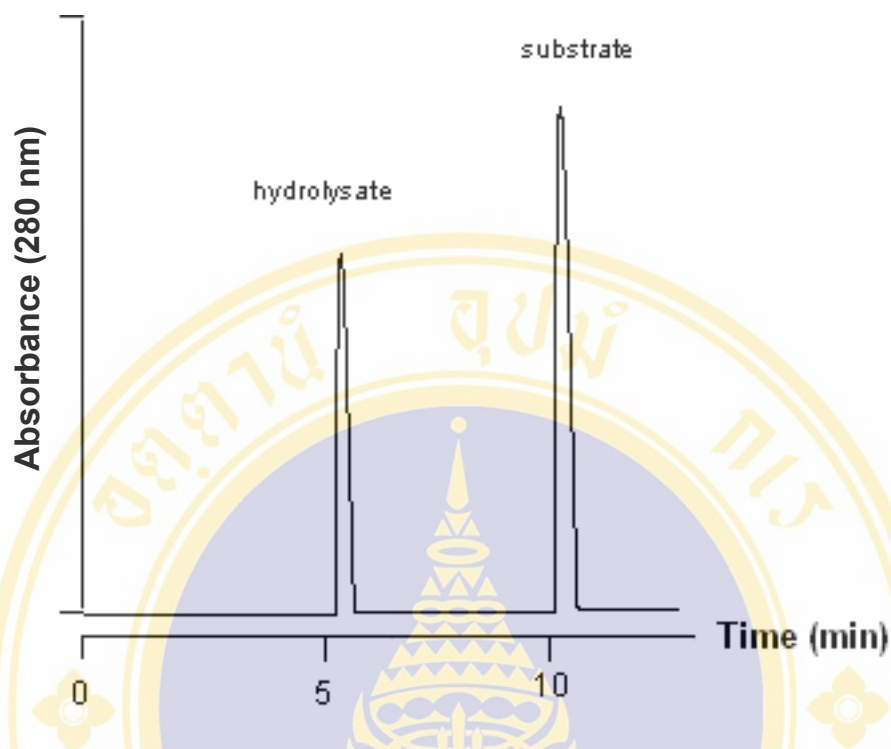


**Figure 16.** Chromatograms of HIV-1 PR inhibitory activity assay.

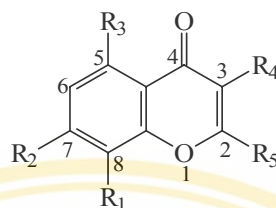
## CHAPTER V

### RESULTS AND DISCUSSION

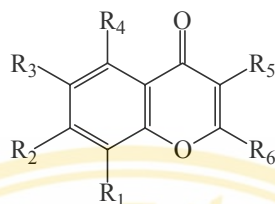
#### A. General discussion

HIV protease is an important enzymes for HIV life cycle due to a crucial step in the replication cycle of the virus involving the processing by virus-encoded protease of the viral *gag* and *gag-pol* polyproteins into structural proteins and enzymes essential for the proper assembly and maturation of fully infection virion. Although the peptide-derived inhibitors are potent HIV-1 protease inhibitors, they are typically not suitable drug candidate. The early problems of peptidic protease inhibitors, poor oral bioavailability and severe side effects caused by the necessarily high doses of the inhibitors, strengthened the development of non-peptidic protease inhibitors that promised better bioavailability and/or pharmacokinetic properties.

In the ongoing to search for new and better HIV-1 protease inhibitors, our research group has designed and synthesized a new class of non-peptidic compounds in chromone series (structures as shown in Table 3). In this study, more derivatives in this chromone series have been synthesized based on the previous 3D QSAR, CoMFA and CoMSIA studies (structure as shown in Table 4). All compounds were prepared using one-pot cyclization reaction with DBU as a base. Their structures were characterized by  $^1\text{H}$  NMR, mass spectrometry, infrared spectrophotometry and elemental analysis. The synthesized compounds were evaluated for their *in vitro* enzyme inhibitory activity by HPLC assay using recombinant HIV-1 protease enzyme expressed in *E.coli* and anthranilyl His-Lys-Ala-Arg-Val-Leu-(*p*-NO<sub>2</sub>-Phe)-Glu-Ala-Nle-Ser-NH<sub>2</sub> as a substrate.

**Table 3.** Structures of the previously synthesized chromone derivatives (22).

Compound	R <sub>1</sub>	R <sub>2</sub>	R <sub>3</sub>	R <sub>4</sub>	R <sub>5</sub>
1	H	OH	H	H	4'-(NO <sub>2</sub> )-Phenyl
2	H	OH	H	H	3'-(CF <sub>3</sub> )-Phenyl
3	H	OH	H	H	4'-(F)-Phenyl
4	H	OH	H	H	3',5'-(diNO <sub>2</sub> )-Phenyl
5	H	OH	H	H	3'-(Cl)-Phenyl
6	H	OH	H	H	3',4'-(diCl)-Phenyl
7	H	OH	H	H	4'-( <i>t</i> -butyl)-Phenyl
8	H	OH	OH	H	3'-(CF <sub>3</sub> )-Phenyl
9	H	OH	OH	H	4'-(F)-Phenyl
10	H	OH	OH	H	3',4'-(diF)-Phenyl
11	H	OH	OH	H	4'-( <i>t</i> -butyl)-Phenyl
12	H	OH	OH	H	3'-(Cl)-Phenyl
13	H	OH	OH	H	3',4'-(diCl)-Phenyl
14	H	OH	OH	H	4'-(OCH <sub>3</sub> )-Phenyl
15	H	OH	OH	H	3'-(OCH <sub>3</sub> )-Phenyl
16	H	OH	OH	H	4'-(NO <sub>2</sub> )-Phenyl
17	H	OH	OH	H	3',5'-(diNO <sub>2</sub> )-Phenyl
18	OH	OH	H	4''-(NO <sub>2</sub> )-Benzoyl	4'-(NO <sub>2</sub> )-Phenyl
19	H	OH	H	4''-(NO <sub>2</sub> )-Benzoyl	4'-(NO <sub>2</sub> )-Phenyl
20	OH	OH	H	3''-(CF <sub>3</sub> )-Benzoyl	3'-(CF <sub>3</sub> )-Phenyl
21	H	OH	H	3''-(CF <sub>3</sub> )-Benzoyl	3'-(CF <sub>3</sub> )-Phenyl
22	OH	OH	H	4''-(F)-Benzoyl	4'-(F)-Phenyl
23	H	OH	H	4''-(F)-Benzoyl	4'-(F)-Phenyl
24	H	OH	H	3'',4''-(diF)-Benzoyl	3',4'-(diF)-Phenyl
25	H	OH	OH	4''-(NO <sub>2</sub> )-Benzoyl	4'-(NO <sub>2</sub> )-Phenyl
26	H	OH	H	4''-(OCH <sub>3</sub> )-Benzoyl	4'-(OCH <sub>3</sub> )-Phenyl
27	H	OH	H	3''-(OCH <sub>3</sub> )-Benzoyl	3'-(OCH <sub>3</sub> )-Phenyl
28	OH	H	H	H	Phenyl
29	H	OH	H	H	CH <sub>3</sub>
30	H	OH	H	H	Phenyl
31	H	OH	H	H	Benzyl
32	OH	OH	H	H	CH <sub>3</sub>
33	OH	OH	H	H	Phenyl
34	OH	OH	H	H	Benzyl
35	H	OH	H	CH <sub>3</sub>	Phenyl
36	H	OH	H	CH <sub>3</sub>	Benzyl

**Table 4.** Structures of chromone derivatives synthesized in this study.

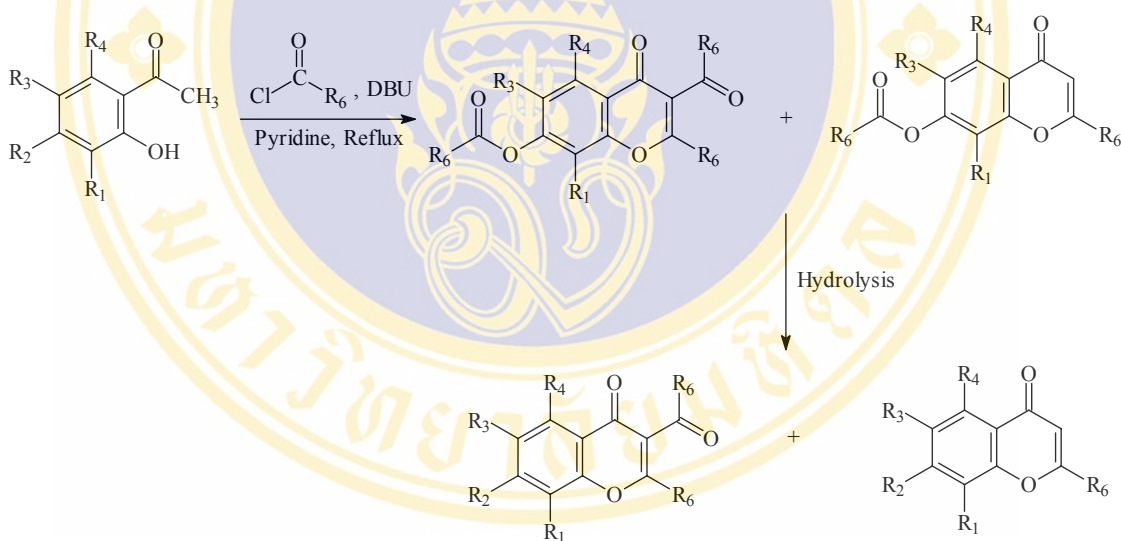
Cpd.	R <sub>1</sub>	R <sub>2</sub>	R <sub>3</sub>	R <sub>4</sub>	R <sub>5</sub>	R <sub>6</sub>
1	H	OH	H	H	4''-( <i>t</i> -butyl)-Benzoyl	4'-( <i>t</i> -butyl)-Phenyl
2	H	OH	H	H	3''-(Cl)-Benzoyl	3'-(Cl)-Phenyl
3	OH	OH	H	H	3''-(Cl)-Benzoyl	3'-(Cl)-Phenyl
4	OH	OH	H	H	4''-(OCH <sub>3</sub> )-Benzoyl	4'-(OCH <sub>3</sub> )-Phenyl
5	OH	OH	H	H	3''-(OCH <sub>3</sub> )-Benzoyl	3'-(OCH <sub>3</sub> )-Phenyl
6	H	OH	H	OH	3''-(OCH <sub>3</sub> )-Benzoyl	3'-(OCH <sub>3</sub> )-Phenyl
7	H	H	OH	H	H	3'-(OCH <sub>3</sub> )-Phenyl
8	H	H	OH	H	H	3'-(Cl)-Phenyl
9	H	H	OH	H	H	4'-(F)-Phenyl
10	H	H	OH	H	H	3'-(CF <sub>3</sub> )-Phenyl

## B. Synthesis of chromone derivatives by one-pot cyclization reaction

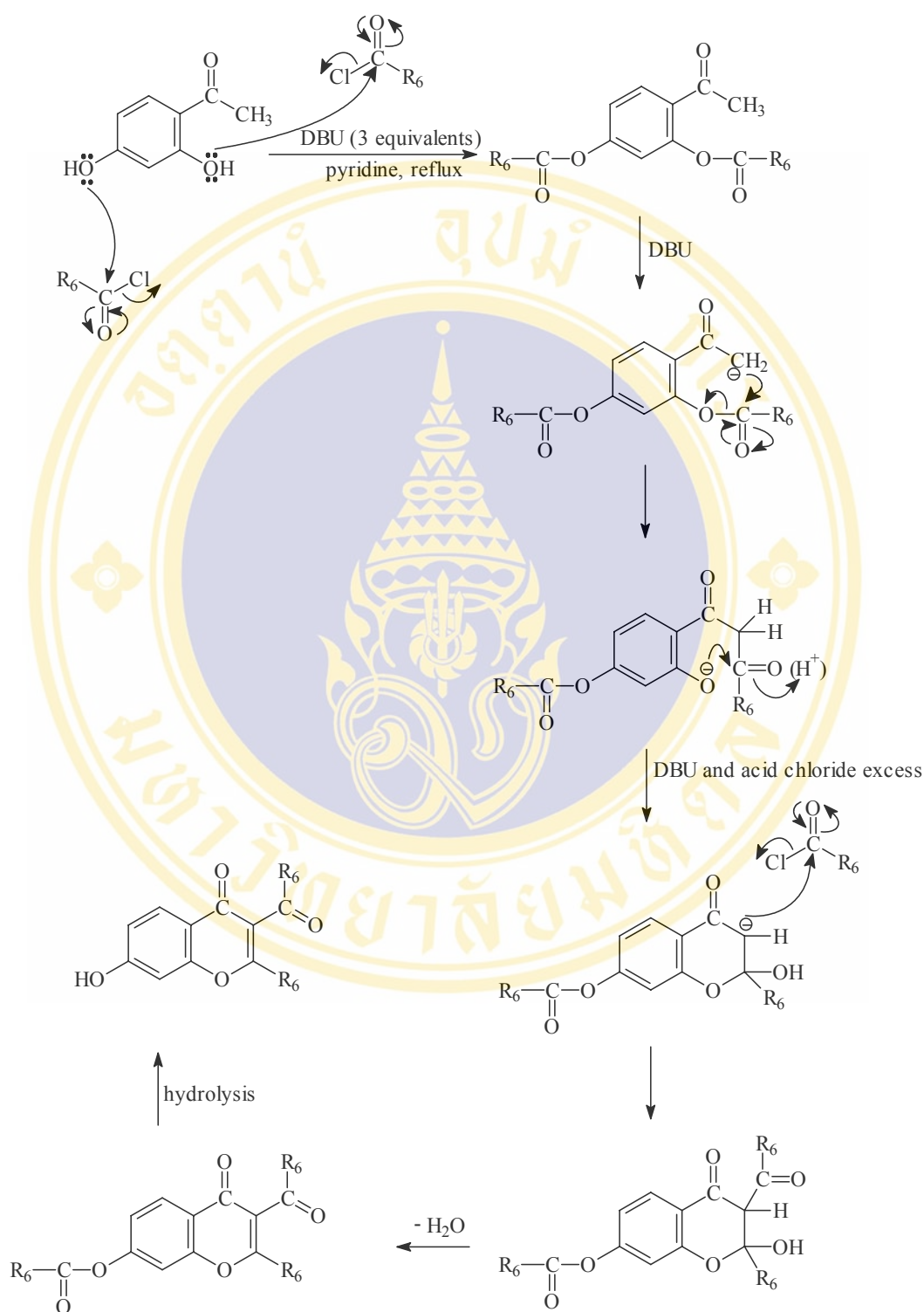
The cyclization of phenolic ketones was carried out in one step by reacting with aroyl chlorides in the presence of 1,8-diazabicyclo[5,4,0]undec-7-ene (DBU), outline as shown in Scheme 1 and Scheme 2. The phenolic ketone was dissolved in pyridine and refluxed with the appropriate aroyl chloride and DBU at 140-160°C for 30 hours. The intermediate ester compound was hydrolyzed using the mixture of NaOH, methanol, water and 1,4-dioxane to yield the desired chromone derivatives.

The synthesized compounds were purified by column chromatography and/or recrystallization. The structures of pure compounds were identified by Fourier transform infrared spectroscopy (FT-IR), nuclear magnetic resonance spectroscopy (NMR), mass spectrometry (MS), and elemental analysis.

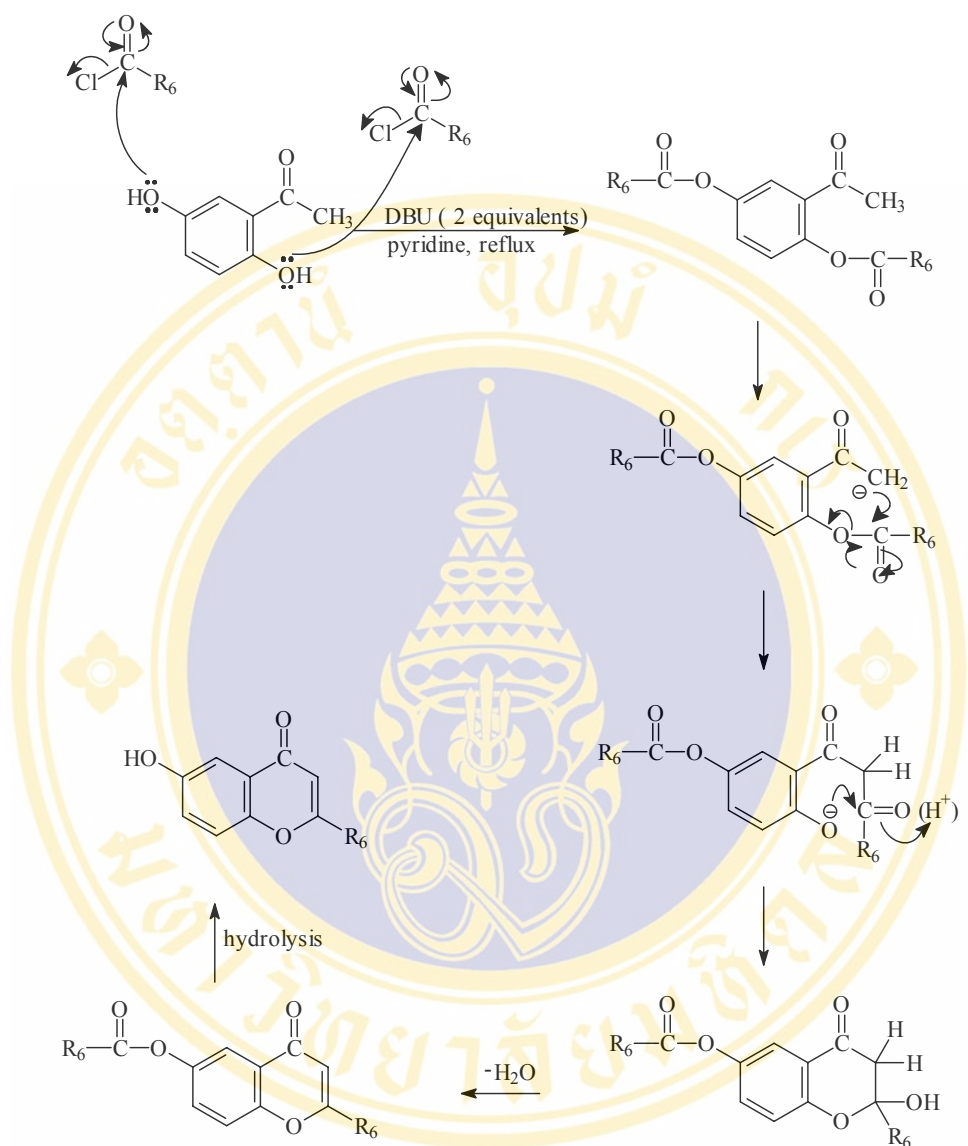
The proposed mechanism of cyclization of compounds **1-6** in Table 4 ( $R_1, R_4 = H, OH; R_2 = OH; R_3 = H$ ) is shown in Scheme 2 using 2,4-dihydroxy acetophenone as an example and compounds **7-10** ( $R_1, R_2, R_4 = H; R_3 = OH$ ) is shown in Scheme 3 using 2,5-dihydroxy acetophenone as an example. The phenolic ester intermediate was initially formed and subsequent abstraction of acidic methylene proton by DBU. The obtained carbanion nucleophile attacked the ester carbonyl carbon leading to  $\beta$ -diketone. Cyclization of  $\beta$ -diketone followed by dehydration leading to the chromone ester. The chromone ester was finally hydrolyzed by the mixture of NaOH in methanol, water and dioxane yielded the desired chromone derivatives. Ten new compounds were accomplished and the percent yields of cyclized products were summarized in Table 5.



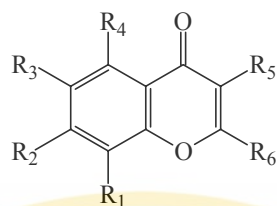
**Scheme 1.** Synthesis of chromone derivatives compounds **1-10**.



**Scheme 2.** Proposed mechanism of one-pot cyclization of compounds 1-6.



**Scheme 3.** Proposed mechanism of one-pot cyclization of compounds **7-10**.

**Table 5.** Melting point (m.p.) and % yield of chromone derivatives.

Cpd.	R <sub>1</sub>	R <sub>2</sub>	R <sub>3</sub>	R <sub>4</sub>	R <sub>5</sub>	R <sub>6</sub>	m.p. (°C)	% yield
1	H	OH	H	H	4''-( <i>t</i> -butyl)-Benzoyl	4'-( <i>t</i> -butyl)-Phenyl	271-273	25.38
2	H	OH	H	H	3''-(Cl)-Benzoyl	3'-(Cl)-Phenyl	303.305	23.14
3	OH	OH	H	H	3''-(Cl)-Benzoyl	3'-(Cl)-Phenyl	256-257	11.50
4	OH	OH	H	H	4''-(OCH <sub>3</sub> )-Benzoyl	4'-(OCH <sub>3</sub> )-Phenyl	253-254	5.81
5	OH	OH	H	H	3''-(OCH <sub>3</sub> )-Benzoyl	3'-(OCH <sub>3</sub> )-Phenyl	255-257	14.97
6	H	OH	H	OH	3''-(OCH <sub>3</sub> )-Benzoyl	3'-(OCH <sub>3</sub> )-Phenyl	167.2-168	6.68
7	H	H	OH	H	H	3'-(OCH <sub>3</sub> )-Phenyl	226-228	11.97
8	H	H	OH	H	H	3'-(Cl)-Phenyl	247-248	28.07
9	H	H	OH	H	H	4'-(F)-Phenyl	261-262.5	6.84
10	H	H	OH	H	H	3'-(CF <sub>3</sub> )-Phenyl	259.1-260.3	2.99

The percentage yields of the cyclized products shown in Table 5 are not high, approximately 3-28 %. The low yield of the desired products might be due to most of starting aroyl chloride have the electron-donating groups (*t*-butyl, methoxy) at *para* or *meta* position. These electron-donating groups will decrease the electrophilicity of the carbonyl group in the aroyl chloride (see also Scheme 2 and Scheme 3). Moreover, the cyclization reactions also gave the other undesired products which were not yet identified. As seen from Table 5, the starting phenolic ketones with R<sub>2</sub> = OH and R<sub>1</sub>, R<sub>2</sub> and R<sub>3</sub> = H or OH gave the resulting cyclized products with double reacted phenolic ketones (compounds **1-6**). When the phenolic ketones possess R<sub>1</sub>, R<sub>2</sub>, and R<sub>4</sub> = H; R<sub>3</sub> = OH, the reaction provided the products with only one phenolic ketone

reacted (compounds **7-10**). The underlie basis for these different types of products is still unclear.

The IR spectrum of the obtained chromone derivatives showed the similar pattern, e.g., IR spectrum 7-hydroxy-2-(4'-*tert*-butylphenyl)-3-(4''-*tert*-butylbenzoyl) chromone **1** (Figure 17.) showed the frequency of O-H stretching of the hydroxyl group at  $3420\text{ cm}^{-1}$ , C=O stretching at  $1683\text{ cm}^{-1}$  and C=C aromatic stretching at  $1624\text{ cm}^{-1}$ .

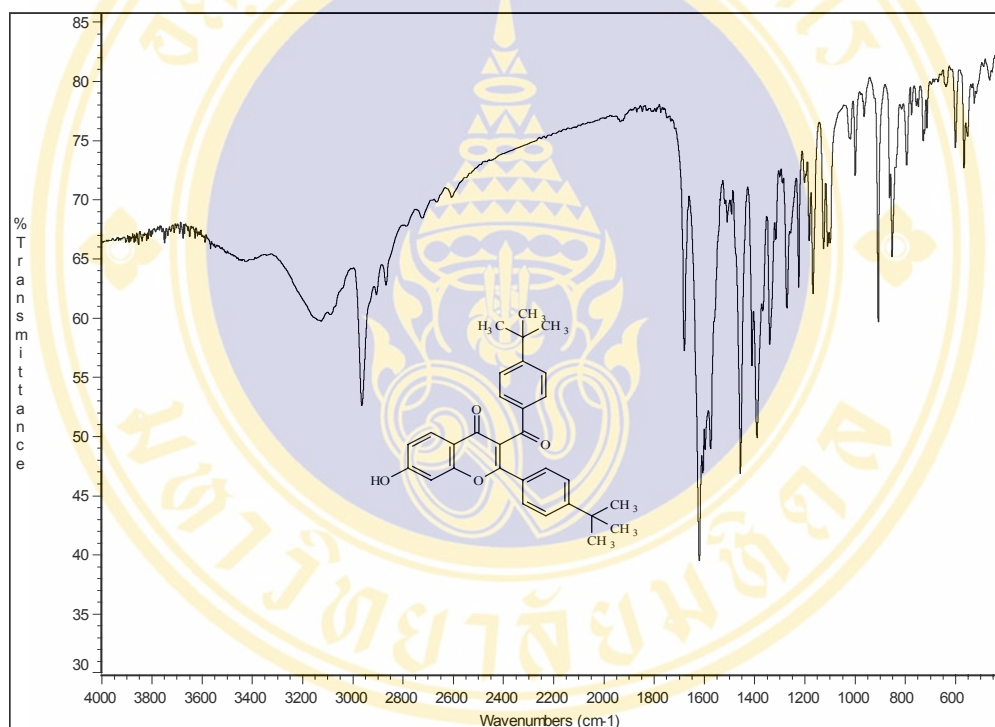


**Figure 17.** IR spectrum of 7-hydroxy-2-(4'-*tert*-butylphenyl)-3-(4''-*tert*-butyl benzoyl) chromone **1**.

$^1\text{H}$  NMR spectrum of compound **1** (taken as an example) is shown in Figure 18. The two singlets at  $\delta$  1.23 ppm and  $\delta$  1.27 ppm represent the *tert*-butyl protons in ring B and ring D, respectively. The doublet of doublet at  $\delta$  6.95 ppm represents one proton of benzopyran H6 *ortho*-coupling with benzopyran H5 ( $J = 7.95$  Hz) and *meta*-coupling with benzopyran H8 ( $J = 1.13$  Hz). The doublet at  $\delta$  6.98 ppm represents one proton of benzopyran H8 *meta*-coupling with benzopyran H6 ( $J = 1.13$  Hz). The doublet at  $\delta$  7.45 ppm represents two protons of H3' and H5' (ring B) *ortho*-coupling with H2' and H6' ( $J = 8.32$ ). The doublet at  $\delta$  7.49 ppm represents two protons of H3'' and H5'' (ring D) *ortho*-coupling with H2'' and H6'' ( $J = 8.48$ ). The doublet at  $\delta$  7.55 ppm represents two protons of H2' and H6' *ortho*-coupling with H3' and H5' ( $J = 8.32$ ). The doublet at  $\delta$  7.82 ppm represents two protons of H2'' and H6'' *ortho*-coupling with H3'' and H5'' ( $J = 8.48$ ). The doublet at  $\delta$  7.86 ppm represents one proton of benzopyran H5 *ortho*-coupling with benzopyran H6 ( $J = 7.95$  Hz).

Most of the EI mass spectra of chromone derivatives had characteristic peaks at  $m/z$   $M^+$ ,  $M^+ - 29$ , 397 and 265 as shown in mass spectrum of compound **1** in Figure 19. The proposed fragmentation mechanism was illustrated in Figure 20, compound **1** was taken as an example.

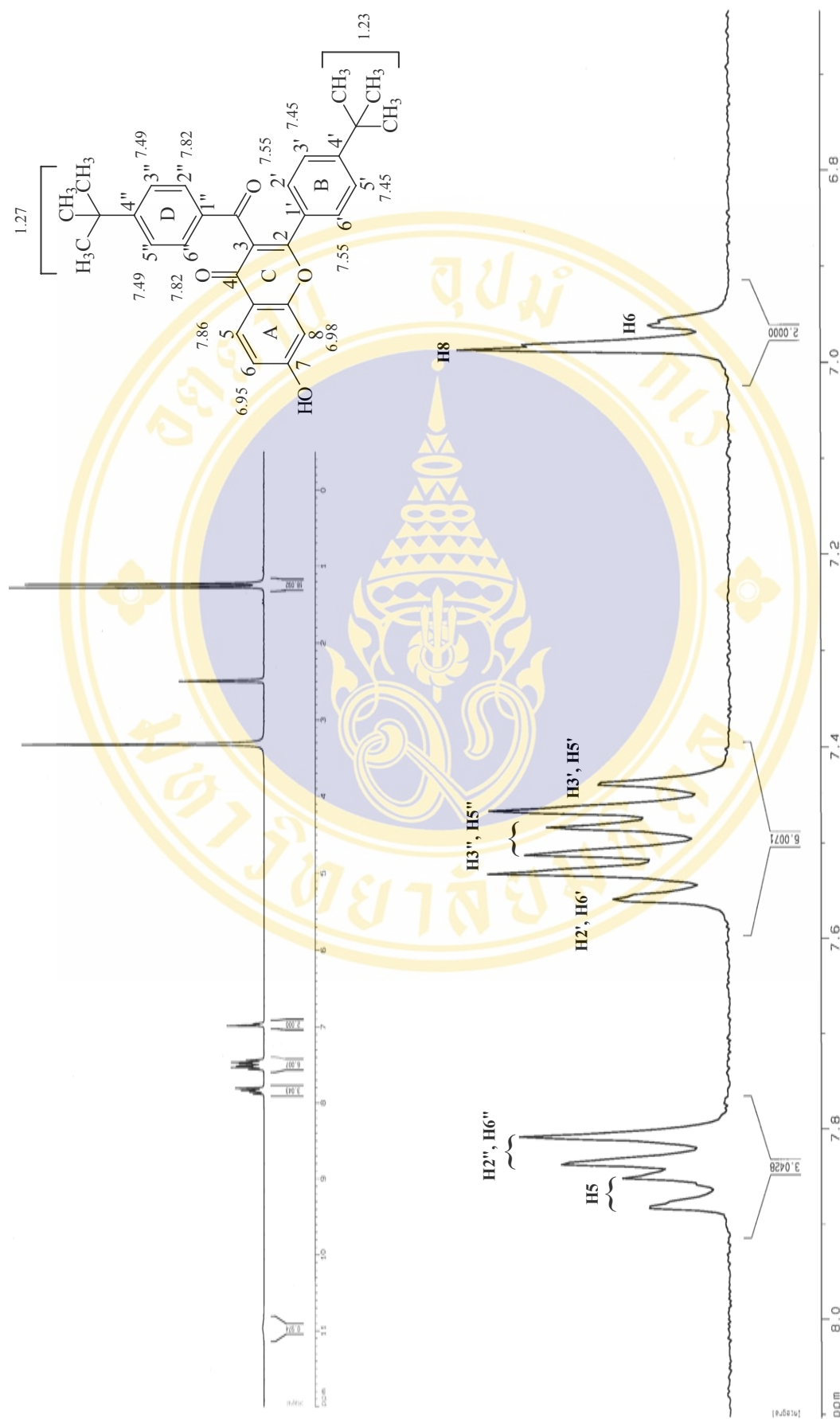


**Figure 18.** <sup>1</sup>H NMR spectrum (300 MHz, DMSO, DMSO-d<sub>6</sub>) of 7-hydroxy-2-(4''-tert-butylphenyl)-3-(4'-tert-butylphenyl)chromone **1**.

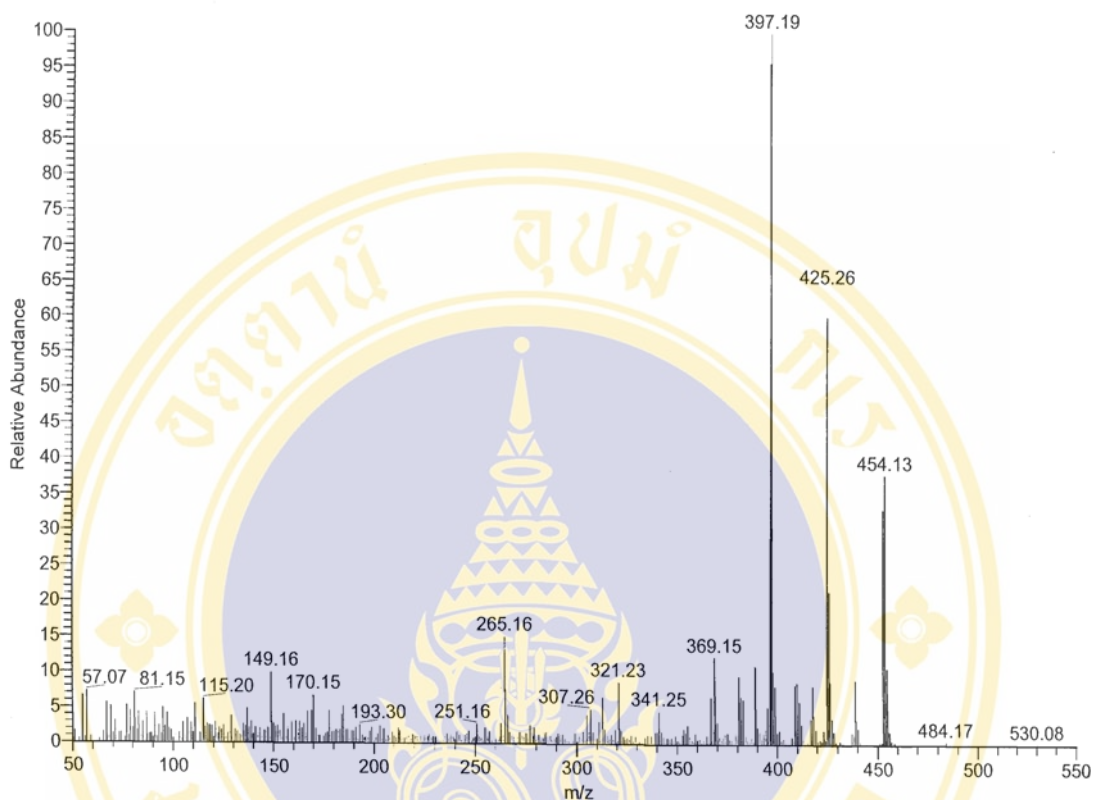


**Figure 19.** EI mass spectrum of 7-hydroxy-2-(4'-*tert*-butylphenyl)-3-(4''-*tert*-butyl benzoyl) chromone **1**.

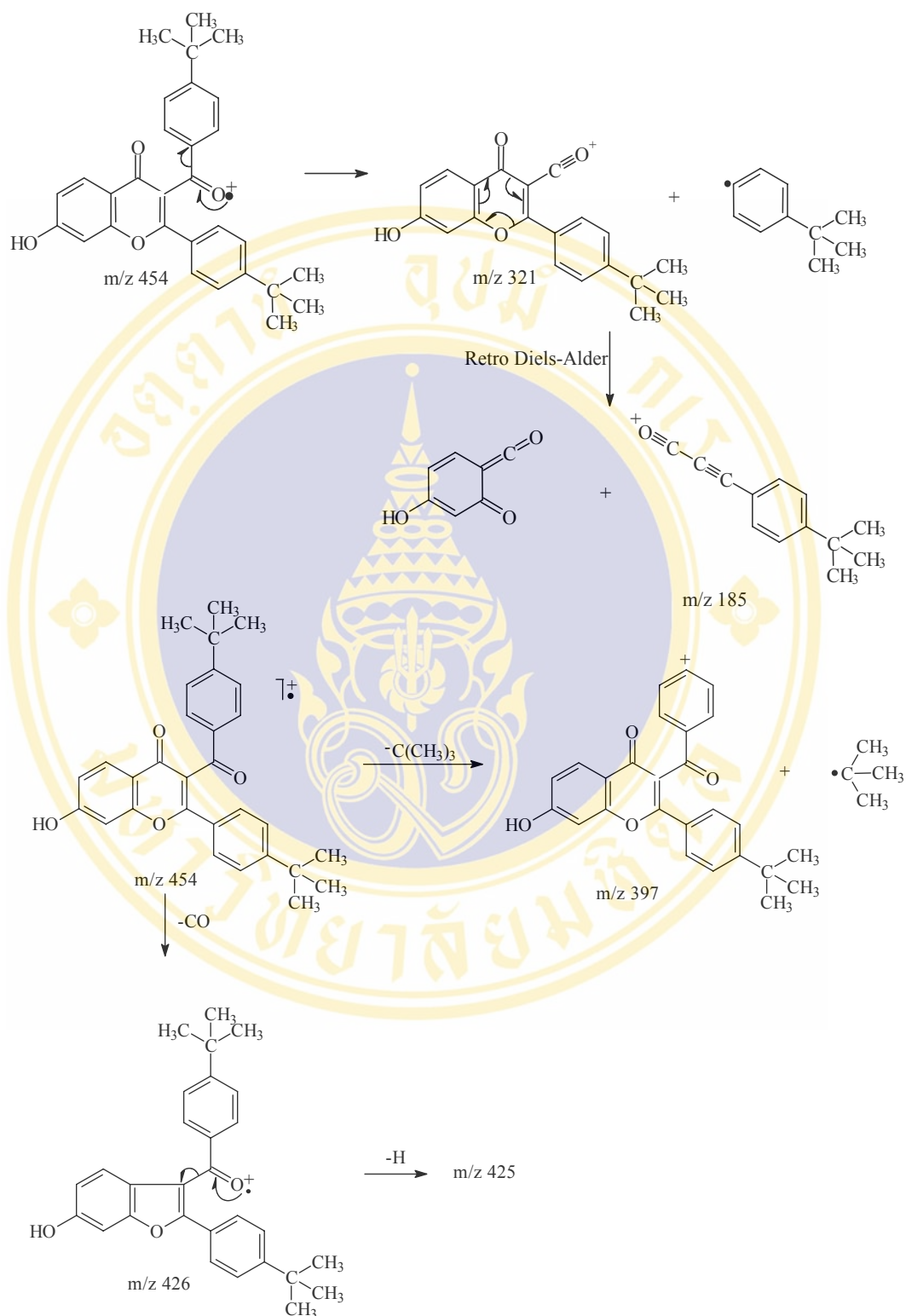


**Figure 20.** Proposed fragmentation mechanism of 7-hydroxy-2-(4'-*tert*-butylphenyl)-3-(4''-*tert*-butylbenzoyl) chromone **1**.

The IR spectrum of 6-hydroxy-2-(3'-fluorophenyl) chromone **9** (Figure 21) showed the frequency of O-H stretching of the hydroxyl group at  $3295\text{ cm}^{-1}$ , C=O stretching at  $1649\text{ cm}^{-1}$  and C=C aromatic stretching at  $1624\text{ cm}^{-1}$ .

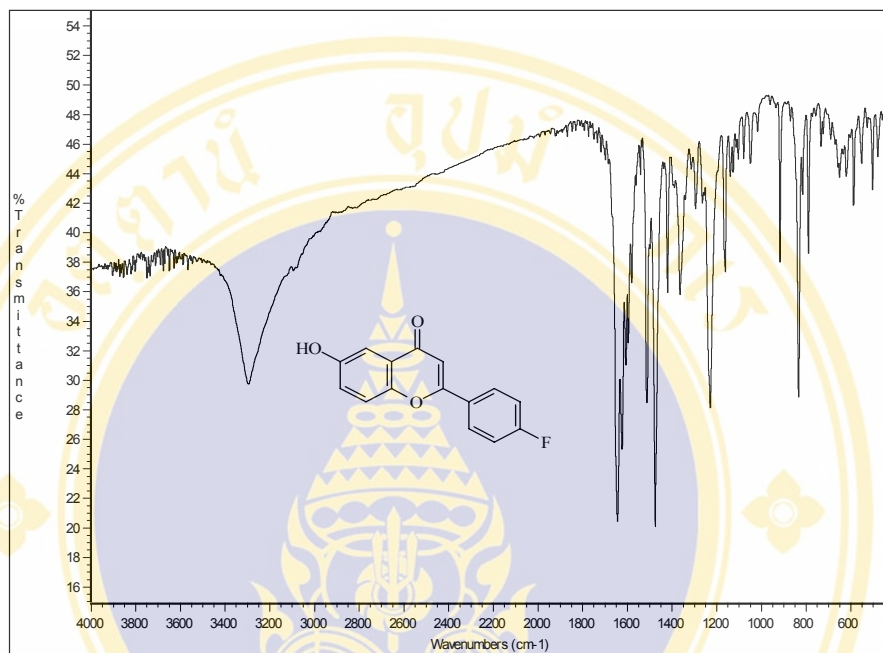


**Figure 21.** IR spectrum of 6-hydroxy-2-(3'-fluorophenyl) chromone **9**.

$^1\text{H}$  NMR spectra of compound **9** (taken as an example) are shown in Figure 22. The singlet at  $\delta$  6.95 ppm represents one proton of benzopyran H3. The doublet of doublet at  $\delta$  7.25 ppm represents one proton of benzopyran H7 ortho-coupling with benzopyran H8 ( $J = 8.93\text{ Hz}$ ) and *meta*-coupling with benzopyran H5 ( $J = 2.67\text{ Hz}$ ). The doublet at  $\delta$  7.30 ppm represents one proton of benzopyran H5 *meta*-coupling with benzopyran H7 ( $J = 2.67\text{ Hz}$ ). The triplet at  $\delta$  7.41 ppm represents two protons of H3' and H'5 (ring B) coupling with H2', H6' ( $J = 8.78\text{ Hz}$ .) and coupling with 4'-F ( $J = 8.78\text{ Hz}$ ).  $^{19}\text{F}$  is a sensitive nucleus which yields sharp signals and has a wide chemical shift range. The doublet at  $\delta$  7.64 ppm represents one proton of benzopyran H8 *ortho*-coupling with benzopyran H7 ( $J = 8.93\text{ Hz}$ ). The multiplet peaks between  $\delta$  8.13-8.17 ppm represent two protons of H2' and H6'. The singlet at  $\delta$  10.04 ppm represents one proton of C<sub>6</sub>-OH of benzopyran.

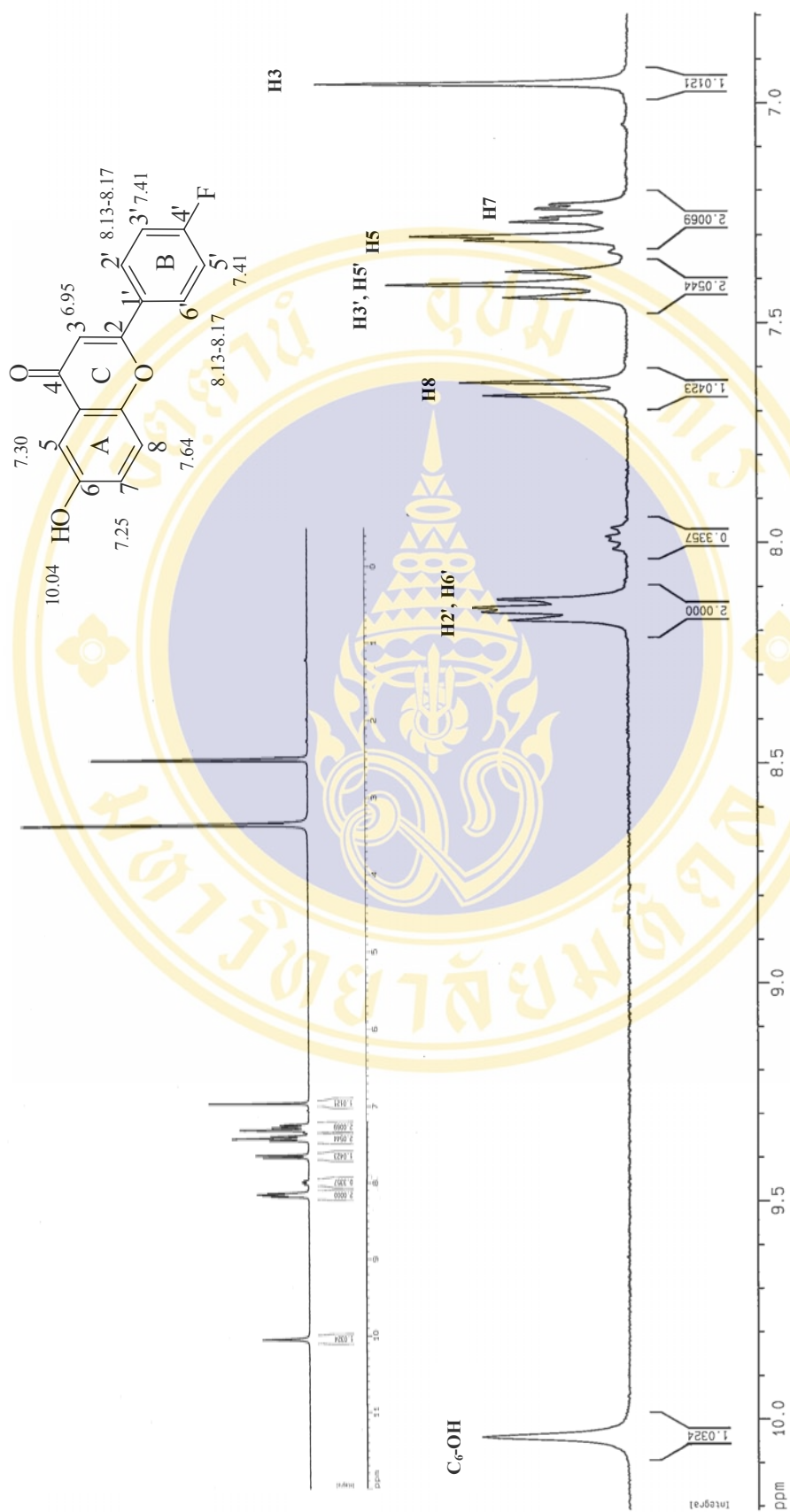


**Figure 22.** <sup>1</sup>H NMR spectrum (300 MHz, DMSO) of 6-hydroxy-2-(3'-fluorophenyl)chromone **9**

The EI mass spectrum of compound **9** had the characteristic peaks at  $m/z$   $M^+$ ,  $M^+-28(228)$  and 136 (Figure 23). The proposed fragmentation mechanism of compound **9** was illustrated in Figure 24.

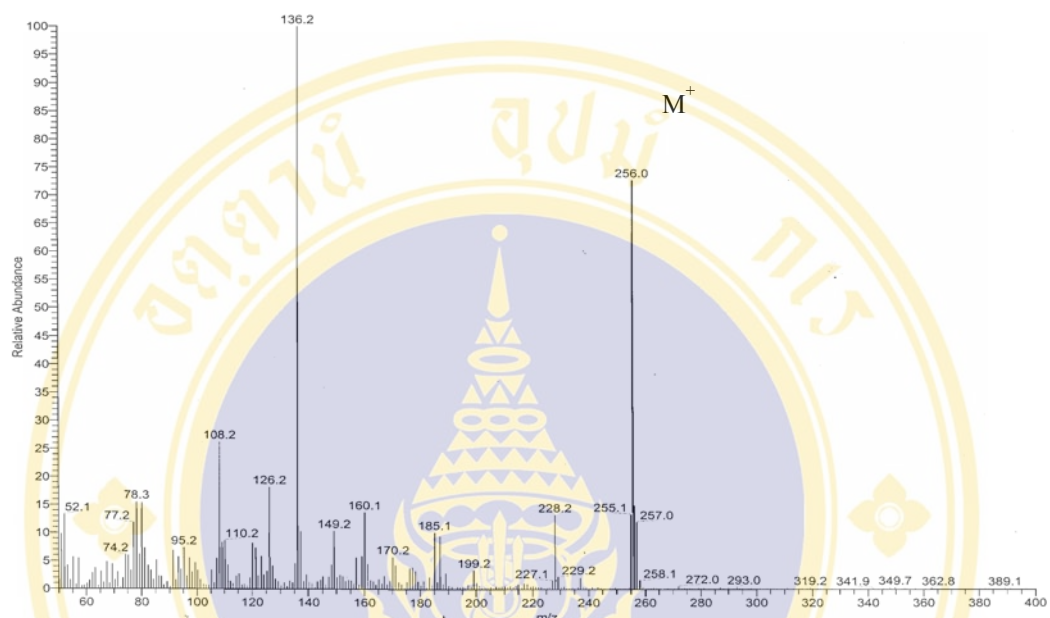


**Figure 23.** EI mass spectrum of 6-hydroxy-2-(3'-fluorophenyl) chromone **9**.

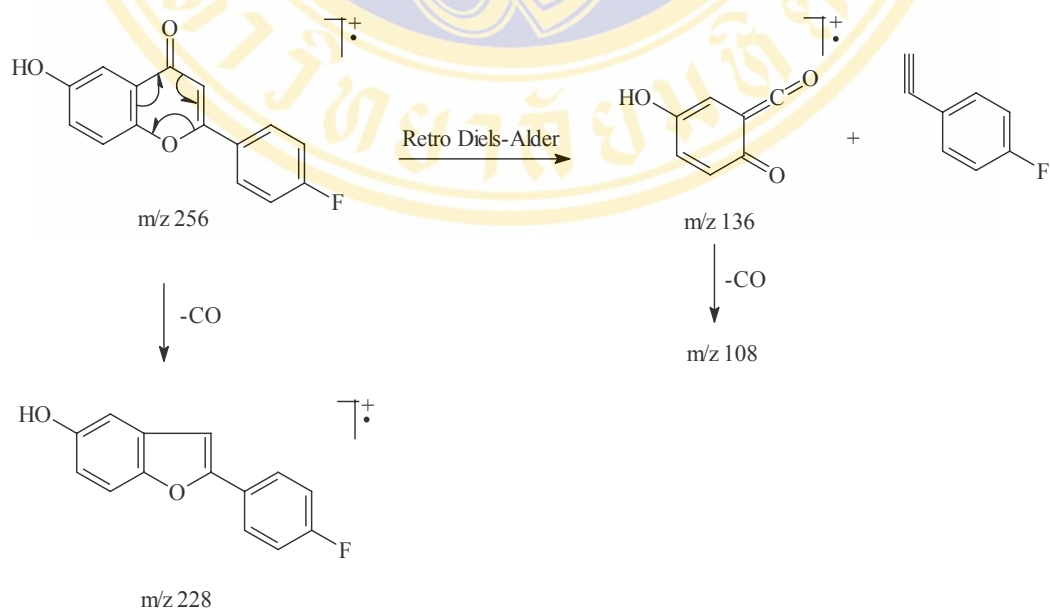


**Figure 24.** Proposed fragmentation mechanism of 6-hydroxy-2-(3'-fluorophenyl) chromone **9**.

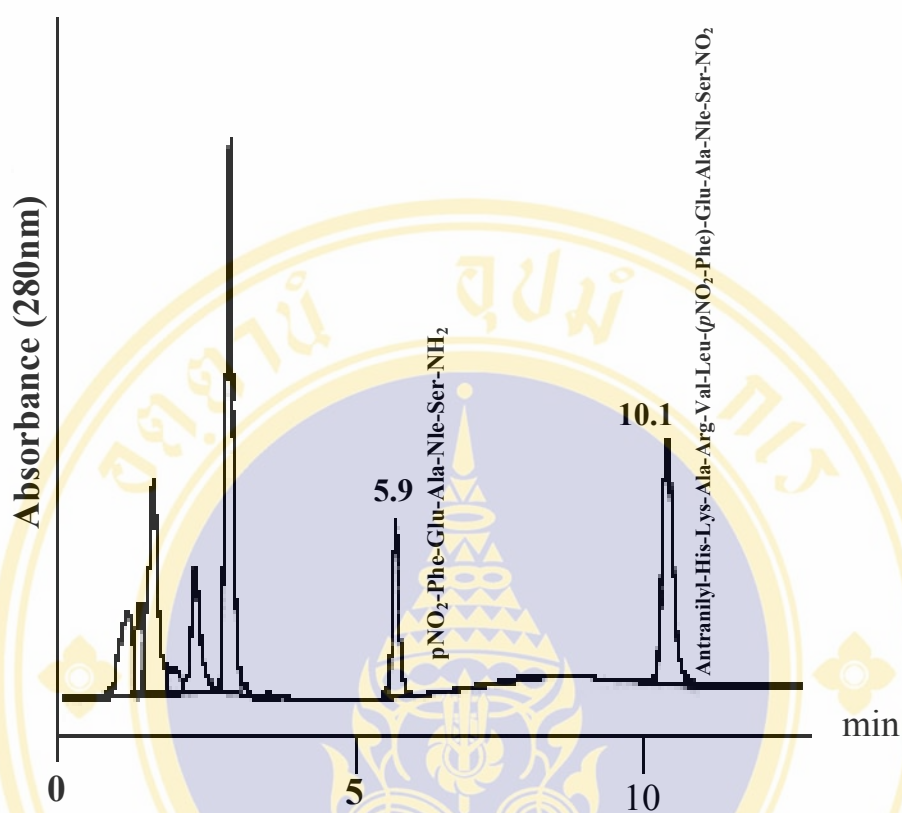
### C. HIV-1 protease inhibitory activity testing.

The *in vitro* HIV-1 protease inhibitory activity in this study was determined by a stopped time HPLC assay, using a peptide, Anthranilyl His-Lys-Ala-Arg-Val-Leu-(*p*-NO<sub>2</sub>-Phe)-Glu-Ala-Nle-Ser-NH<sub>2</sub> as a substrate. A stopped time HPLC assay was performed by incubating peptide substrate with the protease enzyme in small volumes (< 0.1 mL). After quenching with 10 % trifluoroacetic acid at selected times, the sample was subjected to reverse phase HPLC on octadecylsilane column. The resulting peptidolytic products were thereby separated from the remaining substrate using linear gradient of acetonitrile in 0.1 % trifluoroacetic acid (TFA) with spectrophotometric detection at 280 nm. The retention times of the substrate and *p*-NO<sub>2</sub>-Phe-bearing hydrolysate were 5.9 and 10.1 min, respectively (Figure 25). The percent relative inhibitory ratio (% IR), briefly called as % inhibition, was calculated from the ratio of substrate peak area to the hydrolysate peak area.

$$\% \text{ inhibition} = \frac{(A_{\text{Negative control}} - A_{\text{Sample}})}{A_{\text{Negative control}}} \times 100$$

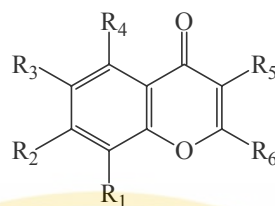
(where A is a relative peak area of the hydrolysate).

In this *in vitro* assay, 100 μM of pepstatin A was used as a positive control and DMSO was used as a negative control.



**Figure 25.** HPLC profile of a reaction mixture of HIV-1 PR and substrate incubated for 2 hours at 37° C.

Ten chromone derivatives were evaluated for their inhibitory activities and the results were reported as % inhibition as shown in Table 6. As seen from Table 6, compound **1** possessed the highest % inhibition with  $88.53 \pm 1.75$  % at concentration  $12.5 \mu\text{g/mL}$ , while pepstatin A, a potent aspartyl protease inhibitor showed  $91.07 \pm 1.53$  % inhibition at  $100 \mu\text{M}$  in the same experiment.

**Table 6.** The inhibitory activity of the synthesized chromone compounds.

Cpd.	R <sub>1</sub>	R <sub>2</sub>	R <sub>3</sub>	R <sub>4</sub>	R <sub>5</sub>	R <sub>6</sub>	% inhibition
<b>1</b>	H	OH	H	H	4''-( <i>t</i> -butyl)-Benzoyl	4'-( <i>t</i> -butyl)-Phenyl	88.53 ± 1.75
<b>2</b>	H	OH	H	H	3''-(Cl)-Benzoyl	3'-(Cl)-Phenyl	54.17± 0.81
<b>3</b>	OH	OH	H	H	3''-(Cl)-Benzoyl	3'-(Cl)-Phenyl	50.59 ± 1.39
<b>4</b>	OH	OH	H	H	4''-(OCH <sub>3</sub> )-Benzoyl	4'-(OCH <sub>3</sub> )-Phenyl	35.23 ± 4.07
<b>5</b>	OH	OH	H	H	3''-(OCH <sub>3</sub> )-Benzoyl	3'-(OCH <sub>3</sub> )-Phenyl	53.13 ± 2.95
<b>6</b>	H	OH	H	OH	3''-(OCH <sub>3</sub> )-Benzoyl	3'-(OCH <sub>3</sub> )-Phenyl	53.39 ± 3.22
<b>7</b>	H	H	OH	H	H	3'-(OCH <sub>3</sub> )-Phenyl	75.29 ± 2.13
<b>8</b>	H	H	OH	H	H	3'-(Cl)-Phenyl	47.48 ± 0.94
<b>9</b>	H	H	OH	H	H	4'-(F)-Phenyl	54.56 ± 4.68
<b>10</b>	H	H	OH	H	H	3'-(CF <sub>3</sub> )-Phenyl	66.68 ± 0.32
Pepstatin A							91.07 ± 1.53

Compounds which exhibited inhibitory activity greater than 65 % inhibition (i.e., compounds **1**, **7** and **10**) were selected for further determination of IC<sub>50</sub> values. The IC<sub>50</sub> values were obtained from linear regression plots between log concentration (log C) versus % inhibition. Compound **1** with the IC<sub>50</sub> value of 6.89 μM has been shown to be the most potent inhibitor in this series. The results of the IC<sub>50</sub> determination of compounds **1**, **7** and **10** are shown in Table 7-9 and Figure 26-28.

1. **IC<sub>50</sub> determination of 7-hydroxy-2-(4'-*tert*-butylphenyl)-3-(4''-*tert*-butylbenzoyl)chromone 1.**

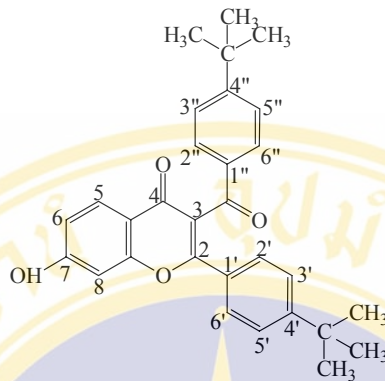


**Table 7.** Results of the determination of IC<sub>50</sub> value of compound 1.

Conc. ( $\mu\text{g/mL}$ )	logC	% inhibition	intercept	slope	R <sup>2</sup>	IC <sub>50</sub>	
						$\mu\text{g/mL}$	$\mu\text{M}$
12.5	1.09691	88.53	16.911	66.661	0.9936	3.13	6.89
5.0	0.69897	67.51					
2.5	0.39794	40.72					
0.625	-0.20412	3.54					

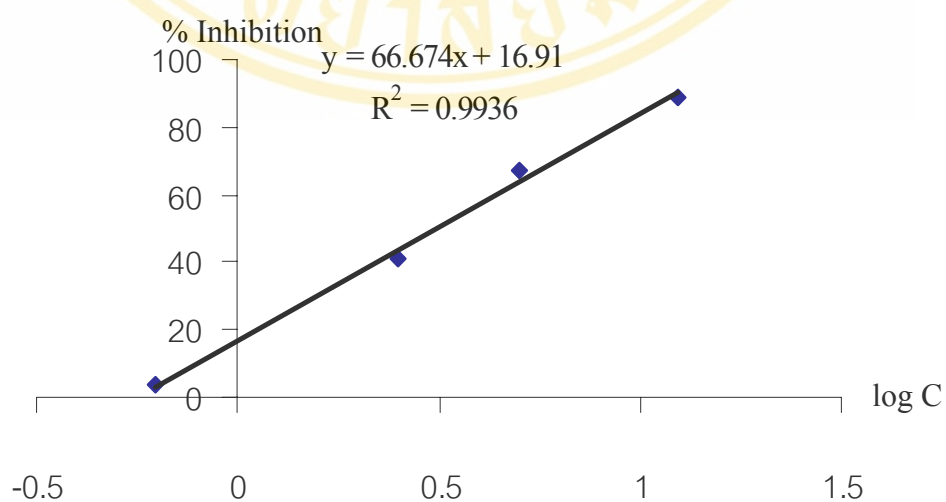


**Figure 26.** The % inhibition vs. log concentration profile of compound 1.

## 2. IC<sub>50</sub> determination of 6-hydroxy-2-(3'-methoxyphenyl)chromone 7.

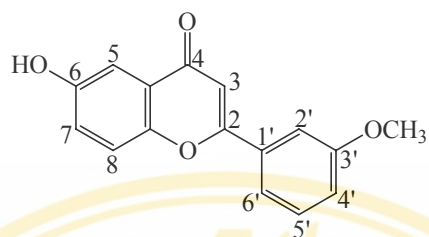


**Table 8.** Results of the determination of IC<sub>50</sub> value of compound 7.

Conc. ( $\mu\text{g/mL}$ )	logC	% inhibition	intercept	slope	R <sup>2</sup>	IC <sub>50</sub>	
						$\mu\text{g/mL}$	$\mu\text{M}$
12.5	1.09690	72.87	-2.3568	65.707	0.9884	6.26	23.35
7.5	0.87506	52.03					
2.5	0.39794	21.36					
1.25	0.09691	6.4					

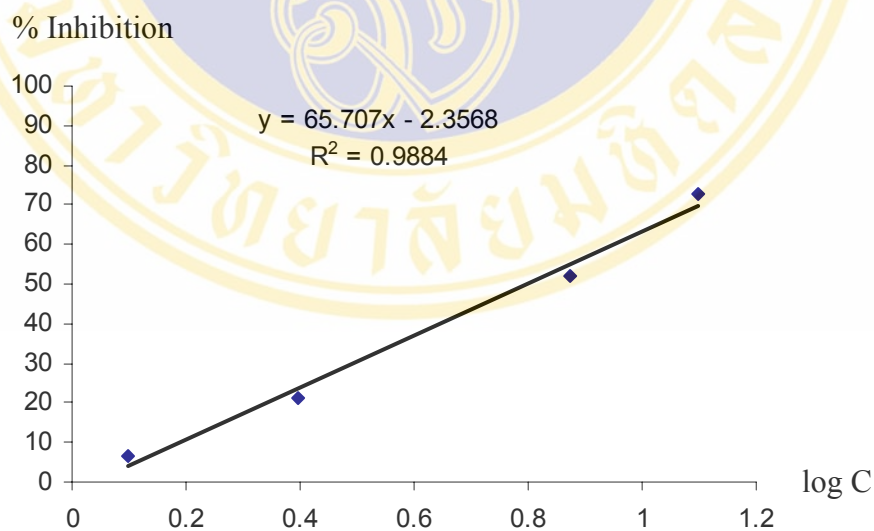


**Figure 27.** The % inhibition vs. log concentration profile of compound 7.

### 3. IC<sub>50</sub> determination of 6-hydroxy-2-(3'-trifluoromethylphenyl)chromone 10.

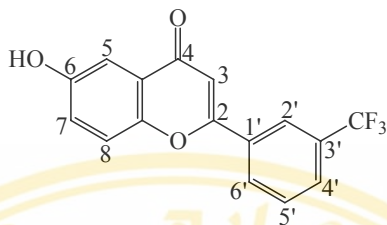


**Table 9.** Results of the determination of IC<sub>50</sub> value of compound 10.

Conc. ( $\mu\text{g/mL}$ )	logC	% inhibition	intercept	slope	R <sup>2</sup>	IC <sub>50</sub>	
						$\mu\text{g/mL}$	$\mu\text{M}$
12.5	1.09690	65.53	-30.125	87.459	0.9851	8.24	26.92
7.5	0.875061	49.52					
2.5	0.39794	26.72					
1.25	0.09691	6.13					

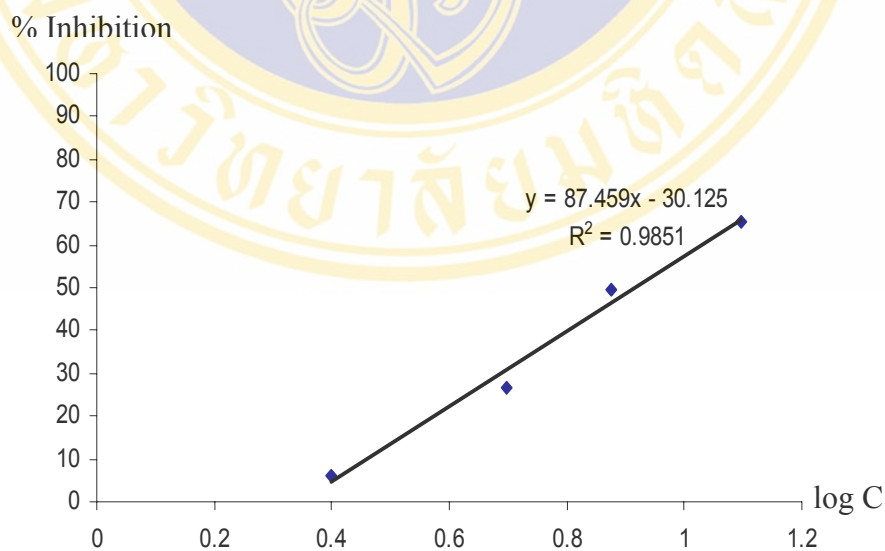


**Figure 28.** The % inhibition vs. log concentration profile of compound 10.

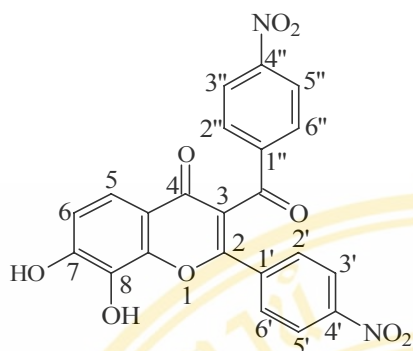
The  $IC_{50}$  values of the selected chromone derivatives were compared with the currently approved HIV-1 PIs, i.e., saquinavir, indinavir, ritonavir, nelfinavir, amprenavir, and atazanavir and fosamprenavir as shown in Table 10. Compound **1**, the most potent derivative in this study, is still less potent than the approved HIV-1 PIs. Compound **1** exhibited 3-4 times higher potency than compound **7** ( $IC_{50} = 23.35 \mu\text{M}$ ) and compound **10** ( $IC_{50} = 26.92 \mu\text{M}$ ).

**Table 10.** The  $IC_{50}$  values of compounds **1**, **7**, **10** and clinically approved HIV-1 PIs.

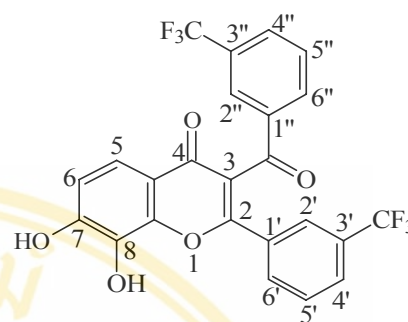
Inhibitors	$IC_{50}$ ( $\mu\text{M}$ )
Compound <b>1</b>	6.89
Compound <b>7</b>	23.35
Compound <b>10</b>	26.92
Saquinavir	0.0035*
Indinavir	0.0250*
Ritonavir	0.0270*
Nelfinavir	0.0220*
Amprenavir	0.0840*
Atazanavir	0.0050*
Fosamprenavir	0.012-0.08*

\* $IC_{50}$  values were taken from reference 137.

The structure-activity relationships obtained from this study agree with the previous study (21). From the previous study, compounds in this chromone series with substituted phenyl and substituted benzoyl groups at position 2 and 3 of the benzopyran nucleus respectively, i.e., compound **18** and compound **20** showed the high potency. These bulky phenyl and benzoyl rings might form hydrophobic interaction with S1 (Val32, Ile50', Pro81, Val82) and S2 (Leu23, Val32, Val82, Ile84) of HIV-1 PR. Moreover, compounds **1**, **18** and **20**, all contain OH group at position 7 (ring A of benzopyran). This OH group can act as hydrogen bond donor and form hydrogen bonding interaction with Asp25 and Asp25' (22).

Compound **18**

92.24 % inhibition

IC<sub>50</sub> = 0.65 μMCompound **20**

93.16 % inhibition

IC<sub>50</sub> = 0.34 μM

\*Note: pepstatin A possessed 95.56 % inhibition in this experiment (22, 138).

The previous CoMSIA study provides the structural features required for good activity which are corresponding to this study. The CoMSIA steric and hydrophobic contour maps in Figure 29a and 29c respectively, indicate that both *meta* and *para* positions of the phenyl and benzoyl rings should contain the bulky substituents. The hydrogen bond donor ability contour map (Figure 29d) provides the information that hydrogen bond donor substituent should be presented in ring A of the benzopyran nucleus (21). The results from this study gave the idea of the structure of the promising high potent HIV-1 PI. The candidate compound(s) should contain the bulky substituted phenyl and benzoyl groups at position 2 and 3, as well as the hydrogen donor group in ring A of the benzopyran. However, the further docking study should also be performed to confirm the structural requirement for inhibitor-enzyme interaction.

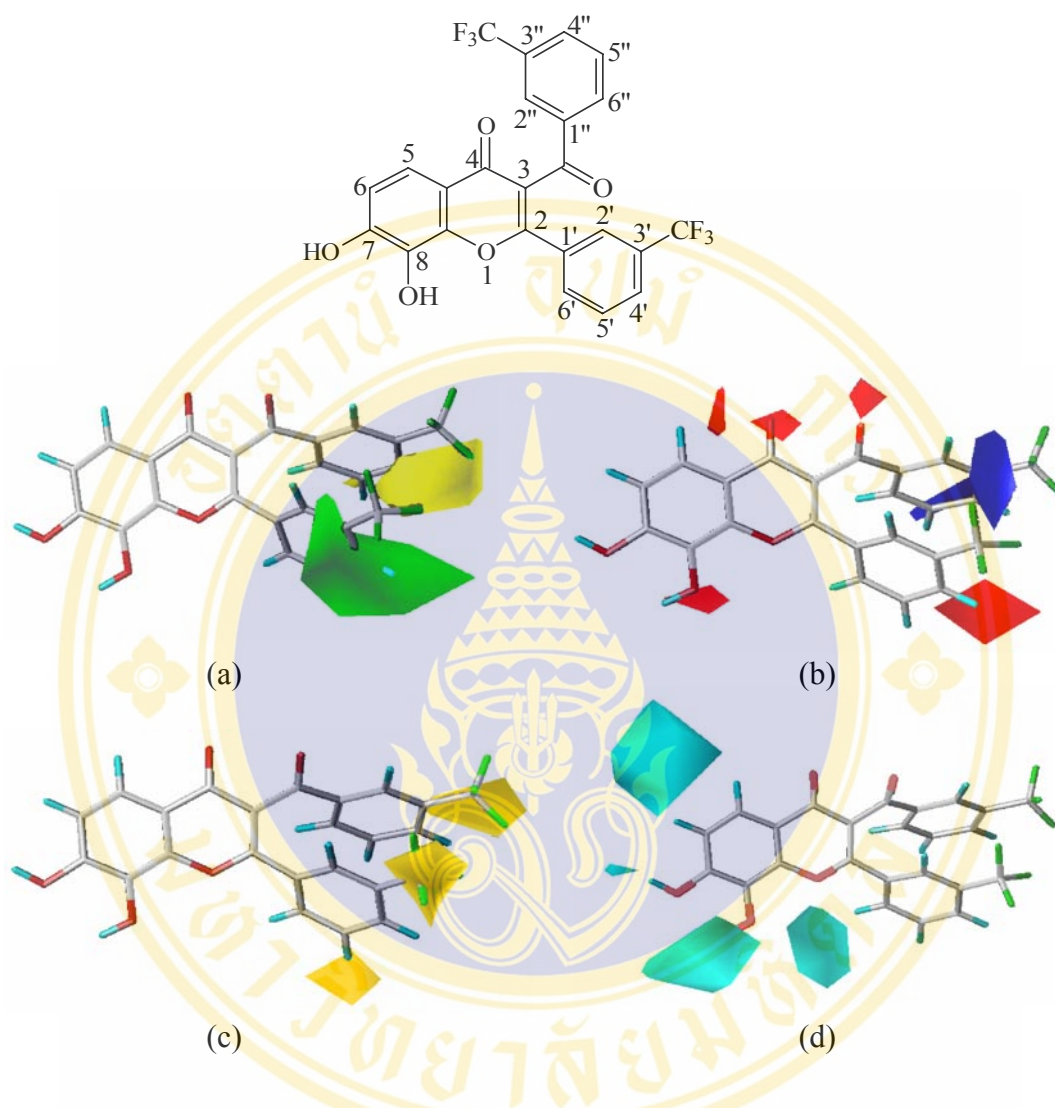


**Figure 29.** CoMSIA contour maps: (a) Steric contour map: green and yellow polyhedra indicate regions where more steric bulk or less steric bulk, respectively, will enhance the activity. (b) Electrostatic contour map: blue and red polyhedra indicate regions where positively charged or negatively charge substituent will enhance the activity. (c) Hydrophobic contour map: yellow and white polyhedra indicate regions where hydrophobic or hydrophilic groups, respectively, will enhance the activity. (d) Hydrogen bond donor ability contour map: cyan polyhedra indicate regions where hydrogen bond donor groups will increase the activity.

## CHAPTER VI

### CONCLUSION

A new series of non-peptidic protease inhibitors, chromone derivatives, has been designed and synthesized in our laboratory based on the previous 3D QSAR, CoMFA and CoMSIA studies. The general structure of molecules in this series consists of benzopyran-4-one (chromone) nucleus with different substituted phenyl and substituted benzoyl groups at position 2 and 3 respectively and different OH substitution patterns at position 5, 6, 7 and 8. Ten derivatives in this series have been synthesized by one-pot cyclization reaction. The synthesized compounds were purified by column chromatography and/or recrystallization. The structures of pure compounds were identified by Fourier transform infrared spectroscopy (FT-IR), nuclear magnetic resonance spectroscopy (NMR), mass spectrometry (MS), and elemental analysis. The percentage yields of the synthesized compounds are in the range of 3-28 %.

The synthesized compounds at concentration 12.5  $\mu\text{g/mL}$  have been evaluated for their *in vitro* inhibitory activity against HIV-1 protease by HPLC assay using recombinant HIV-1 protease and anthranilyl His-Lys-Ala-Arg-Val-Leu-(*p*-NO<sub>2</sub>-Phe)-Glu-Ala-Nle-Ser-NH<sub>2</sub> as substrate. The results obtained from the assay showed the inhibitory activity in the range of 35 % inhibition to 88 % inhibition. Compounds which exhibited inhibitory activity greater than 65 % inhibition were selected for further determination of IC<sub>50</sub> values. The IC<sub>50</sub> values of compounds **1**, **7** and **10** are 6.89  $\mu\text{M}$ , 23.35  $\mu\text{M}$ , and 26.92  $\mu\text{M}$ , respectively.

The results from this study correspond to the previous 3D QSAR, CoMFA and CoMSIA studies that compounds in this chromone series with substituted phenyl and substituted benzoyl groups at position 2 and 3 of the benzopyran nucleus, respectively showed the high potency. Moreover, both *meta* and *para* position of the phenyl and benzoyl rings should contain bulky substituents. The hydrogen bond donor substituent should be presented in ring A of the benzopyran nucleus. The results of this study

give a picture of the main chemical features which are responsible for good inhibitory activity. The future docking study will be performed to review the inhibitor-enzyme interaction. The docking study will be able to confirm this suggested structural requirements for the high potent inhibitor.



## REFERENCES

1. Thaisrivongs S, Romero DL, Tommasi RA, Janakiraman MN, Strohbach JW, Turner SR, et. al. Structure-based design of HIV protease inhibitors: 5,6-dihydro-4-hydroxy-2-pyrones as effective, nonpeptidic inhibitors. *J Med Chem* 1996; 39: 4630-42.
2. Blundell TL, Lapatto R, Wilderspin A F, Hemmings AM, Hobart P M, Danley D E. et. al. The 3-D Structure of HIV-1 protease and the design of antiviral agents for the treatment of AIDS. *Trends Biol Sci* 1990; 15: 425-30.
3. Debouck C, Metcalf B, W. Human immunodeficiency virus protease: a target for AIDS therapy. *Drug Dev Res* 1990; 21: 1-17.
4. Moyle G, Gazzard B. Current knowledge and future prospects for the use of HIV protease inhibitors. *Drug* 1996; 51: 701-12.
5. Surleraux DLNG, de Kock HA, Verschuereen WG, Pille GME, Maes LJR, Peeters A. Design of HIV-1 protease inhibitors active on multidrug-resistant virus. *J Med Chem* 2005; 48: 1965-73.
6. Nobel S, Faulds D. Saquinavir: a review of its pharmacology and clinical potential in the management of HIV-infection. *Drugs* 1996; 52: 93-112.
7. Mealy N, Castaner J. Indinavir sulfate: anti-HIV, HIV-1 protease inhibitor. *Drugs Fut* 1996; 31: 600-9.
8. Lea AP, Faulds D. Ritonavir. *Drugs*. 1996; 52: 541-6.
9. Rabasseda X, Martel AM. Nelfinavir mesylate: Antiviral for AIDS, HIV-1 protease inhibitor. *Drugs Fut*. 1997; 22: 371-7.
10. Adkim JC, Faulds D. Amprenavir. *Drugs* 1998; 5: 837-42.
11. Becker S. Atazanavir: improving the HIV protease inhibitor class. *Expert Rev Anti-Infect Ther* 2003; 1: 403-413.

12. Sham HL, Betebenner DA, Herrin T, Kumar G, Saldivar A, Vasavanonda S, et al. Synthesis and antiviral activities of the major metabolites of the HIV protease inhibitor ABT-378 (Lopinavir). *Bioor Med Chem Let* 2001; 11: 1351-3.
13. Sohma Y, Hayashi Y, Ito T, Matsumoto H, Kimura T, Kiso Y. Development of Water-Soluble prodrugs of the HIV-1 protease inhibitor KNI-727: importance of the conversion time for higher gastrointestinal absorption of prodrugs based on spontaneous chemical cleavage. *J Med Chem* 2003; 46: 4124-35.
14. Wang S, Milne GWA, Yan X, Posey IJ, Nicklaus MC, Graham L, et al. Discovery of novel, non-peptide HIV-1 protease inhibitors by pharmacophore searching. *J Med Chem* 1996; 39: 2047-54.
15. Thaisrivongs S, Tomich PK, Watenpaugh KD, Chong KT, Houe WJ, Yang CP, et al. Structure-based design of HIV protease inhibitors: 4-hydroxy-coumarines and 4-hydroxy-2-pyrones as non-peptidic inhibitors. *J Med Chem* 1994; 37: 3200-04.
16. Thaisrivongs S, Janakiraman MN, Chong KT, Tomich PK, Dolak LA, Turner SR, et al. Structure-based design of novel HIV protease inhibitors: sulfonamide-containing 4-hydroxy-coumarines and 4-hydroxy-2-pyrones as potent non-peptide inhibitors. *J Med Chem* 1996; 39: 2400-10.
17. Lam P, Ru Y, Jadhav PK, Aldrich PE, De Lucca GV, Eyermann CJ, Chang CH, et al. Cyclic HIV protease inhibitors: synthesis, conformational analysis, P<sub>2</sub>/P<sub>2</sub>' structure-activity relationship, and molecular recognition of cyclic ureas. *J Med Chem* 1996; 39: 3514-25.
18. Han Q, Chang CH, Li R, Ru Y, Jadhav PK, Lam PYS. Cyclic HIV protease inhibitors: Design and synthesis of orally bioavailable, pyrazole P<sub>2</sub>/P<sub>2</sub>' cyclic ureas with improved potency. *J Med Chem* 1998; 41: 2019-28.
19. Jadhav PK, Woerner FJ, Lam P, Hodge CN, Eyermann CJ, Man HW, et al. Nonpeptide cyclic cyanoguanidines as HIV-1 protease inhibitors: synthesis, structure-activity relationships, and X-ray crystal structure studies. *J Med Chem* 1998; 41: 1446-55.

20. Turner SR, Strohbach JW, Tommasi RA, Aristoff PA, Johnson PD, Skulnick HI, et al. Tipranavir (PNU-140690): a potent, orally bioavailable non-peptidic HIV protease inhibitor of the 5,6-dihydro-4-hydroxy-2-pyrone sulfonamide class. *J Med Chem* 1998; 41: 3467-76.
21. Ungwitayatorn J, Samee W, Pimthon J. 3D-QSAR studies on chromone derivatives as HIV-1 protease inhibitors. *J Mol Str* 2004; 689: 99-106.
22. Samee W. Synthesis, evaluation and molecular modeling of chromone derivatives as HIV-1 protease inhibitors and molecular modeling of phthalimide derivatives as HIV-1 reverse transcriptase inhibitors [Ph.D. Thesis in pharmaceutical chemistry and phytochemistry]. Bangkok: Faculty of graduate studies, Mahidol university; 2003.
23. Ma C, Nakamura N, Miyashiro H, Hattori M, Shimotohno K. Inhibitory effect of ursolic acid derivatives from *Cynomorium songaricum*, and related triterpenes on human immunodeficiency viral protease. *Phytotherapy Res* 1998; 12: 138-142.
24. Riva C, De Toma C, Donadel L, Boi C, Pennini R, Motta G, et al. New DBU (1,8-diazabicyclo[5.4.0]undec-7-ene) assisted one-pot synthesis of 2,8-disubstituted 4H-1-benzopyran-4-ones. *Synthesis* 1997: 195-201.
25. Wlodawer A, Vondrasek J. Inhibitors of HIV-1 protease: a major success of structure-assisted drug design. *Annu Rev Biophys Biomol Struct* 1998; 27: 249-84.
26. Antia R, Holloran ME. Recent developments in theories of pathogenesis of AIDS. *Trends Microbiol* 1996; 4: 282-5.
27. Phair J, Munoz A, Detels R, Kaslow R, Rinaldo C, Saah A. The risk of *Pneumocystis carinii* pneumonia among men infected with human immunodeficiency virus type 1. *N Engl J Med* 1990; 322: 161-5.
28. HIV infection. Available from: <http://www.answers.com/topic/hiv>.
29. Steinbrook R. The AIDS epidemic in 2004. *NEJM* 2004, 351: 115-7.
30. Ren J, Stammers DK. HIV reverse transcriptase structure: designing new inhibitors and understanding mechanisms of drug resistance. *Trends Pharm Sci* 2005; 26: 4-7.

31. AIDS epidemic update 2004. Available from: [http://www.unaids.org/wad2004/report\\_pdf.html](http://www.unaids.org/wad2004/report_pdf.html) [Accessed 2005 june 9].
32. Amado RG, Chen ISY. Lentiviral vectors-the promise of gene therapy within reach. *Science* 1999; 285: 674-76.
33. Feng S, Holland EC. HIV-1 tat trans-activation requires the loop sequence within tar. *Nature* 1998; 334: 165-7.
34. Rice AP, Mathews MB. Transcriptional but not translational regulation of HIV-1 by the tat gene product. *Nature* 1988; 332: 551-3.
35. Roy S, Delling U, Chen CH. A bulge structure in HIV-1 TAR RNA is required for tat binding and tat-mediated trans-activation. *Genes Dev* 1990; 4: 1365-73.
36. Cullen BR. Posttranscriptional Regulation by the HIV-1 rev protein. *Seminars in Virology* 1998; 8: 327-34.
37. Jowett JB, Planelles V, Poon B, Shah Np, Chen ML, Chen IS. The human immunodeficiency virus type 1 vpr gene arrests infected T cells in the G2 + M phase of the cell cycle. *J Virol* 1995; 69: 6304-13.
38. Schubert U, Bour S, Ferrer-Montiel AV. The two biological activities of human immunodeficiency virus type 1 Vpu protein involve two separable structural domains. *J Virol* 1996; 70: 809-19.
39. Trono D. HIV accessory proteins: leading roles for the supporting cast. *Cell* 1995; 82: 189-92.
40. Turner BG, Summers MF. Structural biology of HIV. *J Mol Biol* 1999; 285: 1-32.
41. Structure of HIV. Available from: <http://www.whfreeman.com/immunology/CH22/figure22-02a..htm> [Accessed 2005 june 9].
42. Deng H, Liu R, Ellmeier W, Choe S, Unutmaz D, Burkhart M, et. al. Identification of a major co-receptor for primary isolates of HIV-1. *Nature* 1996; 381: 661-6.
43. Schwartz SA, Nair MP. Current concepts in human immunodeficiency virus infection and AIDS. *Clin Diagn Lab Immunol* 1999; 6: 295-305.

44. Hammer SM, Squires KE, Hughes MD, Grimes JM, Demeter LM, Currier JS, et al. A controlled trial of two nucleoside analogues plus zidovudine in persons with human immunodeficiency virus infection and CD4 cell counts of 200 per cubic millimeter or less. *N Engl J Med* 1997; 337: 725-33.
45. Goldsmith MA, Warmedam MT, Atchison RE, Miller MD, Green WC. Dissociation of the CD4 down regulation and viral infectivity enhancement functions of human immunodeficiency virus type 1 nef. *J Virol* 1995; 69: 4112-21.
46. How HIV Causes AIDS. Available from: <http://www.niaid.nih.gov/factsheets/howhiv.htm>
47. Devereux HL, Toule M, Johnson MA. Rapid decline in detectability of HIV-1 drug resistance mutation after stopping therapy. *AIDS* 1999; 13: 123-7.
48. Garg R, Gupta SP, Gao H, Babu MS, Debnath AK, Hansch C. Comparative quantitative structure-activity relationship studies on anti-HIV drugs. *Chem Rev* 1999; 99: 3525-601.
49. De Clercq E. Toward improved anti-HIV chemotherapy: therapeutic strategies for intervention with HIV infections. *J Med Chem* 1995; 38: 2491-517.
50. Jones PS. Strategies for antiviral drug discovery. *Antivir Chem Chemother* 1998; 9: 283-302.
51. De clercq E. Human Retroviruses. *Aids Res* 1992; 8: 119-37.
52. Kohlstaedt LA, Wang J, Friedman JM, Rice PA, Steitz TA. Crystal structure at 3.5 Å resolution of HIV-1 reverse transcriptase complexed with an inhibitor. *Science* 1992; 256: 1783-90.
53. Ding J, Das K, Hsiou Y, Sarafianos SG, De Clark A Jr, Jacobo-Molina A, et al. Structure and functional implications of the polymerase active site region in a complex of HIV-1 RT with a double-stranded DNA template-primer and an antibody fab fragment at 2.8 Å resolution. *J Mol Biol* 1998; 284: 1095-1111.
54. Sluis-Cremer N, Temiz NA, Bahar I. Conformational changes in HIV-1 reverse transcriptase induced by nonnucleoside reverse transcriptase inhibitor binding. *Curr HIV Res* 2004; 2: 323-32.

55. Tantillo C, Ding JP, Jacobomolina A, Nanni RG, Boyer PL, Hughes SH, et. al. Locations of anti-aids drug binding sites and resistance mutations in the 3-dimensional structure of HIV-1 reverse transcriptase: implications for mechanisms of drug inhibition and resistance. *J Mol Biol* 1994; 243: 369-387.
56. De Clercq E. HIV Resistance to reverse transcriptase inhibitors. *Biochem. Pharmacol* 1994; 47: 155-169.
57. Ding JK, Das K, Tantillo W, Zhang AD, Clark, Jr. S, Jessen X, et. al. Structure of HIV-1 RT in a complex with NNRTI a-APA R 95845 at 2.8 Å. *Structure* 1995; 3: 365-79.
58. Ren JR, Esnouf E, Garman D, Somers C, Ross I, Kirby J, et. al. High resolution structures of HIV-1 RT from four RT-inhibitor complexes. *Nat Struct Biol* 1995; 2: 293-302.
59. Smith M, Rouzer BK, Taneyhill CA, Smith LA, Hughes NA, Boyer SH, et.al. Molecular Modeling Studies of HIV-1 reverse transcriptase nonnucleoside inhibitors-total-energy of complexation as a predictor of drug placement and activity. *Protein Sci* 1995; 4, 2203-22.
60. Toh H, Ono M, Saigo K, Miyata T. Retroviral protease-like sequence in the yeast transposon<sup>tyl</sup>. *Nature* 1985; 315: 691-92.
61. Seelmeier S, Schmidt H, Turk V, Vonderhelm K. Human immunodeficiency virus has an aspartic-type protease that can be inhibited by pepstatin-A. *Proc Natl Acad Sci USA* 1988; 85: 6612-16.
62. Leung D, Abbenante G, Fairlie DP. Protease inhibitors: current status and future prospects. *J Med Chem* 2000; 43: 305 -41.
63. Pearl LH, Taylor WR. A structural model for the retroviral proteases. *Nature* 1987; 329: 351-4.
64. Turner SR. HIV protease inhibitors-the next generation. *Curr Med Chem* 2002; 1: 141-162.
65. Andersson HO, Fridborg K, Löwgren S, Alterman M, Mühlman A, Björsne M, et al. Optimization of P1-P3 groups in symmetric and asymmetric HIV-1 protease inhibitors. *Eur J Biochem* 2003; 270: 1746-58.

66. Menéndez-Arias L, Weber IT, Oroszlan S. Mutational analysis of the substrate binding pocket of murine leukemia virus protease and comparison with human immunodeficiency virus proteases. *J Biol Chem* 1995; 8: 29162-8.
67. Wlodawer A, Gustchina A. Structural and biochemical studies of retroviral proteases. *Biochim Biophys Acta* 2000; 1477: 16-34.
68. Louis JM, Ishima R, Nesheiwat I, Pannel LK, Lynch SM, Torchia DA, et. al. Revisiting monomeric HIV-1 protease - Characterization and redesign for improved properties. *J Biol Chem* 2003; 278: 6085-92.
69. Sluis-Cremer N, Tachedjian G. Modulation of the oligomeric structures of HIV-1 retroviral enzymes by synthetic peptides and small molecules. *Eur J Biochem* 2002; 269: 5103-11.
70. Hoffmann C. HIV Therapy 2003: Overview of Antiretroviral Drugs. In: Hoffmann C, Kamps BS. *HIV medicine 2003*. Flying Publisher. 2003; p. 61-119.
71. Gogu SR, Agrawal KC. The protective role of zinc and N-acetyl cysteine in modulating zidovudine-induced hematopoietic toxicity. *Life Sci* 1996; 59: 1323-9.
72. Witvrouw M, Pannecouque C, Desmyter J, De Clercq E, Andries K. *In vitro* evaluation of the effect of temporary removal of HIV drug pressure. *Antivir Res* 2000; 46: 215-21.
73. Perry CM, Balfour JA. Didanosine: An update on its antiviral activity, pharmacokinetic properties and therapeutic efficacy in the management of HIV disease. *Drugs* 1996; 53: 928-62.
74. Selected properties of didanosine. Available from: [http://www.tthhivclinic.com/pdf/RTI% 20 didanosine.pdf](http://www.tthhivclinic.com/pdf/RTI%20didanosine.pdf) [Accessed 2005 June 9].
75. Whittington R, Brogden RN. Zalcitabine: a review of its pharmacology and clinical potential in acquire immunodeficiency syndrome (AIDS). *Drugs* 1992; 44: 656-83.

76. Mitsuya H, Broder S. Inhibition of the *in vitro* infectivity and cytopathic effect of human T-lymphotropic virus III/lymphadenopathy-associated virus (HTLV-III/LAV) by 2',3'-dideoxynucleosides. *Proc Natl Acad Sci USA* 1986; 83: 1911-15.
77. Robinson C, Castaner J. Stavudine: Anti-HIV. *Drugs Fut* 1994; 19: 925-32.
78. Erickson JW, Burt SK. Structural mechanism of HIV drug resistance. *Ann Rev Pharmacol Toxicol* 1996; 36: 545-71.
79. Balzarini J, Van Aeschot, A, Herdewijn P, De Clercq E. Rapid communications – 5-chloro-substituted derivatives of 2',3'-didehydro-2',3'-dideoxyeridine, 3'-fluoro-2',3'-dideoxyeridine and 3'-azido-2',3'-dideoxyeridine as anti-HIV agents. *Biochem Pharmacol* 1989; 38: 869-74.
80. Cameron JM, Collis P, Daniel M, Storer R, Wilcox P. Lamivudine: Antiviral. *Drugs Fut* 1993; 18: 319-23.
81. Walsh JS, Reese MJ, Thurmond LM. The metabolic activation of abacavir by human liver cytosol and expressed human alcohol dehydrogenase isozymes. *Chem Biol Interact* 2002; 142: 135-54.
82. Daluge SM, Good SS, Faletto MB, Miller WH, St. Clair MH, Boone LR, et.al. 1592U89, a novel carbocyclic nucleoside analog with potent, selective anti-human immunodeficiency virus activity. *Antimicrob Agents Chemother* 1997; 41: 1082-93.
83. Robbins BL, Srinivas RV, Kim C, Bischofberger N, Fridland A. Anti-HIV activity and cellular metabolism of a potential prodrug of the acyclic nucleoside phosphonate 9-R-(2-phosphonomethoxypropyl)adenine (PMPA), bis(isopropylloxymethyl carbonyl)PMPA. *Antimicrob Agents Chemother* 1998; 42: 612-7.
84. Arimilli MN, Kim CU, Dougherty J, Mulato A, Oliyai R, Shaw JP, et. al., Synthesis *in vitro* biological evaluation and oral bioavailability of 9-[2-[(phosphonomethoxy)propyl]adenine (PMPA) prodrugs. *Antivir Chem Chemother* 1997; 8: 557-64.

85. Molina JM, Ferchal F, Rancinan C, Raffi F, Rozenbaum W, Sereni D, et al. Once-daily combination therapy with emtricitabine, didanosine, and efavirenz in human immunodeficiency virus-infected patients. *J Infect Dis* 2000; 182: 599-602.
86. Darque A, Valette G, Rousseau F, Wang LH, Sommadossi JP, Zhou XJ. Quantitation of intracellular triphosphate of emtricitabine in peripheral blood mononuclear cells from human immunodeficiency virus-infected patients. *Antimicrob Agents Chemother* 1999; 43: 2245-50.
87. Richman DD. Antiretroviral activity of emtricitabine, a potent nucleoside reverse transcriptase inhibitor. *Antivir Ther* 2001; 6: 83-8.
88. Jeong LS, Schinazi RF, Beach JW, Kim HO, Napalli S, Shanmuganathan K, et al. Asymmetric synthesis and biological evaluation of .beta.-L-(2R,5S)- and .alpha.-L-(2R,5R)-1,3-oxathiolane-pyrimidine and -purine nucleosides as potential anti-HIV agents. *J Med Chem* 1993; 36:181-95.
89. Schäfer W, Friebe WG, Leinert H, Merten A, Poll T, Von der Saal W, et al. Non-nucleoside inhibitors of HIV-1 reverse transcriptase: Molecular modeling and X-ray structure investigations. *J Med Chem* 1993; 36: 726-32.
90. Johnson V. Nucleoside reverse transcriptase inhibitors and resistance of human immunodeficiency virus type 1. *J Infect Dis* 1995; 17: 140-9.
91. Eshleman SH, Jackson JB. Nevirapine resistance after single dose prophylaxis. *AIDS Rev* 2002; 4: 59-63.
92. Miller V, Staszewski S, Boucher CAB, Phair JP. Clinical experience with non-nucleoside reverse transcriptase inhibitors. *AIDS* 1997; 11: 157-64.
93. Sulkowski MS, Thomas DL, Chaisson RE, Moore RD. Hepatotoxicity associated with antiretroviral therapy in adults infected with HIV and the role of hepatitis C or B virus infection. *JAMA* 2000; 283: 74-80.
94. Conway B. Initial therapy with protease inhibitor-sparing regimens: evaluation of nevirapine and delavirdine. *Clin Infect Dis* 2000; 2: 130-4.
95. von Giesen HJ, Koller H, Theisen A, Arendt G. Therapeutic effects of nonnucleoside reverse transcriptase inhibitors on the central nervous system in HIV-1 infected patients. *JAIDS* 2002; 29: 363-7.

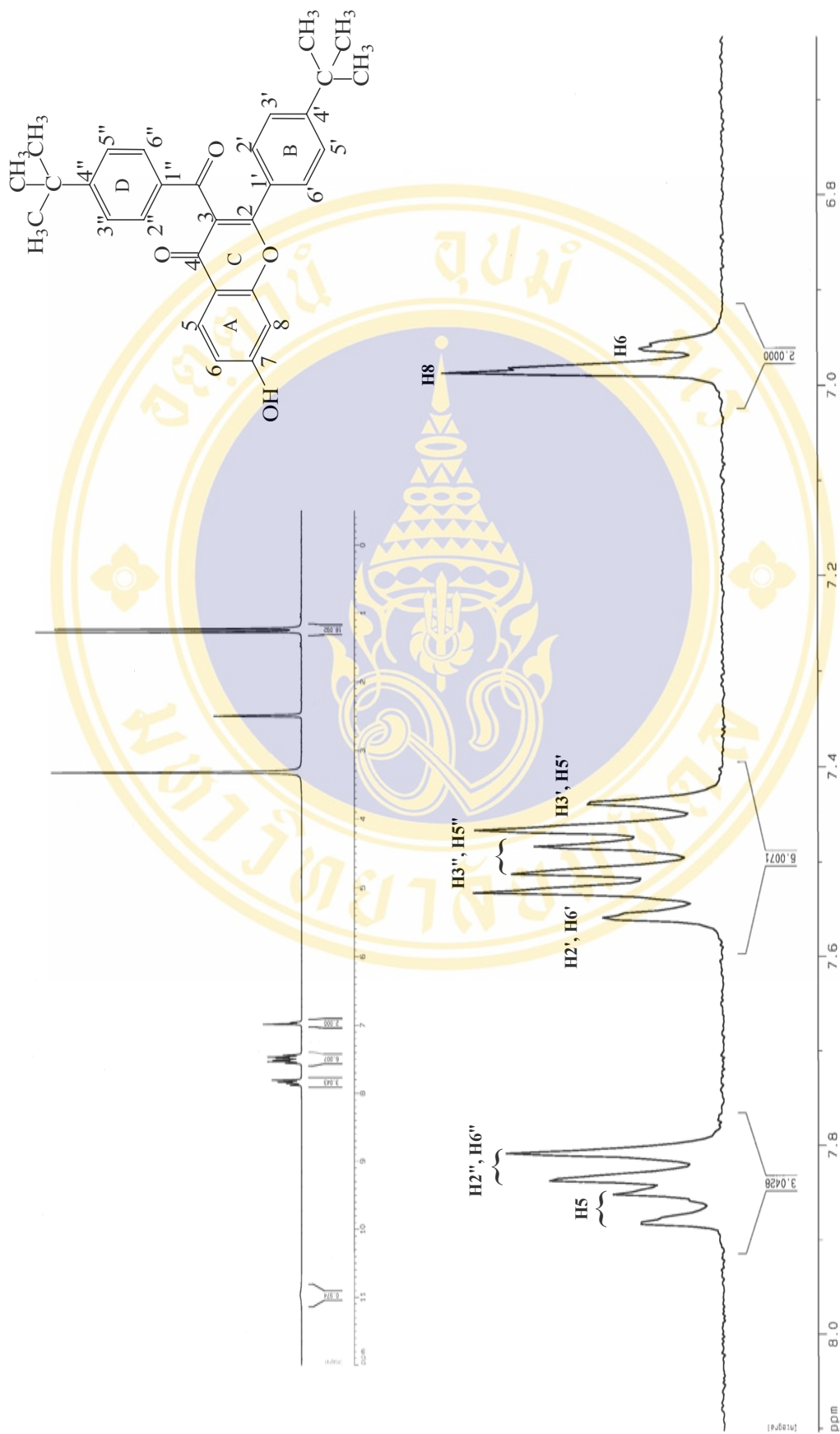
96. Maga G, Ubiali D, Salvetti R, Pregolato M, Spadari S. Selective interaction of the human immunodeficiency virus type 1 reverse transcriptase nonnucleoside inhibitor efavirenz and its thio-substituted analog with different enzyme-substrate complexes. *Antimicrob Agents Chemother* 2000; 44: 1186-94.
97. Young SD, Britcher SF, Tran LO, Payne LS, Lumma WC, Lyle TA, et. al. L-743,726(DMP-266): A novel, highly potent nonnucleoside inhibitor of the human immunodeficiency virus type 1 reverse transcriptase. *Antimicrob Agents Chemother* 1995; 39: 2602-2.
98. Chapman TM, Plosker GL, Perry CM. Fosamprenavir; a review of its use in the management of antiretroviral therapy-naive patients with HIV infection. *Drugs* 2004; 64: 2101-24.
99. Patick AK, Boritzki TJ, Bloom LA. Activities of the human deficiency virus type 1 (HIV-1) protease inhibitor nelfinavir mesylate in combination with reverse transcriptase and protease inhibitors against acute HIV-1 infection in vitro. *Antimicrob Agents Chemother* 1997; 1: 2159-64.
100. Redshaw S, Roberts NA, Thomas GJ. The road to zidovudine a history of saquinavir, the first human immunodeficiency virus protease inhibitor. *Handb. Exp. Pharmacol* 2000; 140: 3-21.
101. Graves BJ, Hatada MH, Miller JK, Graves MC, Roy S, Cook CM, et al. The three-dimensional x-ray crystal structure of HIV-1 protease complexed with a hydroxyethylene inhibitor. *Adv Exp Med Biol* 1991; 306: 455-60.
102. Kravcik S. Pharmacology and clinical experience with saquinavir. *Expert Opin Pharmacother* 2001; 2: 303-315.
103. Figgitt DP, Plosker GL. Saquinavir soft-gel capsule: an updated review of its use in the management of HIV infection. *Drugs* 2000; 60: 481-516.
104. Erickson J, Neidhart DJ, VanDrie J, Kempf DJ, Wang XC, Norbeck DW, et al. Design, activity, and 2.8 Å crystal structure of a C<sub>2</sub> symmetric inhibitor complexed to HIV-1 protease. *Science* 1990; 249: 527-33.

105. Kempf DJ, Marsh KC, Denissen JF, McDonald E, Vasavanonda S, Flentge CA, et al. ABT-538 is a potent inhibitor of human immunodeficiency virus protease and has high oral bioavailability in humans. *Proc Natl Acad Sci USA* 1995; 92: 2484-8.
106. Kempf DJ, Sham HL, Marsh KC, Flentge CA, Betebenner D, Green BE, et al. Discovery of ritonavir, a potent inhibitor of HIV protease with high oral bioavailability and clinical efficacy. *J Med Chem* 1998; 41: 602-17.
107. Kempf DJ, Marsh KC, Kumar G, Rodrigues AD, Denissen JF, McDonald E, et al. Pharmacokinetic enhancement of inhibitors of the human immunodeficiency virus protease by coadministration with ritonavir. *Antimicrob Agents Chemother* 1997; 41: 654-60.
108. Rich DH, Sun CQ, Vara Prasad JV, Pathiasseril A, Toth MV, Marshall GR, et al. Effect of hydroxyl group configuration in hydroxyethylamine dipeptide isosteres on HIV protease inhibition. Evidence for multiple binding modes. *J Med Chem* 1991; 34: 1222-5.
109. Vacca JP, Guare JP, De Solms SJ, Sanders WM, Giuliani EA, Young SD, et al. R. L-687,908, a potent hydroxyethylene containing HIV protease inhibitor. *J Med Chem* 1991; 34: 1225-8.
110. Dorsey BD, Levin RB, McDaniel SL, Vacca JP, Guare JP, Darke PL, et al. L-735,524: the design of a potent and orally bioavailable HIV protease inhibitor. *J Med Chem* 1994; 37: 3443-51.
111. Plosker GL, Noble S. Indinavir: a review of its use in the management of HIV infection. *Drugs* 1999; 58: 1165- 203.
112. Kalish VJ, Tatlock JH, Davies JF, Kaldor SW, Dressman BA, Reich S, et al. Structure-based drug design of nonpeptidic P2 substituents for HIV-1 protease inhibitors. *Bioorg Med Chem Lett* 1995; 5: 727-32.
113. Creus TM, Meda MJM, Jane CC, Garcia IN, Sala RJ. Nelfinavir: review of its pharmacokinetics and drug interactions. *Farm. Hosp.* 1999; 23: 79-93.
114. Kim EE, Baker CT, Dwyer MD, Murcko MA, Rao BG, Tung RD, et al. Crystal structure of HIV-1 protease in complex with VX-478, a potent and orally bioavailable inhibitor of the enzyme. *J Am Chem Soc* 1995; 117: 1181-2.

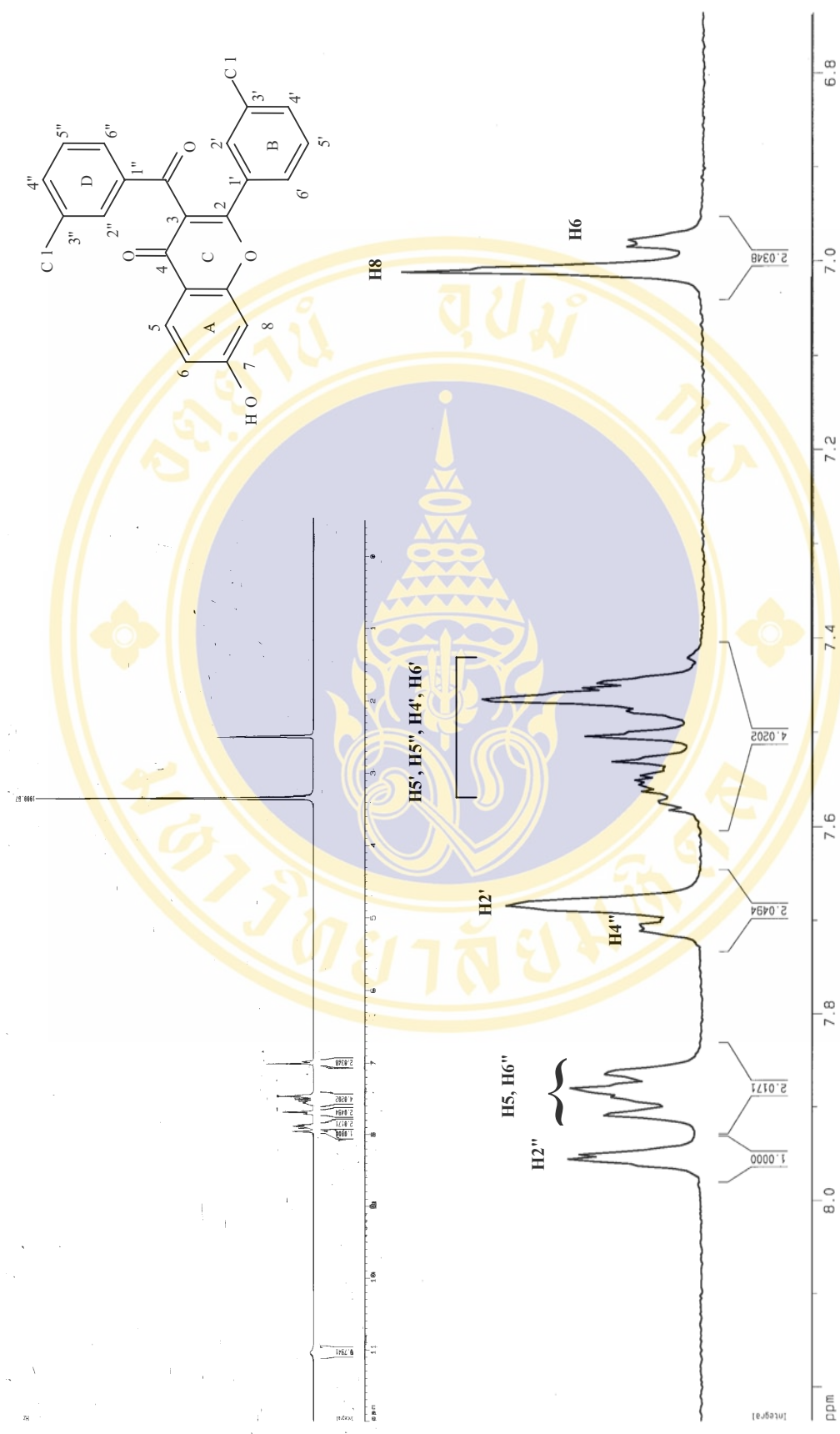
115. Billich A. Amprenavir vertex pharmaceuticals. *Curr Opin Investig Drugs* 1999; 1: 251-67.
116. Murphy R, Gulick RM, De Gruttola V, D'Aquila RT, Eron JJ, Sommadossi JP, et al. Treatment with amprenavir alone or amprenavir with zidovudine and lamivudine in adults with human immunodeficiency virus infection. *J Infect Dis* 1999; 179: 808-16.
117. Sham HL, Kempf DJ, Molla A, Marsh KC, Kumar GN, Chen CM, et al. ABT-378, a highly potent inhibitor of the human immunodeficiency virus protease. *Antimicrob Agents Chemother* 1998; 42: 3218-24.
118. Wlodawer A. Rational approach to AIDS drug design through structural biology. *Annu Rev Med* 2002; 53: 595-614.
119. Hurst M, Faulds D. Lopinavir. *Drugs* 2000; 60: 1371-79.
120. Kumar GN, Dykstra J, Roberts EM, Jayanti VK, Hickman D, Uchic J, et al. Potent inhibition of the cytochrome P-450 3A-mediated human liver microsomal metabolism of a novel HIV protease inhibitor by ritonavir: a positive drug-drug interaction. *Drug Metab Dispos* 1999; 27: 902-908.
121. Cvetkovic RS, Goa KL. Lopinavir/Ritonavir; a review of its use in the management of HIV infection. *Drugs* 2003; 63: 769-802.
122. Abbott Laboratories. Kaletra<sup>®</sup> (lopinavir/ritonavir) capsules and oral solution. Product label information. Available from: <http://www.kaletra.com> [Accessed 2002 Oct 2].
123. Orrick JJ, Corklin R, Steinhart CR. Atazanavir. *Annal Pharmacother* 2004; 38: 1664-70.
124. Raja A, Lebbos J, Kirkpatrick P. Atazanavir sulphate. *Nature Reviews Drug Discovery* 2003; 2: 857-8.
125. Xu Z, Singh J, Schwinden MD, Zhieng B, Kissick TP, Patel B, et al. Process research and development for an efficient synthesis of the HIV protease inhibitor BMS-232632. *Org Proc Res Dev* 2002; 6: 323-8.
126. Witherell G. BMS-232632 (Novartis/Bristol-Myers Squibb). *Curr Opin Investig Drugs* 2001; 2: 340-7.
127. Goldsmith DR, Perry CM. Atazanavir. *Drugs* 2003; 63: 1679-93.

128. Colonna R, Rose R, McLaren C, Thiry A, Parkin N. Identification of I50L as the signature atazanavir (ATV) resistance mutation in treatment-naive HIV-1 infected patients receiving ATV-containing regimens. *J Infect Dis* 2004; 189: 1802-10.
129. Ellis JM, Roos JW, Coleman CI. Fosamprenavir a novel protease inhibitor and prodrug of amprenavir. *Formulary* 2004; 39: 151-60.
130. Fung HB, Guo Y. Enfuvirtide: a fusion inhibitor for the treatment of HIV infection. *Clin Ther* 2004; 26: 352-78.
131. Dando TM, Perry CM. Enfuvirtide. *Drugs*. 2003; 63: 2755-66.
132. Cooper DA, Lange JMA. Peptide inhibitors of virus–cell fusion: enfuvirtide as a case study in clinical discovery and development. *Lancet Infect Dis* 2004; 4: 2004.
133. Eraikhuemen N, Branch E, Boston N, Honeywell M, Sneed K. Enfuvirtide: a novel agent for inhibiting the entry of HIV-1 into immune cells. *Drug Forecast* 2003; 28: 571-83.
134. Hyland LJ, Bayton BD, Moore ML, Shu AYL, Heys JR, Meek TD. A radiometric assay for HIV-1 protease. *Anal Biochem* 1990; 188: 408-15.
135. Wang GT, Matayoshi E, Huffaker HJ, Krafft GA. Design and synthesis of new fluorogenic HIV protease substrates based on resonance energy transfer. *Tetrahedron Letter*. 1990; 31: 6493-6.
136. Matayoshi ED, Wang GT, Krafft GA, Erickson J. Novel fluorogenic substrates for assaying retroviral protease by resonance energy transfer. *Science* 1990; 247: 954-8.
137. AIDSinfo: Antiretroviral drugs. Available from: <http://aidsinfo.nih.gov/drugs/> [Accessed 2005 June 9].
138. Ungwitayatorn J, Samee W. Docking study of chromone derivatives as HIV-1 protease inhibitors. *Mahidol University Journal of Pharmaceutical Science* 2002; 29: 11-7.

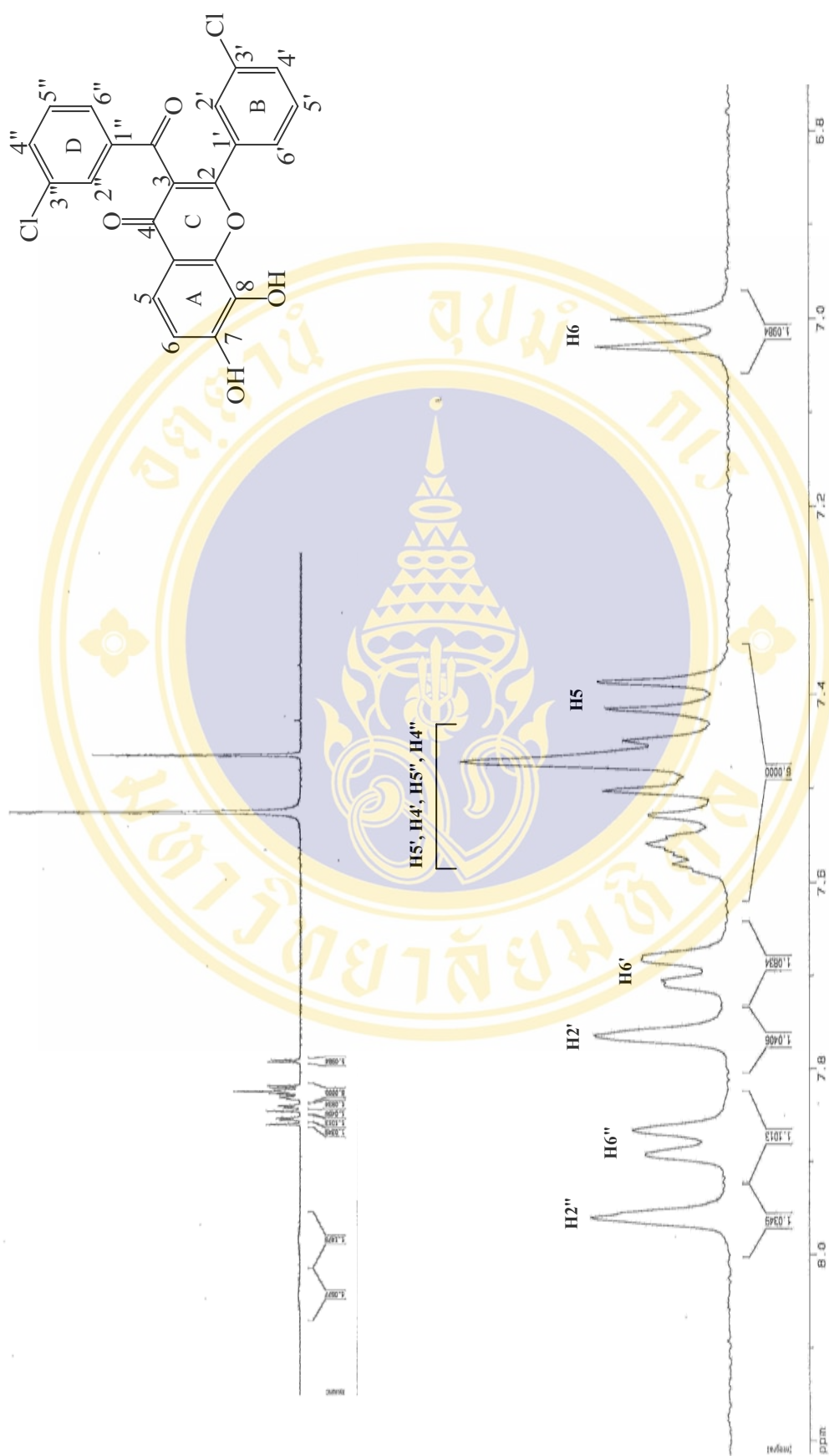




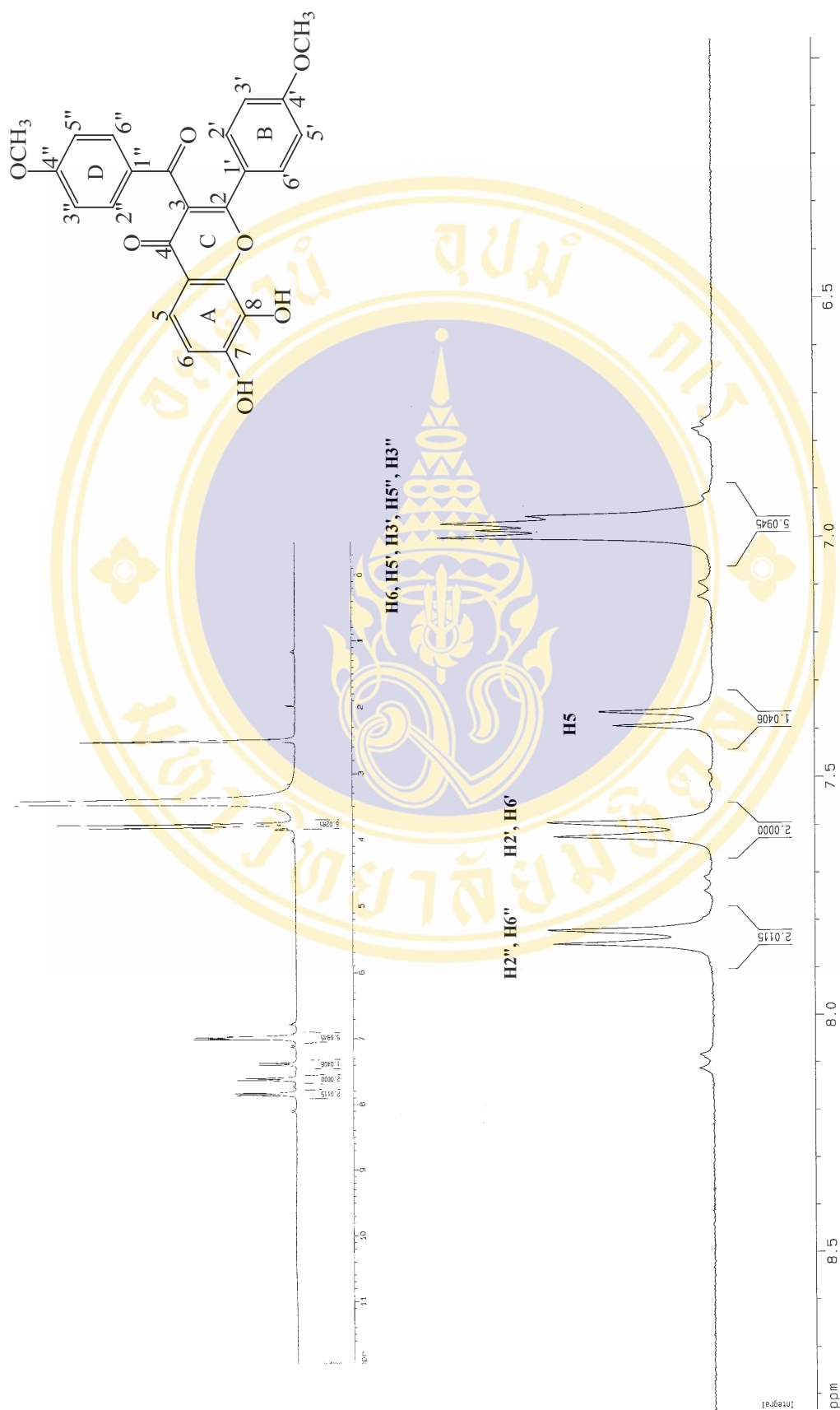
<sup>1</sup>H NMR spectrum (300 MHz, DMSO) of 7-Hydroxy-2-(4-(4'-tert-butylphenyl)-3-(4''-tert-butylbenzoyl)chromone) 1.



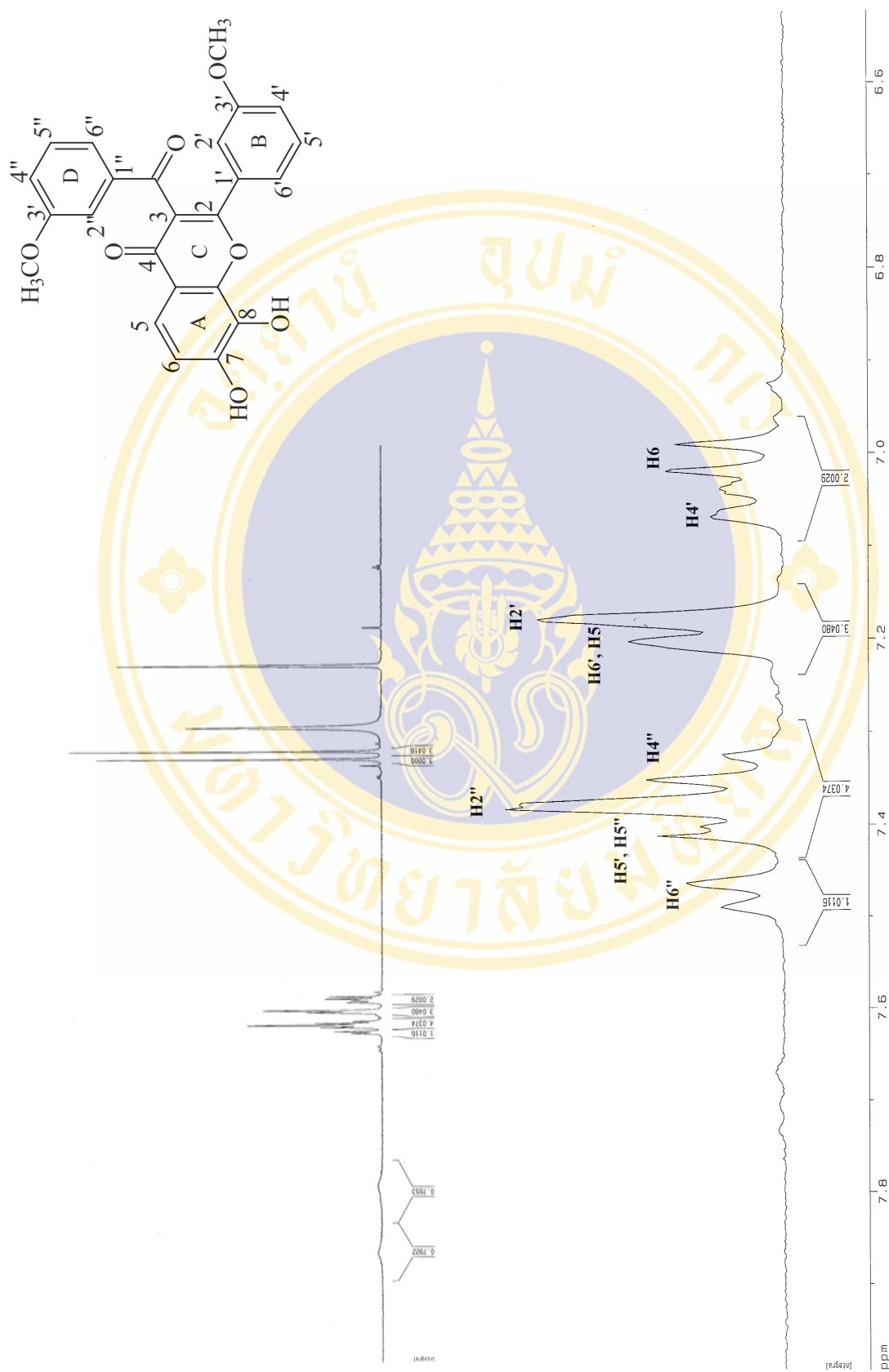
<sup>1</sup>H NMR spectrum (300 MHz, DMSO) of 7-Hydroxy-2-(3-chlorophenyl)-3-(3''-chlorophenyl)chromone 2.



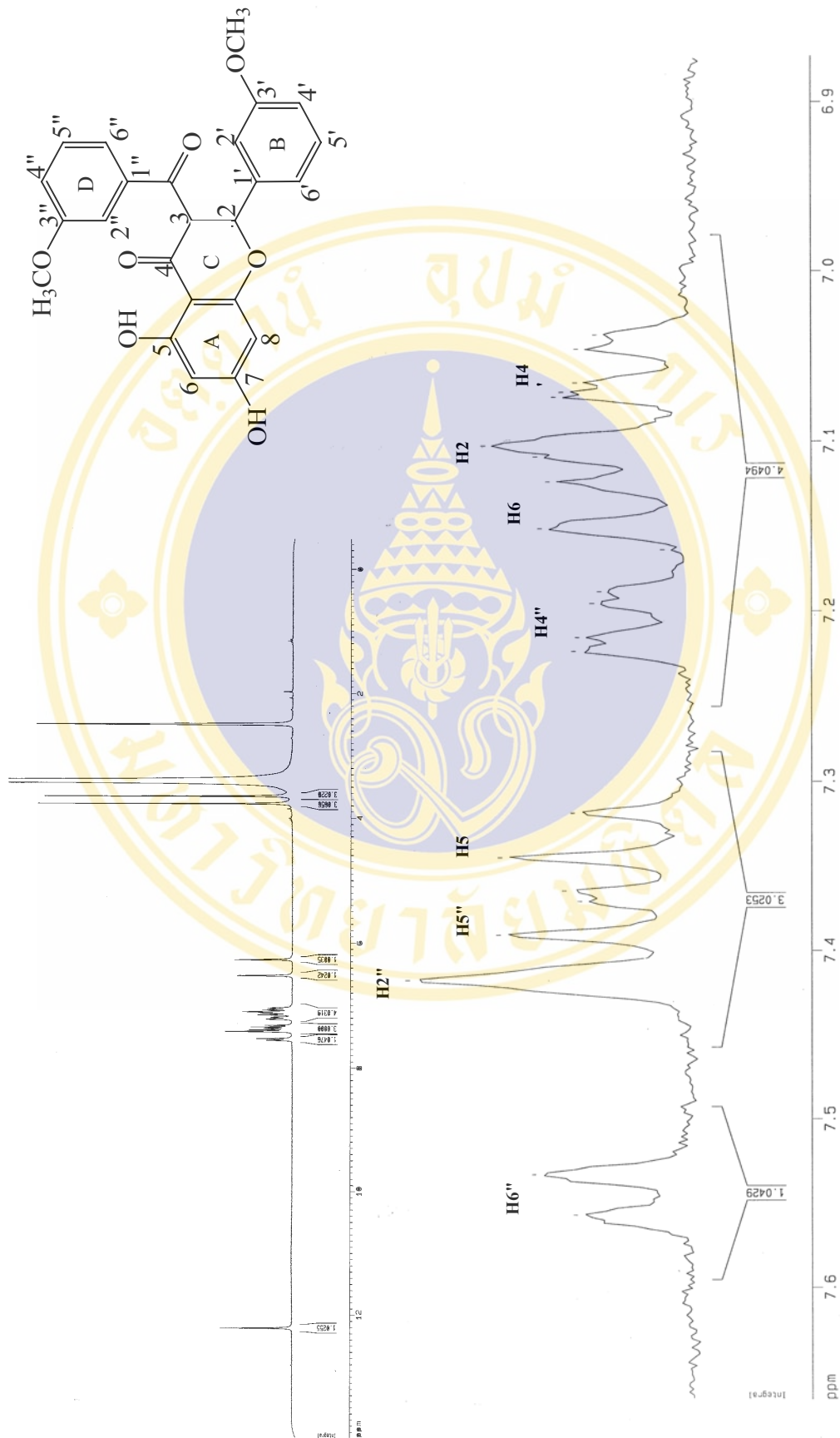
<sup>1</sup>H NMR spectrum (300 MHz, DMSO) of 7,8-Dihydroxy-2-(3'-chlorophenyl)-3-(3''-chlorobenzoyl)chromone 3.



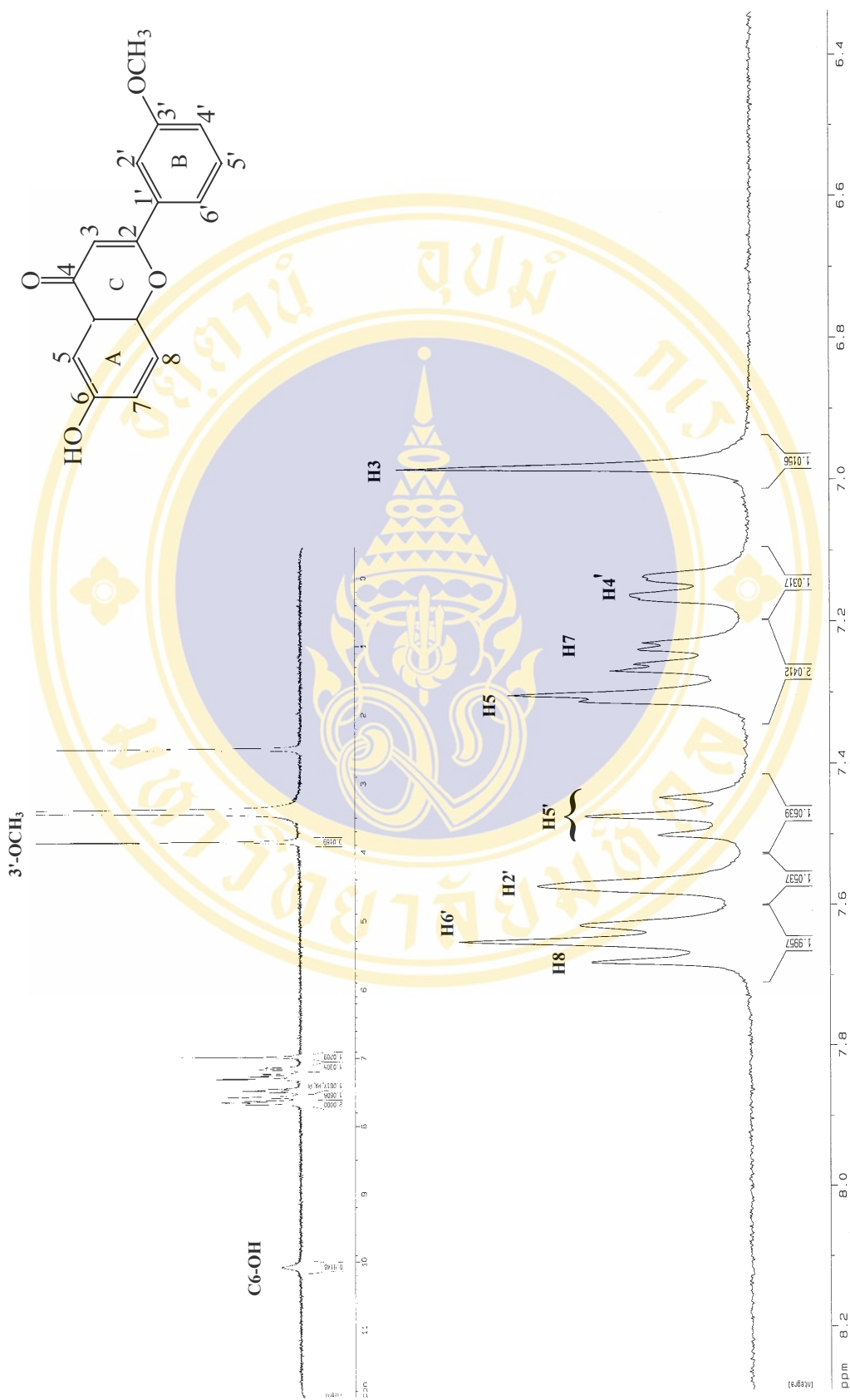
<sup>1</sup>H NMR spectrum (300 MHz, DMSO) of 7,8-Dihydroxy-2-(4'-methoxyphenyl)-3-(4''-methoxyphenyl) chromone **4**.



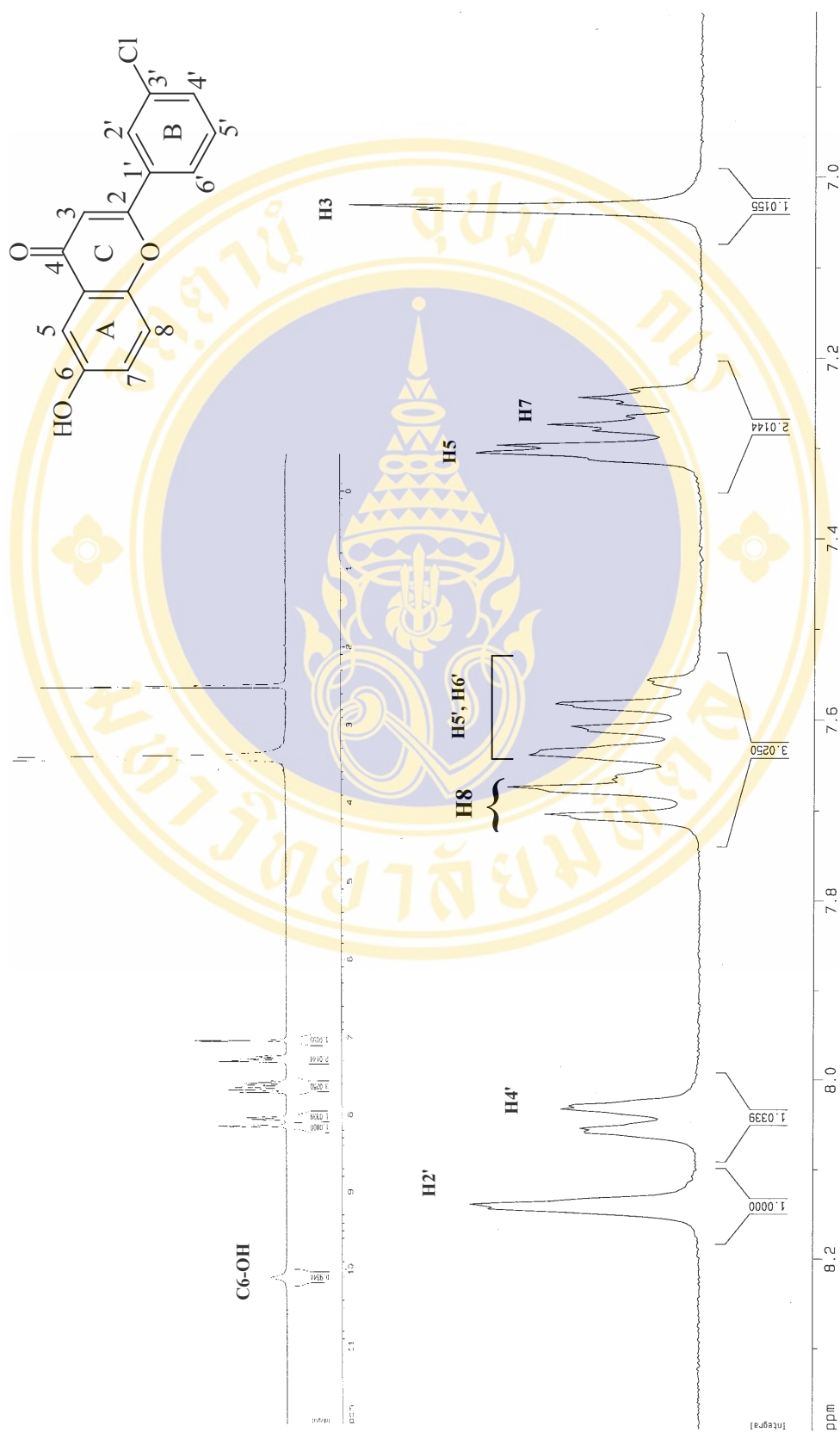
<sup>1</sup>H NMR spectrum (300 MHz, DMSO) of 7,8-Dihydroxy-2-(3'-methoxyphenyl)-3-(3''-methoxyphenyl)chromone **5**



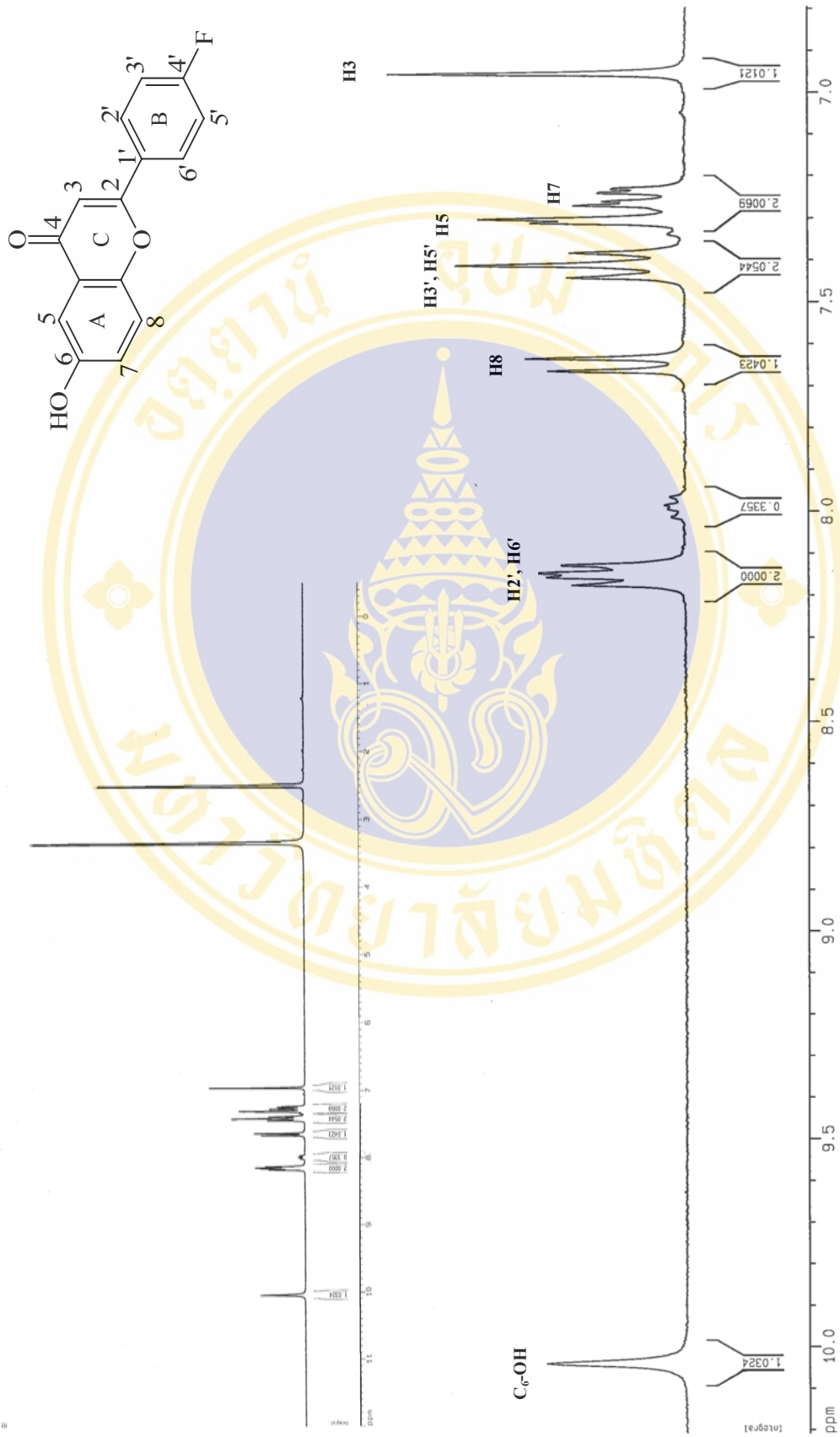
<sup>1</sup>H NMR spectrum (300 MHz, DMSO) of 5,7-Dihydroxy-2-(3'-methoxyphenyl)-3-(3''-methoxybenzoyl)chromone 6



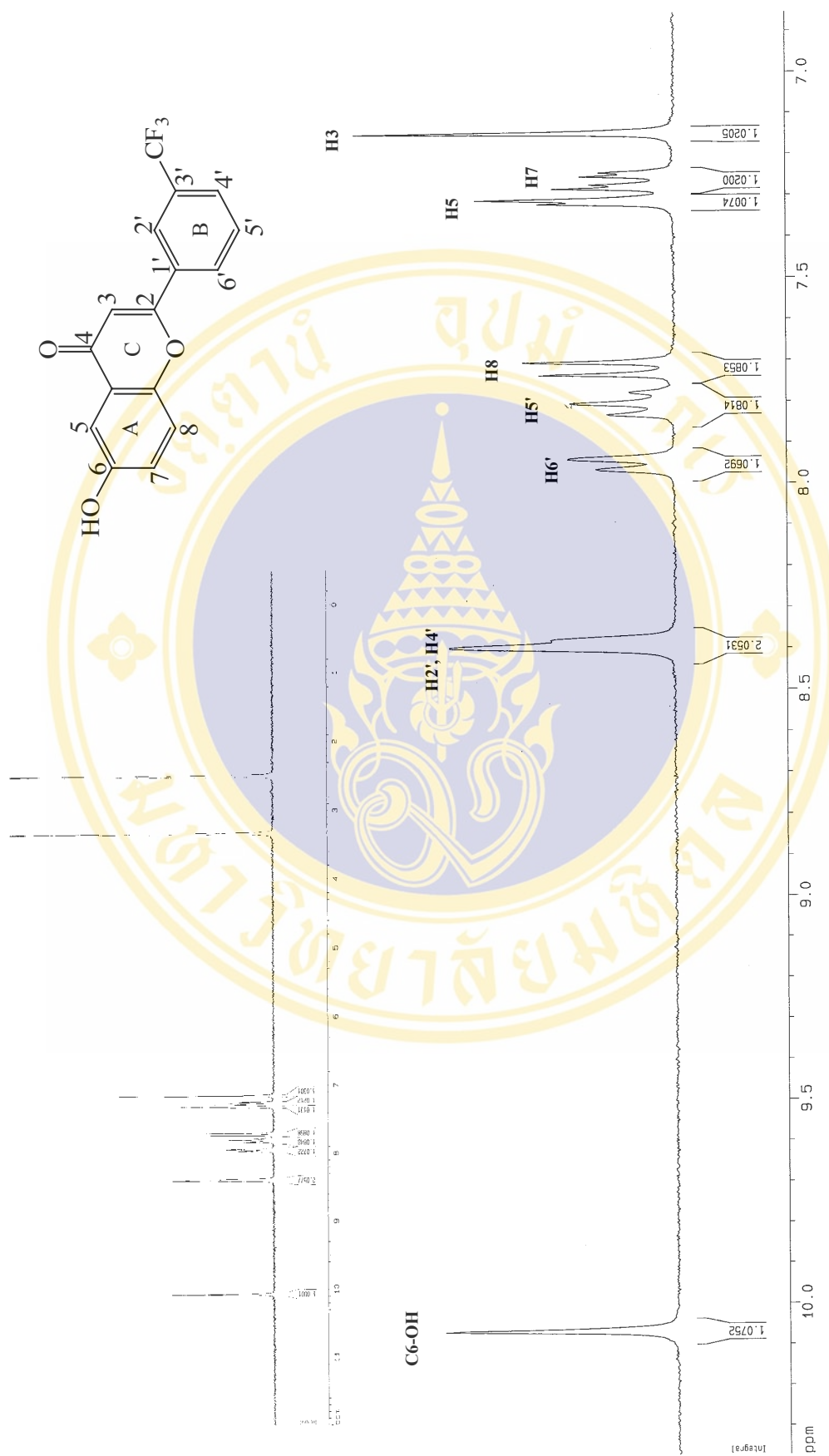
<sup>1</sup>H NMR spectrum (300 MHz, DMSO) of 6-Hydroxy-2-(3'-methoxyphenyl)chromone 7.



<sup>1</sup>H NMR spectrum (300 MHz, DMSO) of 6-Hydroxy-2-(3'-chlorophenyl)chromone 8.

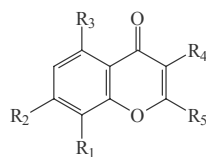


<sup>1</sup>H NMR spectrum (300 MHz, DMSO) of 6-Hydroxy-2-(4'-fluorophenyl)chromone **9**.



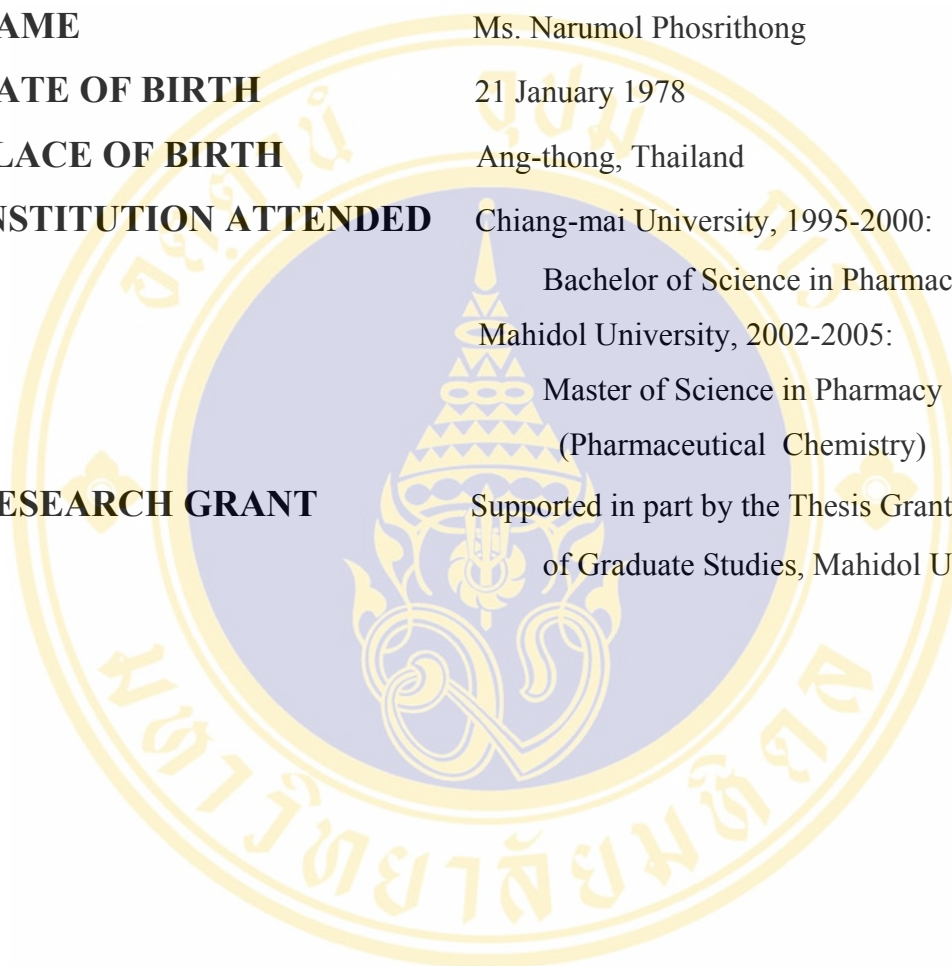
<sup>1</sup>H NMR spectrum (300 MHz, DMSO) of 6-Hydroxy-2-(3'-trifluoromethylphenyl)chromone **10**.

The inhibitory activity of the previously synthesized chromone compounds.



Cpd.	R <sub>1</sub>	R <sub>2</sub>	R <sub>3</sub>	R <sub>4</sub>	R <sub>5</sub>	% inhibition (previous study)	% inhibition (this study)
<b>1</b>	H	OH	H	H	4'-(NO <sub>2</sub> )-Phenyl	63.52 ± 1.63	56.17 ± 7.25
<b>7</b>	H	OH	H	H	4'-( <i>t</i> -butyl)-Phenyl	78.89 ± 5.71	78.97 ± 3.85
<b>8</b>	H	OH	OH	H	3'-(CF <sub>3</sub> )-Phenyl	74.80 ± 0.26	78.32 ± 2.68
<b>9</b>	H	OH	OH	H	4'-(F)-Phenyl	88.13 ± 2.33	90.14 ± 0.96
<b>10</b>	H	OH	OH	H	3',4'-(diF)-Phenyl	80.25 ± 3.25	78.76 ± 2.14
<b>11</b>	H	OH	OH	H	4'-( <i>t</i> -butyl)-Phenyl	89.29 ± 3.47	88.96 ± 4.27
<b>12</b>	H	OH	OH	H	3'-(Cl)-Phenyl	73.62 ± 0.58	69.12 ± 0.77
<b>13</b>	H	OH	OH	H	3',4'-(diCl)-Phenyl	85.26 ± 1.20	81.11 ± 3.63
<b>14</b>	H	OH	OH	H	4'-(OCH <sub>3</sub> )-Phenyl	88.68 ± 2.27	86.12 ± 3.15
<b>15</b>	H	OH	OH	H	3'-(OCH <sub>3</sub> )-Phenyl	97.48 ± 1.72	92.16 ± 3.02
<b>18</b>	OH	OH	H	4''-(NO <sub>2</sub> )-Benzoyl	4'-(NO <sub>2</sub> )-Phenyl	92.24 ± 1.70	92.55 ± 1.36
<b>21</b>	H	OH	H	3''-(CF <sub>3</sub> )-Benzoyl	3'-(CF <sub>3</sub> )-Phenyl	74.98 ± 3.86	74.99 ± 5.48
<b>22</b>	OH	OH	H	4''-(F)-Benzoyl	4'-(F)-Phenyl	84.94 ± 1.54	83.56 ± 5.39
<b>25</b>	H	OH	OH	4''-(NO <sub>2</sub> )-Benzoyl	4'-(NO <sub>2</sub> )-Phenyl	88.39 ± 0.11	87.87 ± 2.84
<b>26</b>	H	OH	H	4''-(OCH <sub>3</sub> )-Benzoyl	4'-(OCH <sub>3</sub> )-Phenyl	34.06 ± 9.89	22.96 ± 1.16
Pepstatin A						95.56 ± 0.17	91.07 ± 1.53

## BIOGRAPHY



<b>NAME</b>	Ms. Narumol Phosrithong
<b>DATE OF BIRTH</b>	21 January 1978
<b>PLACE OF BIRTH</b>	Ang-thong, Thailand
<b>INSTITUTION ATTENDED</b>	Chiang-mai University, 1995-2000: Bachelor of Science in Pharmacy Mahidol University, 2002-2005: Master of Science in Pharmacy (Pharmaceutical Chemistry)
<b>RESEARCH GRANT</b>	Supported in part by the Thesis Grant, Faculty of Graduate Studies, Mahidol University